Chondroitin sulfate conjugation facilitates tumor cell internalization of albumin nanoparticles for brain-targeted delivery of temozolomide via CD44 receptor-mediated targeting

Ritu R. Kudarha & Krutika K. Sawant

Drug Delivery and Translational Research
An Official Journal of the Controlled Release Society

ISSN 2190-393X

Drug Deliv. and Transl. Res.
DOI 10.1007/s13346-020-00861-x

Springer

Drug Delivery and Translational Research
https://doi.org/10.1007/s13346-020-00861-x

ORIGINAL ARTICLE

Chondroitin sulfate conjugation facilitates tumor cell internalization of albumin nanoparticles for brain-targeted delivery of temozolomide via CD44 receptor-mediated targeting

Ritu R. Kudarha[1] · Krutika K. Sawant[1]

Accepted: 17 September 2020

Abstract

In the present investigation, temozolomide (TMZ) loaded chondroitin sulfate conjugated albumin nanoparticles (CS-TNPs) were fabricated by desolvation method were chondroitin sulfate (CS) was used as the surface exposed ligand to achieve CD44 receptor mediated targeting of brain tumor. The developed CS-TNPs were characterized for particle size, zeta potential, entrapment efficiency and drug loading and evaluated by FTIR, DSC, XRD and TEM analysis. BBB (blood brain barrier) passage study using in vitro BBB model indicated that CS-TNPs were able to efficiently cross the BBB. Cell viability assay data demonstrated higher cytotoxicity of CS-TNPs as compared with pure TMZ. The CD44 receptor blocking assay and receptor poisoning assay in U87 MG cells confirmed the CD44 receptor and endocytosis-mediated (caveolae pathway) uptake of CS-TNPs. CS-TNPs were able to generate ROS in U87 MG cells. In vivo pharmacokinetic and biodistribution studies were performed in Wistar rats. In vivo results revealed significant enhancement in pharmacokinetic profile of CS-TNPs as compared with TMZ alone. Biodistribution results demonstrated higher accumulation of TMZ in the brain by CS-TNPs as compared with the pure drug that confirmed the brain targeting ability of nanoparticles. From all obtained results, it may be concluded that CS-TNPs are promising carrier to deliver TMZ to the brain for targeted therapy of brain tumor.

Keywords BSA nanoparticles · Chondroitin sulfate · Temozolomide · Brain targeting · CD44 blocking assay · Toxicity and Stability study

Introduction

Temozolomide (TMZ) is a first-line drug used for the treatment of brain tumors. It is basically an alkylating agent and a prodrug which firstly gets converted into highly unstable compound 5-(3-methyltriazen-1-yl) imidazole-4-carboxamide (MTIC) at physiological pH and then MTIC is further converted into 5-aminoimidazole-4-carboxamide (AIC) and methyldiazonium ion. Formation of these methyldiazonium ions causes breakage of double strand of DNA and leads to cell cycle arrest and cell death by methylation of DNA [1]. Although TMZ has the ability to cross the blood brain barrier (BBB), it needs a high systemic dose to reach a therapeutic concentration in the brain because of its short half-life. Due to this, various systemic side effects like oral ulceration, bone marrow suppression, fatigue, vomiting, nausea, and headache are associated with TMZ therapy [2, 3]. To overcome these side effects and to improve its therapeutic activity via brain targeting, a novel drug delivery system is required.

Albumin-based nanoparticles are widely explored to treat cancers due to the unique properties and targeting potential of albumin for passive as well as active targeting. Other important properties of albumin nanoparticles are non-antigenicity, biodegradability, and ease of surface modification to avoid the undesirable toxicity of drugs [4]. In surface-modified albumin nanocarriers, various ligands have been used for either altering various properties of therapeutic moiety (like pharmacokinetic properties, stability, circulation half-life, and release behavior) or as a targeting moiety [5, 6].

CD44 receptors are highly overexpressed in various cancers like breast cancer, brain tumor, hepatic and cervical

✉ Krutika K. Sawant
dr_krutikasawant@rediffmail.com

[1] Drug Delivery Research Laboratory, Centre of Relevance and Excellence in NDDS, Faculty of Pharmacy, The Maharaja Sayajirao University of Baroda, Donor's Plaza, Fathegunj, Vadodara 390002, India

Published online: 07 October 2020

cancers, etc. which can be targeted using various targeting moieties [4, 7–9]. Chondroitin sulfate (CS), (sulfated glycosaminoglycans), is a natural anionic mucopolysaccharide found in mammals [10] that is used for targeting the CD44 receptor and also facilitates crossing the blood brain barrier (BBB) [9].

The present research work focused on fabrication of temozolomide-loaded CS-conjugated bovine serum albumin (BSA) nanoparticles (CS-TNPs) and its investigation in brain targeting for enhancing the therapeutic concentration of TMZ in the brain. The developed CS-TNPs were characterized for different quality attributes like particle size, PDI, zeta potential, entrapment, efficiency, conjugation efficiency, and drug loading. In vitro release of TMZ from CS-TNPs was determined by dialysis method. The cytotoxic potential of TMZ after encapsulation in CS-TNPs was assessed by cell viability assay and BBB passage was estimated by in vitro monolayer and co-culture model. Cellular uptake mechanism was identified using different cell uptake inhibitors and CD44-mediated targeting was estimated by CD44 receptor blocking assay. In vivo pharmacokinetic and biodistribution studies were performed to confirm brain targeting and biochemical parameters were estimated to assess the toxicity potential of prepared CS-TNPs in the rat model.

Experimental

Materials, cells, and animals

Temozolomide (TMZ) was obtained as a gift sample from Cipla Ltd., Mumbai (India). Bovine serum albumin (BSA), chondroitin sulfate (CS), acetic acid, sodium acetate, sodium hydroxide, glutaraldehyde, N-hydroxysuccinimide (NHS), dialysis membrane (12000 MWCO), cell culture plates (96, 12 and 6 well plates), culture flasks, Dulbecco's Modified Eagle Medium (DMEM), fetal bovine serum (FBS), Trypsin-EDTA, penicillin-streptomycin solution (100 U/ml), fluorescein isothiocyanate (FITC) and 1-(4,5-dimethylthiazol-2-yl)-3,5-diphenyl-formazan (MTT) were purchased from Himedia (India). Transwell inserts were purchased from Corning, NY, (USA). Ethanol and N-Ethyl-N'-(3-dimethylaminopropyl) carbodiimide HCl (EDC) were purchased from Spectrochem Pvt Ltd, Mumbai (India). Hexadecyltrimethylammonium bromide (CTAB) and mannitol were purchased from SD Fine chemicals, Mumbai (India). HPLC grade acetonitrile and methanol were purchased from Renkem, (India). All other chemicals and solvents used were of analytical grade. The U-373 MG, U-87 MG, and MDCK II cell lines were purchased from the National Center for Cell Science (NCCS) Pune (India).

Wistar rats (150–200 g) were obtained and housed at 25 °C ± 1 °C in an animal house under 12 h/12 h dark/light cycle with free access to water and food. All animal experimental procedures were reviewed and approved by the Institutional Animal Ethics Committee and CPCSEA (Committee for the Purpose of Control and Supervision of Experiments on Animals, New Delhi, India with registration no IAEC/2018-19/1830.

Fabrication of nanoparticles

TMZ-loaded albumin nanoparticles (TNPs) were fabricated by a previously reported desolvation method with slight modification [11]. Firstly, preliminary optimization by OVAT (one variable at a time) analysis was carried out to identify the critical variables and their ranges for fabrication of TNPs. As per the obtained results of preliminary optimization, the optimized values for different variables are summarized in Table 1 according to which, final optimized batch of TNPs was prepared. Briefly, TMZ (7 mg) was incubated in albumin solution (16.6 mg/ml) (pH 5.7 ± 0.2) under magnetic stirring for 2 h. Then 9-ml ethanol (aqueous:organic phase ratio 1:3) was added dropwise in the albumin solution to form the nanoparticles. In the next step, 10 μl of glutaraldehyde (8% w/v GA) at a concentration of 0.58 μl/mg of BSA was added for hardening the formed nanoparticles. TNPs were separated by centrifugation (12,000 rpm × 30 min), washed thrice with ethanol, and freeze-dried using trehalose (5% w/w) as cryoprotectant. Placebo albumin nanoparticles (PNPs) were prepared with the same method without addition of TMZ.

CS was conjugated with TNPs by carbodiimide chemistry [12]. Briefly, CS, EDC, and NHS at a molar ratio of 1:2:2 were dissolved in 0.01-M MES (2-(N-morpholino) ethane sulfonic acid) buffer (pH 4.7) to activate the carboxylic groups of CS. Subsequently, TNPs were added in the mixture (CS:TNPs ratio = 1:1 w/w) and kept under continuous stirring for 12 h at RT. The conjugated CS-TNPs were separated by centrifugation at 15,000 rpm for 30 min and washed thrice with water to remove unreacted materials. Percent conjugation efficiency of CS with TNPs was determined by previously reported CTAB turbidimetric method [13]. Conjugation of CS with TNPs was optimized by OVAT analysis on the basis of effect of CS:TNPs ratio (1:1, 2:1, and 3:1) and stirring time (1 h, 2 h, 4 h, and 12 h) on size, PDI, zeta potential, and % conjugation efficiency.

Characterization of CS-TNPs

The developed TNPs and CS-TNPs were characterized for particle size and zeta potential using Malvern Zetasizer (ZS Nano, USA) after suitable dilution with double distilled water [9]. The obtained size of nanoparticles was expressed as Z-

Table 1 Optimized values of variables after preliminary optimization

Variables	Values
BSA concentration	16.67 mg/ml
Aqueous phase	Water (5.7 ± 0.2 pH adjusted with dilute acetic acid)
Organic phase	Ethanol
Polymer to drug ratio	1:7
Aqueous:organic phase ratio	1:3
Amount of GA (8%)	0.58 μl/mg BSA (~ 10 μl)
Rate of addition of organic phase	1 ml/min

average (d.nm) value using intensity distribution. The Smoluchowski method was utilized for measurement of zeta potential of developed nanoparticles. DSC analysis was carried out using a differential scanning calorimeter (Shimadzu, Japan) over a temperature range of 30 °C to 300 °C at a heating rate of 10 °C per minute in inert nitrogen atmosphere at a flow rate of 40 ml/min. FTIR analysis was performed for TMZ, BSA, CS, PNPs, TNPs, and CS-TNPs using FTIR spectrometer, IR Affinity-1S (Shimadzu, Japan) in the range from 4000 to 400 cm^{-1}. Powder XRD spectra were obtained using an X-ray diffractometer (Rigaku Ultima IV; Japan). Morphology of CS-TNPs was observed using TEM (TEM CM 200, Philips) [14].

Estimation of entrapment efficiency and drug loading

The quantity of TMZ entrapped in TNPs and CS-TNPs was determined indirectly by measuring concentration of free TMZ in the supernatant using UV–visible spectrophotometer (Shimadzu UV-1700) at 330 nm. The percentage entrapment efficiency (%EE) of TMZ in TNPs and drug loading (%DL) in TNPs and CS-TNPs were then determined using the equation:

$$\%EE = \frac{(\text{Total added drug} - \text{free drug})}{\text{Total added drug}} \times 100$$

$$\%DL = \frac{\text{Entrapped drug}}{\text{Weight of lyophilized nanoparticles}} \times 100$$

In vitro drug release

The dialysis method was used to carry out in vitro drug release studies [15]. Dialysis bags (MWCO = 12,000) containing pure TMZ, TNPs, and CS-TNPs (equivalent to 5 mg drug) were immersed into beakers containing 30-ml sodium acetate buffer (pH 5.5 ± 0.2) and maintained at 37 °C under mild stirring (50 rpm). At predetermined intervals, 1.0-ml samples were collected and replaced with fresh buffer solution to maintain sink condition. UV spectrophotometry at 330 nm was used to determine amount of TMZ released.

In vitro BBB permeation study

The permeation of TMZ, TNPs, and CS-TNPs across the BBB was assessed by in vitro BBB model (co-culture model and monolayer model) [16]. In the co-culture model, U-373 MG cells (density = 7.5×10^4 cells/well) were seeded and grown onto the apical side of inserts. Then inserts were transferred to 12-well culture plates containing DMEM medium (1 ml) and were incubated for 24 h at 37 °C. After incubation, MDCKII (density = 150×10^4 cells/well) were seeded and incubated at 37 °C for 24 h onto the inner side of the insert. After incubation, 1 ml of TMZ, TNPs, and CS-TNPs at TMZ concentration of 2 mg/ml were added to the luminal compartment of inserts. Then, 200 μl of the medium was withdrawn from the basal compartment at predetermined time intervals (0, 2, 24, and 48 h), replacing with fresh medium. The permeation of drug through the in vitro BBB model was determined by HPLC (Agilent Technologic 1260 Infinity II) analysis [16] and the transport ratio of TMZ, TNPs, and CS-TNPs was determined using the following equation:

$$Transportatio(\%) = \left(\frac{Wn}{W}\right) * 100$$

where, Wn = amount of TMZ in basal chamber at time "n" (n = 2, 24 and 48 h); W = amount of TMZ added in apical chamber.

In the monolayer model, only a single cell line at a time was grown in a similar manner to the co-culture model, and the above mentioned procedure was followed.

In vitro cell cytotoxicity assay

The in vitro cell cytotoxicity of synthesized nanoparticles (TNPs and CS-TNPs along with pure TMZ) against U-87 MG cells was estimated by the MTT assay. Briefly, the cells were seeded in a 96-well cell culture plate at a density of 2500 cells/well and incubated for 24 h at 37 °C and 5% CO_2 in culture media. After incubation, the old medium was replaced with fresh medium containing different concentrations (5–100 μg/ml) of pure TMZ, TNPs, and CS-TNPs and incubated

again for 24 and 72 h, respectively. Then, the MTT solution at a concentration of 5 mg/ml (20 μl) was added to the cells and was further incubated overnight in the dark at 37 °C. After incubation, the MTT solution was removed and a150-μl DMSO was added to dissolve the formazan crystals. Thereafter, the absorbance was immediately measured at 570 nm by a microplate reader (Bio-Rad, Hercules, CA, USA) [17].

Cell cycle analysis

U87 MG cells at a density of 1×10^5 cells/well were seeded on plates and incubated at 37 °C for 24 h. After 24 h, the old medium was discarded, replaced with a fresh medium containing TMZ, TNPs, and CS-TNPs at a concentration equivalent to 100 μg/ml of pure drug and incubated for another 24 h. Then cells were detached using trypsin-EDTA, washed with PBS, and fixed using 70% ethanol. Staining of the fixed cells were done with 0.5 ml of PBS containing 0.5μg/ml propidium iodide, 10-μg/ml RNase A, and 0.1% Triton X-100. The cells were incubated for 30 min at room temperature in the dark and cell cycle analysis was performed using BD FACS Aria III (BD Biosciences, CA). Data was analyzed using BD FACS Diva software version 6.1.3 [18].

Cellular uptake study and cellular uptake mechanism

The cellular uptake of TNPs and CS-TNPs (qualitative uptake) in U87 MG cell line was performed using confocal microscopy. The cells at a density of 5×10^3 cell/well were grown on cover slips (coated with poly l-lysine) at 37 °C for 24 h. After 24 h, the old medium was replaced and the cells were treated with a medium containing FITC-tagged TNPs and CS-TNPs for 2 h. The cells were then fixed using 1% PFA after washing with PBS. The cover slips were washed thrice using PBS and mounted on glass slides using 2.5% DABCO and sealed. Cellular uptake of FITC-tagged TNPs and CS-TNPs was then analyzed using Zeiss LSM 510 confocal microscope (Oberkochen, Germany) at ×63 [16].

The cellular uptake mechanism and endocytosis of TNPs and CS-TNPs in the U87 MG cell was determined by pretreating the cells with specific membrane entry inhibitors. The U87 MG cells (density = 1×10^5 cells/well) were seeded and grown on a 6-well plate. After monolayer formation, the cells were pretreated with a fresh medium containing amiloride (25 μg/ml), chlorpromazine (10 μg/ml), and nystatin (50 μg/ml) and incubated at 37 °C for 1 h. After 1 h, TNPs and CS-TNPs (25 μg/ml) were added and co-incubated with inhibitor solutions for 12 h and 24 h, respectively.

The CD44 blocking assay was used to study the uptake of CS-TNPs by the CD44 receptor. For that, the cells were pretreated with 10 mg/ml free HA polymer (175–350 kDa and hydrated overnight in serum- and antibiotic-free medium) for 1 h before addition of CS-TNPs for an additional 12 h and 24 h. After incubation, the cells were lysed using 1% Triton X-100 and the amount of TMZ inside the cells was analyzed by HPLC [19].

Estimation of reactive oxygen species (ROS) generation

The dichlorofluorescein (DCF) assay was used to estimate ROS generation in U87 MG cells. The cells were seeded in a 96-well plate and incubated for 24 h. After 24 h, the medium was replaced with a fresh medium containing TMZ, TNPs, and CS-TNPs (5-100 μg/ml). In this analysis, 10 μg ml^{-1} of H_2O_2 was used as a positive control while untreated cells were used as negative control. Cells were harvested, washed once with PBS, and incubated with 10-μM H_2DCFDA (2,7-dichlorodihydrofluorescein diacetate) (in PBS ×1) for 30 min at 37 °C prior to analysis. The DCF fluorescence was then recorded at 535 nm using a plate reader (Fluoroskan Ascent CF (Labsystems, USA)). The generated ROS was expressed as a ratio of the fluorescence of DCF of treated cells to that of untreated cells [19, 20].

In vivo pharmacokinetic study

Wistar rats were used to perform pharmacokinetic studies of TMZ, TNPs, and CS-TNPs. The animals were divided into three groups ($n = 6$ in each group) and were fasted overnight before the experiment but allowed to drink water freely. Animals in group one, two, and three received pure TMZ dispersion, TNPs, and CS-TNPs at a dose of 3 mg/animal equivalent of TMZ (dose: 200 mg/m^2), respectively, via intravenous route through tail vein [2]. Blood samples were collected retro-orbitally in tubes containing EDTA at predetermined intervals (0.5 h, 1 h, 3 h, 6 h, 12 h, 24 h, 48 h, 60 h, and 72 h). Collected blood was centrifuged (5000 rpm × 20 min) to separate plasma by a cold centrifuge (Remi Equipments Ltd) and separated plasma was stored at − 20 °C until further analysis [16].

Biodistribution study

Wistar rats were randomly divided into three groups with six animals for each time point. Rats in group one, two, and three received pure TMZ dispersion, TNPs, and CS-TNPs, respectively, at a dose of 3 mg/animal equivalent to TMZ (dose: 200 mg/m^2) via tail vein. The rats were sacrificed at predetermined time intervals (12 h and 24 h) by euthanization through overdose of thiopentone sodium and different organs like the brain, lung, heart, kidney, liver, and spleen were isolated and blood was collected. Blood samples were processed as mentioned earlier in pharmacokinetic study. Organs were rinsed and homogenized with cold saline by homogenizer. The homogenates were centrifuged and stored at − 20 °C till further

analysis. The TMZ level in plasma and different organs was determined by HPLC analysis [21].

In vivo toxicity study

Rats were randomly divided into four groups (n = 6 in each group). Animals in group one, two, three, and four received saline, pure TMZ, TNPs, and CS-TNPs, respectively, at a dose containing TMZ equivalent to 30 mg/kg via intravenous route through tail vein. After 7 days, blood was collected retro-orbitally and subjected to biochemical parameter estimation using standard kits through standard procedures in an automated bioanalyzer (Mythic hematology analyzer) [21, 22].

Stability studies

The stability of the lyophilized TNPs and CS-TNPs was investigated according to ICH guidelines by storing samples at refrigerated condition (4 °C) and at room temperature (25 °C ± 2 °C, 65% ± 5% RH) for 3 months. At time intervals of 1 month, samples were withdrawn and redispersed in saline solution and different quality attributes like particle size, assay, and zeta potential were checked to assess their stability [23, 24].

Statistical data analysis

Results are given as mean ± SD. Statistical significance was tested by two-tailed Student's t test or one-way ANOVA. Statistical significance was set at $P < 0.05$.

Results and discussion

Fabrication and optimization of CS-TNPs

TNPs were successfully fabricated by desolvation method followed by CS conjugation (CS-TNPs) by carbodiimide chemistry (Fig. 1A). CS-TNPs optimization was done by

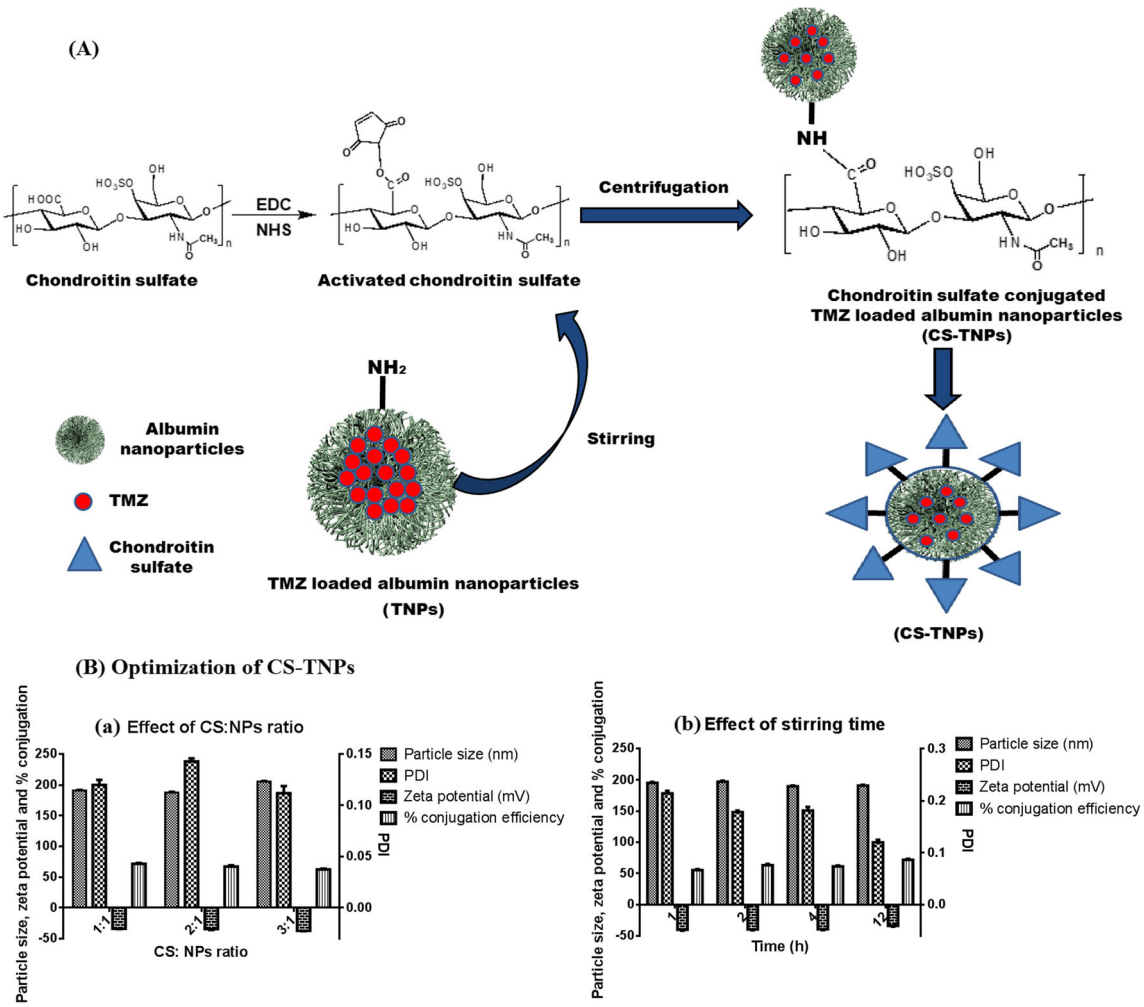

Fig. 1 **A** Schematic representation of fabrication of CS-TNPs and **B** optimization of CS-TNPs: (a) effect of CS:NPs ratio on conjugation and (b) effect of stirring time

varying single factor at a time and observed its effect on particle size, PDI, zeta potential, and % conjugation efficiency of CS with the TNPs.

Effect of CS:NPs ratio on conjugation

Three different CS:NPs ratios were selected to optimize CS-TNPs, viz., 1:1, 2:1, and 3:1. Obtained results are shown in Fig. 1B (a). The results indicated that the CS:NPs ratio does not have a significant effect on particle size, PDI, and zeta potential but has a significant effect on conjugation efficiency. The insignificant effect of CS:NPs ratio on size, PDI, and zeta potential may be correlated with the fact that after increasing the ratio, the surface area of nanoparticles and the number of amine groups present on NPs (to bind with carboxylic groups of CS) remain constant. So, the size, PDI, and zeta potential will not be affected to any large extent after increasing number of CS molecules but may affect conjugation efficiency. This may be attributed to the fact that more the number of CS molecules, more will be the chances of its conjugation on NPs and vice versa. So on the basis of higher conjugation efficiency, 1:1 was selected as HA:NPs ratio and used for further optimization.

Effect of stirring time on conjugation

Effect of stirring time on the conjugation of CS was optimized on the basis of different stirring times (1 h, 2 h, 4 h, and 12 h). Results indicated no significant effect of stirring time on particle size, PDI, and zeta potential but had a significant effect on % conjugation efficiency as shown in Fig. 1B (b). As stirring time increased, % conjugation efficiency of CS with nanoparticles also increased; this may be correlated with the fact that as time passed, more interaction between the carboxylic groups of activated CS and amine groups of albumin took place that led to enhancement of conjugation efficiency of CS with nanoparticles. So based upon these results, 12 h was selected as stirring time for conjugation.

Finally, it can be concluded that for the conjugation of CS with TNPs, the CS:NPs ratio 1:1 and 12-h stirring time were optimum and selected as optimized parameters for preparing the final optimized CS-TNPs.

Characterization of CS-TNPs

The prepared TNPs and CS-TNPs were characterized on the basis of particle size, PDI, and zeta potential using Zetasizer. The particle size of TNPs and CS-TNPs was found to be 160.6 ± 2.87 nm and 222.3 ± 1.57 nm with a PDI of 0.153 ± 0.012 and 0.217 ± 0.05, respectively. Increase in the particle size and PDI indicated conjugation of CS with TNPs. The zeta potential was found to be − 25.3 ± 1.5 mV and − 32.8 ± 1.87 mV for TNPs and CS-TNPs. In case of CS-TNPs, higher negative zeta potential was due to conjugation of CS with TNPs. The CS contains various functional groups such as hydroxyl, carboxyl, and sulfonic acid which impart a negative charge on CS, and due to this, the zeta potential of CS-TNPs shifted toward the higher side. Zeta potential value of TNPs and CS-TNPs indicated stability of prepared nanoparticles as it may produce sufficient repulsion to overcome gravitational attraction between the nanoparticles and leads to better stability [8].

The conjugation efficiency of CS with TNPs was found to be 71.60% ± 1.20% as determined by the CTAB turbidimetric method.

DSC thermograms of BSA, TMZ, CS, PNPs, CS-PNPs (placebo), and CS-TNPs are shown in Fig. 2a. The sharp exothermic peak at 207.89 °C was observed for TMZ which indicates its crystalline nature. As the thermogram of CS-TNPs did not show any exothermic peak of TMZ, it may be said that TMZ was encapsulated in CS-TNPs in the form of molecular dispersion [16].

The FTIR spectra of BSA, TMZ, CS, TNPs, and CS-TNPs are shown in Fig. 2b. Characteristic peaks for TMZ were found at 3417.63 cm^{-1} and 3382.57 cm^{-1} {–N-H stretch for amines}; 3111.11 cm^{-1}, 3183.45 cm^{-1}, and 3281.75 cm^{-1} {=C-H- (alkene) stretch}; 1755.17 cm^{-1}, 1731.15 cm^{-1}, and 1673.25 cm^{-1} {–C=O stretch contributed by aldehydes, ketones, or amide group}; 1597.93 cm^{-1} and 1670.21 cm^{-1} {–C=C- (alkene) stretch}; and 1361 cm^{-1} to 1179 cm^{-1} {-C-N stretch from amines}. BSA showed characteristic peaks at 3275.16 cm^{-1} {–NH stretching}, 2871–2952 cm^{-1} {-C-H and -C-H methoxy stretching}, 1642.45 cm^{-1} {-C=O stretching of amide} and 1533.35 cm^{-1} {-N–H bending -C–N stretching of amide}. FTIR spectrum of CS showed characteristic peaks at 3340.71 cm^{-1} {-OH stretching}, ~ 1562.34 cm^{-1} {amide II - N-H band}, 1612.49 cm^{-1}, and ~ 1408.04 cm^{-1} {-C=O stretching vibration}. In case of TNPs, all characteristic peaks of TMZ were also present but intensity of peaks decreased. In case of CS-TNPs, new peaks at 1527.62 cm^{-1} {attributed to amide bond}, 3307.92 cm^{-1}, and 1450.47 cm^{-1} {for–NH and CN group} were observed which confirmed the conjugation of CS with TNPs [8, 16].

X-ray diffractograms (XRD) of pure TMZ, BSA, CS-PNPs, and CS-TNPs are shown in Fig. 2c. XRD of TMZ showed intense and characteristic sharp peaks at 2θ values of 10.5°, 14.59°, 26.5°, and 27.9° which indicated the highly crystalline nature of drug. The XRD pattern of BSA showed amorphous behavior of polymer as no sharp peak was observed. PNPs and CS-PNPs also did not show any sharp peak. In diffractograms of CS-TNPs, characteristic peaks of TMZ were present but their intensity was decreased. This may be due to conversion of crystalline TMZ into amorphous form after encapsulating in nanoparticles [16]. Apart from this, some additional peaks were also present which may be due to trehalose. The conversion of crystalline TMZ

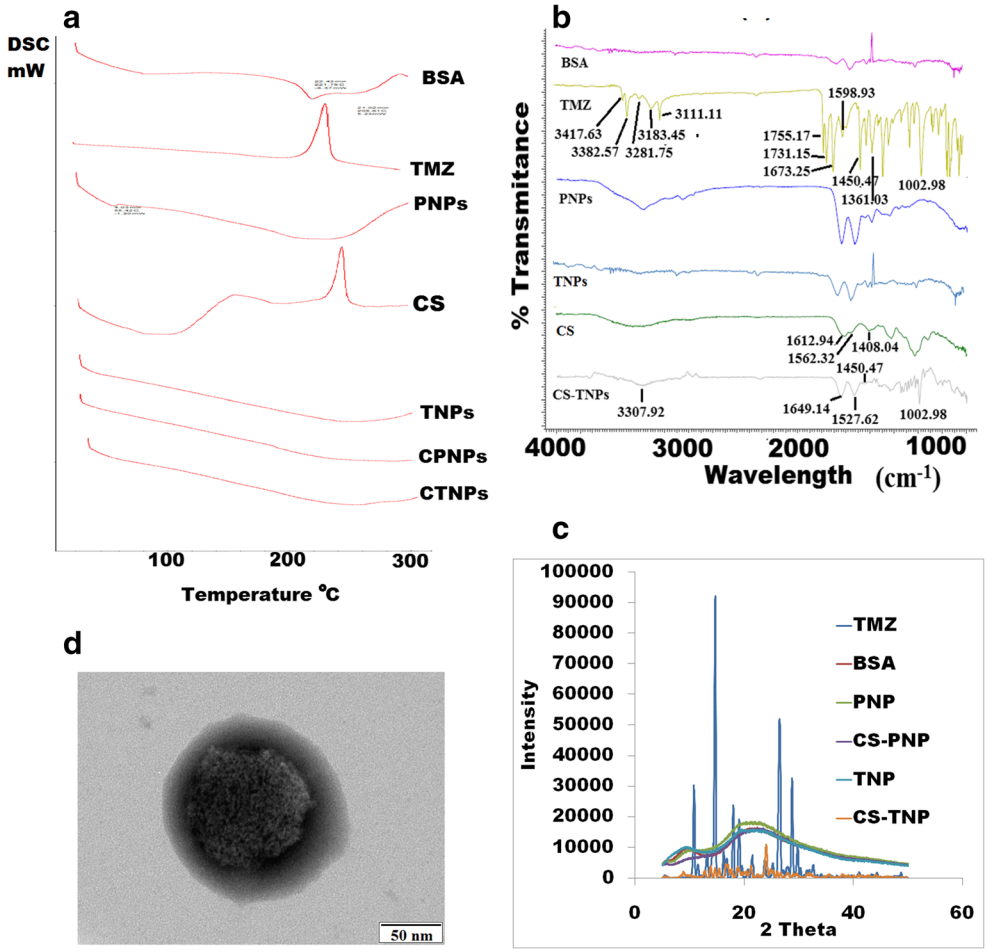

Fig. 2 Characterization of CS-TNPs: **a** DSC thermogram, **b** FTIR spectrum, **c** XRD spectrum, and **d** TEM image

into amorphous TMZ after encapsulating in nanoparticles may also beneficial in terms of solubility and bioavailability as amorphous form is more soluble as compared with crystalline.

TEM image of CS-TNPs indicated the core shell type structure of CS-TNPs in which the dark core represented TNPs and the surrounding lighter gray rim represented CS conjugation with TNPs. The morphology of CS-TNPs was spherical as seen in Fig. 2d. Size of CS-TNPs obtained by TEM was lesser than that obtained by Zetasizer (DLS measurement). Higher particle size in case of DLS may be due to the presence of hydration layer over nanoparticles, while in the case of TEM, the size was measured in a dried state [14].

Entrapment efficiency and drug loading

The percent entrapment efficiency of TNPs and CS-TNPs were found to be 71% ± 2% and 62% ± 3%, respectively, while percent drug loading was found to be 10% ± 1% and 4% ± 1%, respectively. The decrease in the % EE of CS-TNPs may be correlated with the fact that some amount of entrapped TMZ in TNPs may get released during conjugation of CS with TNPs as the conjugation reaction took place in the aqueous condition for 12 h. The decrease in the % DL can be correlated with the fact that in case of CS-TNPs, total weight of the nanoparticles increased as compared with TNPs which led to reduction in the % DL because total weight of nanoparticles is inversely proportional to % DL.

In vitro drug release

The in vitro drug release from TNPs and CS-TNPs was demonstrated at pH 5.5 ± 0.2 to mimic the tumor environment. The obtained results as shown in Fig. 3a indicated that almost 100% drug release of pure TMZ was observed within 1.5 h while only 45.83% ± 1.30% and 26.63% ± 1.50% of drug release took place after 2 h from TNPs and CS-TNPs, respectively. After 24 and 48 h, 58.68% ± 1.48% and 63.11% ± 1.30% of drug was released from TNPs, respectively, while from CS-TNPs, only 32.53% ± 1.51% and 42.42% ± 1.54% of drug release was observed after 24 h and 48 h, respectively. A biphasic release pattern of TMZ was observed from developed TNPs and CS-TNPs characterized by an initial rapid release of 29.30 ± 1.49% and 24.05 ± 0.49% respectively within half an

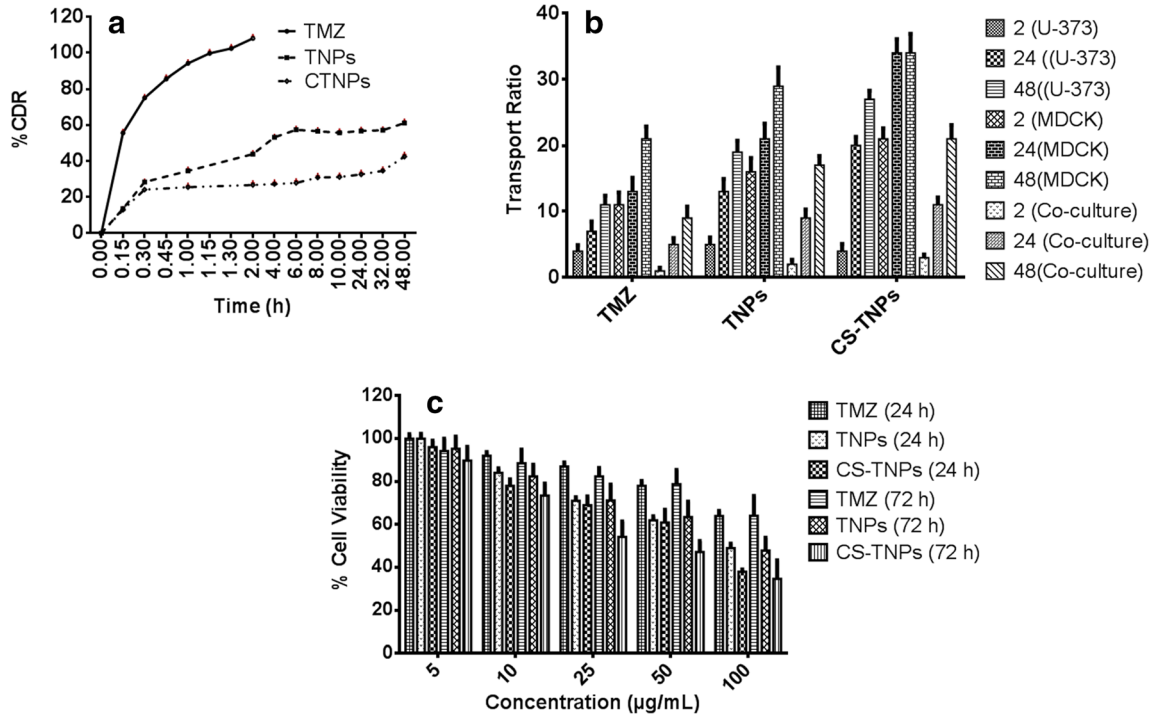

Fig. 3 Evaluations of CS-TNPs: **a** in vitro drug release, **b** in vitro BBB passage studies, and **c** in vitro cell viability study in U87 MG cells. Data are presented as mean ± SD ($n = 3$)

hour which may be due to the presence of the surface-adsorbed drug, followed by slower and sustained release. The slower and sustained release may be due to slow diffusion of drug from TNPs and CS conjugated TNPs. As compared with TNP, much slower release was observed in case of CS-TNPs which may be due to the presence of CS over TNPs which acted as a barrier for drug release from the nanoparticles [25].

In vitro BBB permeation study

In vitro BBB permeation of pure TMZ, TNPs, and CS-TNPs across the in vitro BBB model was determined and the results are shown in Fig. 3b. The transport ratio of TNPs and CS-TNPs was higher than pure TMZ through the co-culture model at all the tested time points which indicated a higher BBB passage ability of TNPs and CS-TNPs as compared with pure TMZ. When TNPs and CS-TNPs were compared, the transport ratio was found to be more for CS-TNPs which may be due to the conjugation of CS with TNPs that facilitated the transport of TNPs across BBB apart from CD44 receptor targeting; CS also facilitates BBB crossing [26]. In case of monoculture model, similar results were seen as in the co-culture model. But when transport ratio of CS-TNPs across the co-culture model was compared with the monolayer model, the ratio was found to be lesser, which may be due to the formation of a tight junction in the co-culture model [19].

In vitro cell cytotoxicity assay

The MTT assay was performed to assess cell cytotoxicity of TMZ, TNPs, and CS-TNPs. The obtained results are shown in Fig. 3c. The results indicated concentration-dependent suppression of cell viability. As compared with TMZ, TNPs and CS-TNPs demonstrated more suppression of cell viability. After 24 h at 100-μg/ml concentration, TMZ showed 64.0% ± 2.0% cell viability while TNPs and CS-TNPs demonstrated 50.5% ± 2.1% and 38.0% ± 1.0% cell viability, respectively. As compared with TMZ, the suppression in the cell viability was 1.27-fold and 1.68-fold higher for TNPs and CS-TNPs which indicated higher cytotoxic potential of prepared nanoparticles as compared with pure drug. CS-TNPs showed enhanced cell cytotoxicity as compared with TNPs which may be correlated with its higher cellular uptake and CD44 receptor targeting ability that led to higher suppression of cell growth. No significant change in cell cytotoxicity was seen after the incubation of cells for 72 h which may be due to slow drug release from nanoparticles and short half-life of TMZ [17].

Cell cycle analysis

The effect of TMZ, TNPs, and CS-TNPs on cell cycle is demonstrated in Fig. 4. TMZ causes cell cycle arrest in the G2/M phase [18]. In U87 MG cells, TMZ at a concentration of 100 μg/ml induced cell cycle arrest in the G2/M phase with

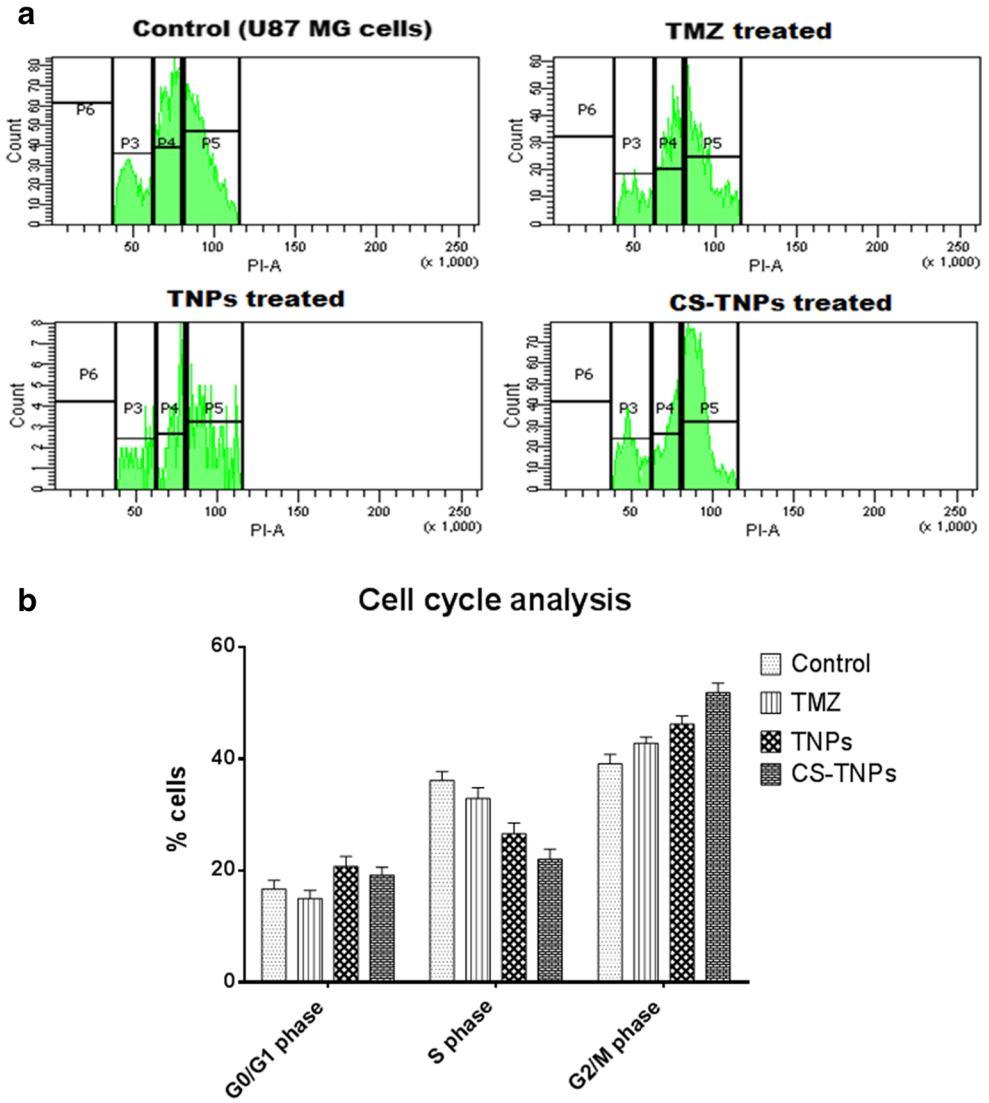

Fig. 4 Cell cycle analysis of control, pure TMZ, TNPs, and CS-TNPs on U87 MG cells (A) flow cytometry analysis using propidium iodide staining for cell cycle phase analysis. (B) Percentage cell distribution at different phases of cell cycle. Data are presented as mean ± SD (n = 3)

43.67% accumulation of cells which was approximately 1.17-fold higher as compared with control cells. TNPs and CS-TNPs induced 48.8% and 51.81% accumulation of cells in the G2/M phase respectively which was 1.25-fold and 1.33-fold higher respectively than untreated control cells. As compared with pure drug, higher accumulation of cells in the G2/M phase was observed in both TNPs and CS-TNPs which suggested that both caused significant inhibition of cell growth. When percent cell accumulation in the G2/M phase after treating with TNPs and CS-TNPs was compared, CS-TNPs demonstrated higher cell cycle arrest which may be correlated with CD44 receptor-mediated higher uptake of CS-TNPs than TNPs. This higher uptake of CS-TNPs led to increased concentration of loaded TMZ inside the cells which caused enhanced cell cycle arrest in the G2/M phase and indicated higher suppression of cell growth. The observed results were also similar with previous findings in which the authors reported the G2/M phase cell cycle arrest by TMZ-loaded nanoparticles [18].

Cellular uptake and cellular uptake mechanism

Cellular uptake of FITC-tagged TNPs and CS-TNPs was qualitatively assessed by confocal microscopy and uptake was clearly seen in the confocal image (Fig. 5). As compared with TNPs, higher uptake of CS-TNPs took place which may be due to the presence of CS over the surface of TNPs. U87 MG cells are CD44 receptors positive cell line. The surface modification of TNPs with CS facilitated the CD44 receptor-mediated uptake of CS-TNPs and led to a higher uptake than TNPs [26]. To further verify this, cellular uptake mechanism was also studied.

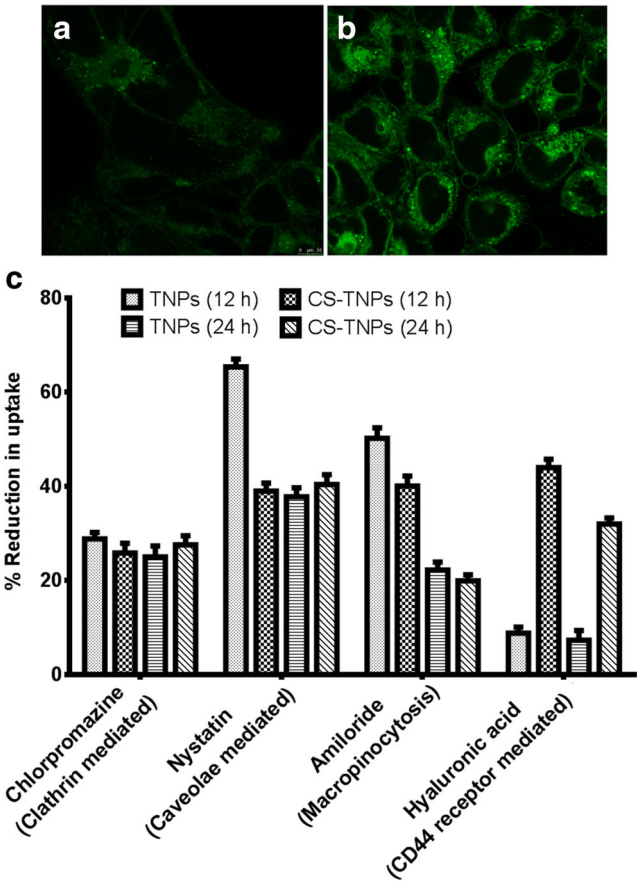

Fig. 5 Cellular uptake of (**a**) TNPs and (**b**) CS-TNPs in U87 MG cells and (**c**) elucidation of cellular uptake mechanism. Data are presented as mean ± SD ($n = 3$)**Fig. 5** Cellular uptake of (**a**) TNPs and (**b**) CS-TNPs in U87 MG cells and (**c**) elucidation of cellular uptake mechanism. Data are presented as mean ± SD ($n = 3$)

Various receptor poisons were used to study the uptake mechanism in which chlorpromazine, nystatin, amiloride, and HA were used to inhibit clathrin, caveolae, macropinocytosis, and CD44 receptor-mediated uptake, respectively [19]. The results (Fig. 5) indicated that in the presence of chlorpromazine, the cellular uptake of TNPs was significantly reduced to 26.7% ± 3.4% and 23.0% ± 2.3% after 12-h and 24-h incubation, respectively, while in the presence of nystatin, reduction in uptake was 63.5% ± 4.7% and 35.7% ± 4.9% after 12 h and 24 h, respectively. In the presence of amiloride, reduction in cellular uptake after 12 h and 24 h was found to be 49.2% ± 4.2% and 20.2% ± 1.7%. Cellular uptake of CS-TNPs in the presence of chlorpromazine was significantly reduced to 25.8% ± 1.4% and 27.6% ± 2.3% after 12-h and 24-h incubation, respectively, while in the presence of nystatin, reduction in uptake was 39.0% ± 3.7% and 40.4% ± 3.9% after 12 h and 24 h, respectively. Reduction in cellular uptake after 12 h and 24 h in the presence of amiloride was found to be 40.1% ± 3.2% and 19.9% ± 1.7%. From the results, it can be concluded that reduction in uptake was maximum when nystatin (caveolae pathway inhibitor) was used; so caveolae-mediated endocytosis may be involved in the uptake of TNPs and CS-TNPs across the U87 MG cell monolayer. The obtained results were also in accordance with previously reported literature [27]

To verify the CD44 receptor-mediated uptake of CS-TNPs, CD44 receptor blocking assay using excess amount of HA (10 mg/ml) as CD44 receptor inhibitor was used. The results revealed (Fig. 5) a significant reduction in cellular uptake of CS-TNPs in HA-treated U87 MG cells as before CD44 receptor blocking, uptake was higher. Free HA as an inhibitor hindered the binding of CS-TNPs with the receptor, so after 12 h and 24 h, the percent reduction in cellular uptake of CS-TNPs was found to be 44.0% ± 1.4% and 32.0% ± 1.8%, respectively, which confirmed the CD44-mediated uptake of CS-TNPs in U87 MG cells. As the uptake of TNPs was not CD44-mediated, after CD44 receptor blockage, no significant reduction in the uptake of TNPs was observed.

From all the obtained results, we can conclude that cellular uptake and internalization of CS-TNPs were predominantly by caveolae-mediated endocytosis and CD44 receptor-mediated uptake.

Estimation of ROS generation

To assess the ROS generation potential of TNPs and CS-TNPs, we used the DCF assay. Basically, H_2DCFDA is a non-fluorescent dye, and after entering the cells, it firstly gets hydrolyzed by the esterase into DCFH which was further oxidized into DCF in the presence of intracellular reactive oxygen species. This DCF is a fluorescent compound and its intensity of fluorescence is used as a marker for investigating the extent of oxidative stress [28]. Based on this principle, the ROS-generation potential of developed TNPs and CS-TNPs in U87 MG cells was estimated and compared with the ROS of pure TMZ. The results as shown in Fig. 6 demonstrated concentration-dependent ROS generation of TNPs and CS-TNPs. The untreated cells (negative control) did not show any ROS generation while TMZ, TNPs, and CS-TNPs demonstrated higher ROS generation as compared with the positive control (H_2O_2). The TNPs and CS-TNPs indicated 2.57-fold and 4.55-fold increase in ROS generation, respectively, as compared with pure TMZ. The obtained results may be correlated with the fact that increase in concentration of TNPs and CS-TNPs led to increased concentration of released TMZ leading to increase in ROS generation. CS-TNPs showed higher ROS generation as compared with pure TMZ and TNPs. This may be due to higher uptake of CS-TNPs via the CS-mediated CD44 receptor which led to increased TMZ concentration in the cells that ultimately caused increased ROS generation that led to oxidative stress to the cells, inhibited the cell proliferation, and caused cell death.

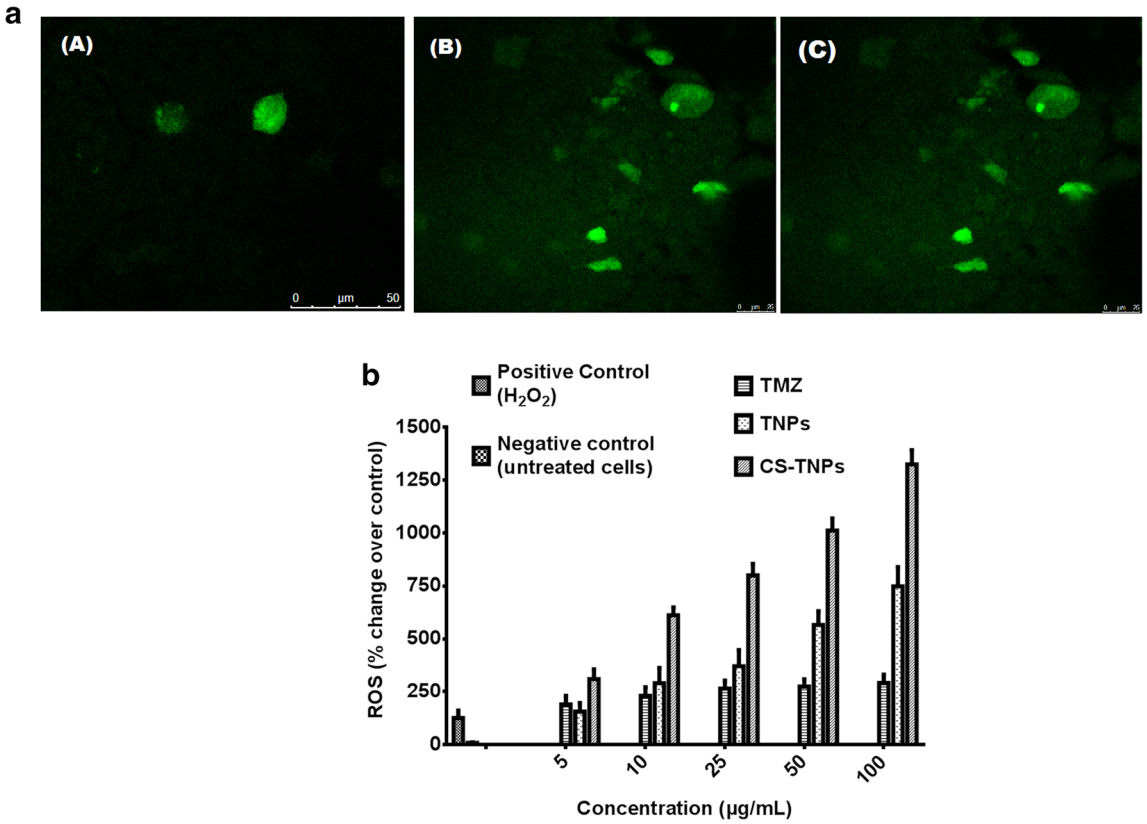

Fig. 6 (**A**) ROS generation of (A) TMZ, (B) TNPs, and (C) CS-TNPs in U87 MG cells and (**B**) elucidation of ROS generation. Data are presented as mean ± SD ($n = 3$)

In vivo pharmacokinetic study

The results of pharmacokinetic study of TMZ, TNPs, and CS-TNPs are shown in Fig. 7a. After intravenous administration of CS-TNPs, significant enhancement in mean plasma drug concentration was observed as compared with TMZ and TNPs (Table 2). TMZ showed Cmax of 4.91 ± 0.11 μg/ml at 0.5 h, and TMZ concentration was maintained up to 12 h. The Cmax of TNPs and CS-TNPs was observed as 2.27 ± 0.12 μg/ml and 3.47 ± 0.15 μg/ml at a Tmax of 3.0 h and 6.0 h respectively. As compared with TNPs and CS-TNPs, TMZ was quickly removed from the circulation. No TMZ was detected after 12 h, while TNPs and CS-TNPs were still present in the plasma until 72-h post-injection of TMZ, TNPs, and CS-TNPs. The difference in obtained results of TMZ and nanoparticles (TNPs and CS-TNPs) may be due to slow diffusion of TMZ from nanoparticles which continued for more than 72 h [16]. Student's *t* test showed significant differences in the mean concentration of TMZ in plasma after IV administration of pure TMZ, TNPs, and CS-TNPs at all time points. TNPs

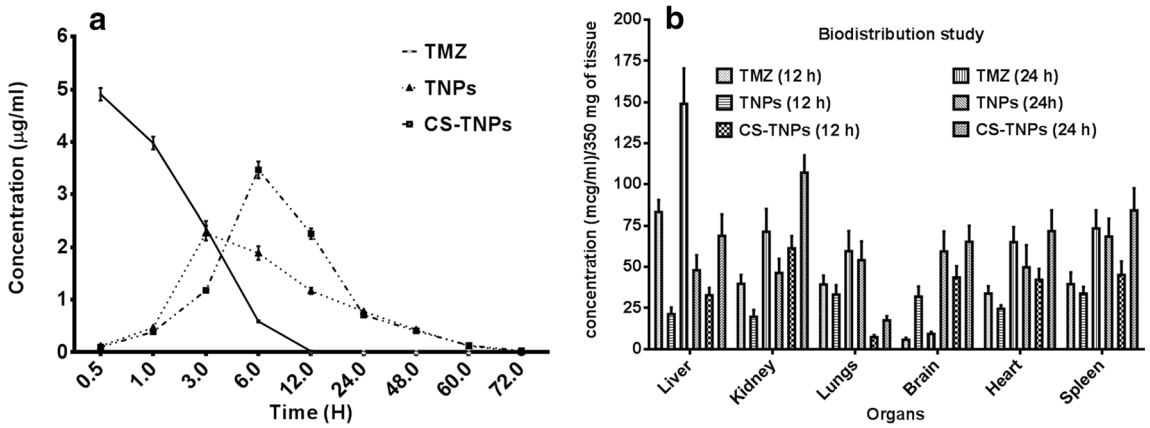

Fig. 7 **a** In vivo pharmacokinetic study: plasma concentration-time profile of TMZ, TNPs, and CS-TNPs after intravenous injection in rats ($n = 6$) and **b** biodistribution pattern of TMZ, TNPs, and CS-TNPs in different organs of a rat. Data are presented as mean ± SD ($n = 6$)

Table 2 Pharmacokinetic parameters of TMZ, TNPs, and CS-TNPs estimated in rats

Parameters	TMZ	TNPs	CS-TNPs
C_{max} (μg/ml)	4.91 ± 0.11	2.27 ± 0.12	3.47 ± 0.15
T_{max} (H)	0.5	3.0	6.0
AUC	17.58 ± 2.15	48.67 ± 3.13	61.37 ± 3.12
$t_{1/2}$ (H)	1.29 ± 1.07	4.42 ± 1.50	6.36 ± 1.34
MRT (H)	2.33 ± 1.25	20.50 ± 2.10	18.45 ± 2.14

**TMZ* temozolomide, *TNPs* temozolomide-loaded bovine serum albumin nanoparticles, *CS-TNPs* chondroitin sulfate-modified TNPs, *Cmax* maximum plasma concentration, *Tmax* time at maximum plasma concentration, *AUC* area-under-the-curve, *t1/2* half-life, *MRT* mean residence time

Data represented as mean ± SD ($n = 6$)

and CS-TNPs showed significant enhancement in the pharmacokinetic profile of TMZ as compared with plain drug solution, in terms of Area Under Curve (AUC), half-life ($t_{1/2}$), and mean residence time (MRT). The AUC of TNPs and CS-TNPs was approximately 2.8-fold and 3.5-fold higher than pure TMZ, respectively, while the $t_{1/2}$ of TMZ was approximately 3.4-fold and 4.9-fold increased when administered as TNPs and CS-TNPs. Enhancement in $t_{1/2}$ may be due to the small particle size of TNPs and CS-TNPs. The small particle size significantly reduces the affinity of macrophages, thus prolonging the $t_{1/2}$ of TMZ in vivo [29]. The $t_{1/2}$ prolongation was more in CS-TNPs as compared with TNPs which may be due to the presence of CS over TNPs creating a barrier for the drug release and prolonging the release of drug. The MRT of TNPs and CS-TNPs was found to be 8.8-fold and 7.9-fold higher, respectively, than pure TMZ which demonstrated long circulating properties of the nanoparticles [16]. All obtained results can also be correlated with the metabolic pattern of TMZ in vivo. IV-administered TMZ got quickly metabolized and degraded in physiological pH. However, when administered in nanoparticles (TNPs and CS-TNPs), they acted as a reservoir for TMZ, provided sustained release, and decreased direct contact of the drug with blood which reduced its metabolism and degradation, leading to prolonged MRT and higher AUC [1, 30]. From all these results, it may be concluded that TNPs and CS-TNPs enhanced the activity of TMZ by enhancing its half-life, bioavailability, and circulating properties.

Biodistribution study

The quantitative biodistribution study of TMZ, TNPs, and CS-TNPs was performed to assess the passage of TMZ

Table 3 Biochemical parameters estimation after IV administration of TMZ, TNPs, and CS-TNPs after 7 days

Parameters	Control	TMZ	TNPs	CS-TNPs
HB%	15.18 ± 0.22	14.19 ± 0.35	14.80 ± 0.44	14.96 ± 0.35
RBC $*10^3$/cmm	8.93 ± 0.87	8.21 ± 0.23	8.42 ± 0.71	8.35 ± 0.47
WBC$*10^3$/cmm	11.28 ± 1.54	10.47 ± 0.89	10.80 ± 2.03	11.02 ± 0.64
PLT$*10^5$/cmm	5.11 ± 0.63	4.83 ± 0.37	5.03 ± 1.77	4.98 ± 0.39
N%	55.7 ± 5.57	54.25 ± 3.12	54.95 ± 2.28	55.01 ± 5.72
E%	0.68 ± 0.25	0.64 ± 0.13	0.69 ± 0.54	0.68 ± 0.05
L%	35.27 ± 2.47	34.32 ± 1.77	35.75 ± 3.17	34.90 ± 3.75
M%	0.93 ± 0.13	0.87 ± 0.12	0.92 ± 0.32	0.88 ± 0.02
PCV%	49.5 ± 3.61	48.3 ± 7.12	48.4 ± 5.99	49.15 ± 5.88
Bil (mg/dl)	0.37 ± 0.01	0.35 ± 0.11	0.37 ± 0.11	0.36 ± 0.02
SGOT (IU/L)	201.9 ± 21.54	198.5 ± 18.3	200.8 ± 22.5	199.7 ± 24.1
SGPT (IU/L)	147.5 ± 19.80	146.9 ± 21.4	152.5 ± 17.6	151.8 ± 19.0
ALK (IU/L)	134.7 ± 18.90	133.9 ± 17.6	133.7 ± 18.1	137.9 ± 21.7
PRO (g/dl)	8.13 ± 1.18	7.93 ± 1.33	7.97 ± 1.16	8.05 ± 1.19
ALB (g/dl)	3.24 ± 0.49	3.11 ± 0.73	3.14 ± 0.49	3.21 ± 0.49
GLB (g/dl)	4.21 ± 0.39	4.18 ± 0.31	4.18 ± 0.15	4.20 ± 0.41
BUN (mg/dl)	12.35 ± 1.12	12.12 ± 2.18	12.15 ± 1.70	12.51 ± 1.92
CREAT (mg/dl)	1.37 ± 0.31	1.36 ± 0.23	1.35 ± 0.81	1.36 ± 0.41

**TMZ* temozolomide, *TNPs* temozolomide-loaded bovine serum albumin nanoparticles, *CS-TNPs* chondroitin sulfate-modified TNPs, *HB* hemoglobin, *RBC* red blood cells, *WBC* white blood cells, *PLT* platelet, *N* neutrophils, *E* eosinophils, *L* lymphocytes, *M* monocytes, *PCV* packed cell volume, *Bil* bilirubin, *SGOT* serum glutamic-oxaloacetic transaminase, *SGPT* serum glutamic pyruvic transaminase, *ALK* alkaline phosphatase, *ALB* albumin, *GLB* globulin, *BUN* blood urea nitrogen, *CREAT* creatinine

Data is represented as mean ± SD ($n = 6$)

Table 4 Stability studies of lyophilized TNPs and CS-TNPs

Time (month)	Particle size (nm)		Zeta potential (mV)		% Assay
	TNPs	CS-TNPs	TNPs	CS-TNPs	CS-TNPs
At refrigerated condition (4 °C)					
0	160.6 ± 2.87	222.3 ± 1.57	− 35.3 ± 1.5	− 32.8 ± 1.87	100.0 ± 1.50
1	159.3 ± 1.48	225.5 ± 3.81	− 35.3 ± 1.3	− 31.6 ± 2.5	99.22 ± 1.53
2	158.1 ± 2.37	228.8 ± 2.87	− 34.8 ± 2.8	− 31.3 ± 1.9	98.43 ± 2.91
3	157.7 ± 3.51	230.5 ± 2.53	− 34.1 ± 1.5	− 30.5 ± 2.3	97.49 ± 2.11
At room temperature (25 °C ± 2 °C and 65% ± 5% relative humidity)					
0	160.6 ± 2.87	222.3 ± 1.57	− 35.3 ± 1.5	− 32.8 ± 1.87	100.0 ± 1.50
1	159.1 ± 3.17	227.6 ± 3.67	− 36.1 ± 3.5	− 31.4 ± 2.9	98.70 ± 2.43
2	157.8 ± 4.29	232.1 ± 2.35	− 35.7 ± 2.9	− 30.6 ± 3.3	98.15 ± 1.86
3	157.5 ± 5.47	238.5 ± 4.87	− 34.2 ± 3.5	− 30.1 ± 4.3	97.37 ± 2.49

**TNPs* temozolomide-loaded bovine serum albumin nanoparticles, *CS-TNPs* chondroitin sulfate-modified TNPs
Data is represented as mean ± SD (n = 3)

through the BBB and its distribution in various vital organs, viz., the brain, liver, heart, lungs, kidney, and spleen after intravenous injection via tail veins. The obtained results are demonstrated in Fig. 7b. The distribution of TMZ in the brain was approximately 6-fold (31.9 ± 6.30 μg/ml) and 9-fold higher (43.5 ± 6.87 μg/ml) with TNPs and CS-TNPs, respectively, as compared with free TMZ (5.7 ± 1.21 μg/ml). This may be due to enhanced BBB permeability, passive targeting ability of TNPs, and receptor-mediated targeting along with the passive targeting ability of CS-TNPs. When CS-TNPs were compared with TNPs, higher brain distribution of TMZ was observed which may be due to surface modification of TNPs with CS. As mentioned earlier, CS also plays role in enhancing BBB permeation; the presence of CS over the nanoparticles facilitated the BBB crossing which led to enhanced concentration of drug in the brain [26]. The obtained results showed correlation with in vitro BBB permeation study of CS-TNPs, where permeation of TMZ was enhanced by 2-fold. The results indicated enhanced permeation of drug through the tight junctions of the BBB when given as nanoparticles.

Further, the results revealed significant reduction in the distribution of drug to highly perfused organs when given as nanoparticles (TNPs and CS-TNPs). This may be attributed to surface modification of nanoparticles that prevented opsonization [16]. After 24 h, TMZ released from TNPs and CS-TNPs was more or less similar in the spleen and heart, whereas in the liver and lungs, distribution was significantly decreased as compared with pure TMZ. This may be due to reduced opsonization and decreased passive accumulation of drug in case of lungs [16] and due to hydrophilicity of nanoparticles in case of liver [31]. As compared with TNPs, more accumulation of CS-TNPs in the liver was observed which may be due to the presence of hydrophilic polymer (CS) over TNPs which enhanced their hydrophilicity. CS-TNPs showed much lesser accumulation of TMZ in the lungs as compared with TMZ and TNPs. Distribution of CS-TNPs was high in the kidney as compared with free TMZ and TNPs which may be also due to more hydrophilicity of CS-TNPs than TMZ and TNPs [32, 33].

In vivo toxicity study

The in vivo toxicity of prepared TNPs and CS-TNPs was demonstrated by single-dose IV administration in rats. The estimated biochemical parameters are summarized in Table 3. Even at 30 mg/kg TMZ (highest dose), no animal died or showed any abnormalities up to 7 days. The suppression of immune cells (white blood cells, neutrophils, monocytes) were lesser in CS-TNPs-treated rats as compared to TMZ and TNPs treated rats which may be due to sustained release of TMZ from CS-TNPs. The results also demonstrated no significant changes in the blood parameters (red blood cells, hemoglobin) and serum enzyme marker levels (bilirubin, serum glutamic-oxaloacetic transaminase, serum glutamic pyruvic transaminase, alkaline phosphatase, albumin, globulin, blood urea nitrogen, creatinine) in TNPs- and CS-TNPs-treated rats and were found to be closely similar to non-treated control rats. These results revealed minimal toxicity of the drug toward normal cells after encapsulation in TNPs and CS-TNPs and indicated as safe for administration. Similar studies were also reported by Kumari et al. 2017, where drug-related toxicity was minimized after encapsulating in nanoparticles.

Stability studies

The results of stability studies (table 4) indicated no significant change in particle size, % assay and zeta potential of prepared TNPs and CS-TNPs at both refrigerated condition and room temperature for 3 months which indicated their stability.

Conclusions

In the present work, temozolomide-loaded chondroitin sulfate-modified albumin nanoparticles (CS-TNPs) were fabricated for efficient tumor internalization to target brain tumor. The developed nanoparticles were characterized and evaluated for various physicochemical properties like particles size, PDI, zeta potential, morphology, drug release, and stability. The results demonstrated that TNPs and CS-TNPs both have the ability to improve the therapeutic efficacy of TMZ after encapsulation in nanoparticles. As compared with TNPs, CS-TNPs showed better tumor-targeting efficiency in cell line studies. The BBB permeability study confirmed the BBB crossing ability of CS-TNPs and the uptake study indicated higher accumulation of CS-TNPs in the tumor cells via caveolae-mediated endocytosis and CD44 receptor targeting. In vivo pharmacokinetic and biodistribution studies revealed improvement in pharmacokinetic profile and therapeutic concentration of TMZ in the brain. The biodistribution and toxicity data suggested safety of developed nanoparticles as accumulation of TMZ in vital organs other than the brain decreased and no significant changes were seen in biochemical parameters of rats treated with the developed nanoparticles. Finally, it may be concluded that CS-TNPs are promising carriers to deliver TMZ to the brain for targeted therapy of brain tumor.

Acknowledgments The authors would like to thank Cipla Ltd, Mumbai for providing gift sample of temozolomide and Dr. Vikram Sarabhai Institute of Cell and Molecular Biology, Maharaja Sayajirao University of Baroda for providing necessary cell line facilities. The authors would also like to thank the Indian Institute of Technology (IIT) Bombay and Indian Institute of Science Education and Research (IISER) Mohali for providing TEM and XRD facility, respectively.

Funding The authors would like to thank DST- INSPIRE, New Delhi, India for providing financial support in the form of INSPIRE fellowship to Ritu Kudarha.

Compliance with ethical standards

Conflict of interest The authors declare that they have no conflict of interest.

Human and animal rights and informed consent All animal experimental procedures were reviewed and approved by the Institutional Animal Ethics Committee and CPCSEA (Committee for the Purpose of Control and Supervision of Experiments on Animals), New Delhi, India with registration no IAEC/2018-19/1830.

References

1. Lopes IC, de Oliveira SCB, Oliveira-Brett AM. Temozolomide chemical degradation to 5-aminoimidazole-4-carboxamide – electrochemical study. J Electroanal Chem. 2013;704:183–9.
2. Khan A, Imam SS, Aqil M, Ahad A, Sultana Y, Ali A, et al. Brain targeting of temozolomide via the intranasal route using lipid-based nanoparticles: brain pharmacokinetic and scintigraphic analyses. Mol Pharm. 2016;13:3773–82.
3. Lee CY. Strategies of temozolomide in future glioblastoma treatment. Onco Targets Ther. 2017;10:265–70.
4. Kudarha RR, Sawant KK. Albumin based versatile multifunctional nanocarriers for cancer therapy: fabrication, surface modification, multimodal therapeutics and imaging approaches. Mater Sci Eng C Mater Biol Appl. 2017;81:607–26.
5. Elzoghby AO, Samy WM, Elgindy NA. Albumin-based nanoparticles as potential controlled release drug delivery systems. J Control Release. 2012;157:168–82.
6. Yewale C, Baradia D, Vhora I, Misra A. Proteins: emerging carrier for delivery of cancer therapeutics. Expert Opin Drug Deliv. Taylor & Francis. 2013;10:1429–48.
7. Agrawal S, Dwivedi M, Ahmad H, Chadchan SB, Arya A, Sikandar R, et al. CD44 targeting hyaluronic acid coated lapatinib nanocrystals foster the efficacy against triple-negative breast cancer. Nanomedicine. 2018;14:327–37.
8. Liu P, Chen N, Yan L, Gao F, Ji D, Zhang S, et al. Preparation, characterisation and in vitro and in vivo evaluation of CD44-targeted chondroitin sulphate-conjugated doxorubicin PLGA nanoparticles. Carbohydr Polym. 2019;213:17–26.
9. Lo Y-L, Chou H-L, Liao Z-X, Huang S-J, Ke J-H, Liu Y-S, et al. Chondroitin sulfate-polyethylenimine copolymer-coated superparamagnetic iron oxide nanoparticles as an efficient magneto-gene carrier for microRNA-encoding plasmid DNA delivery. Nanoscale. 2015;7:8554–65.
10. Zhao L, Liu M, Wang J, Zhai G. Chondroitin sulfate-based nanocarriers for drug/gene delivery. Carbohydr Polym. 2015;133:391–9.
11. Kamali M, Dinarvand R, Maleki H, Arzani H, Mahdaviani P, Nekounam H, et al. Preparation of imatinib base loaded human serum albumin for application in the treatment of glioblastoma. RSC Adv. 2015;5:62214–9.
12. Bishnoi M, Jain A, Hurkat P, Jain SK. Aceclofenac-loaded chondroitin sulfate conjugated SLNs for effective management of osteoarthritis. J Drug Target. 2014;22:805–12.
13. Oueslati N, Leblanc P, Harscoat-Schiavo C, Rondags E, Meunier S, Kapel R, et al. CTAB turbidimetric method for assaying hyaluronic acid in complex environments and under cross-linked form. Carbohydr Polym. 2014;112:102–8.
14. Huang D, Chen Y-S, Rupenthal ID. Hyaluronic acid coated albumin nanoparticles for targeted peptide delivery to the retina. Mol Pharm. 2017;14:533–45.
15. Fang C, Wang K, Stephen ZR, Mu Q, Kievit FM, Chiu DT, et al. Temozolomide nanoparticles for targeted glioblastoma therapy. ACS Appl Mater Interfaces. 2015;7:6674–82.
16. Jain D, Bajaj A, Athawale R, Shrikhande S, Goel PN, Nikam Y, et al. Surface-coated PLA nanoparticles loaded with temozolomide for improved brain deposition and potential treatment of gliomas: development, characterization and in vivo studies. Drug Deliv. 2016;23:999–1016.
17. Ananta JS, Paulmurugan R, Massoud TF. Temozolomide-loaded PLGA nanoparticles to treat glioblastoma cells: a biophysical and cell culture evaluation. Neurol Res. 2016;38:51–9.
18. Ananta JS, Paulmurugan R, Massoud TF. Nanoparticle-delivered antisense MicroRNA-21 enhances the effects of temozolomide on glioblastoma cells. Mol Pharm. 2015;12:4509–17.
19. Pandey A, Singh K, Patel S, Singh R, Patel K, Sawant K. Hyaluronic acid tethered pH-responsive alloy-drug nanoconjugates for multimodal therapy of glioblastoma: an intranasal route approach. Mater Sci Eng C Mater Biol Appl. 2019;98:419–36.
20. Song X, Xie L, Wang X, Zeng Q, Chen TC, Wang W, et al. Temozolomide-perillyl alcohol conjugate induced reactive oxygen

species accumulation contributes to its cytotoxicity against non-small cell lung cancer. Sci Rep. 2016;6:1–10.
21. Jain DS, Bajaj AN, Athawale RB, Shikhande SS, Pandey A, Goel PN, et al. Thermosensitive PLA based nanodispersion for targeting brain tumor via intranasal route. Mater Sci Eng C Mater Biol Appl. 2016;63:411–21.
22. Semete B, Booysen L, Lemmer Y, Kalombo L, Katata L, Verschoor J, et al. In vivo evaluation of the biodistribution and safety of PLGA nanoparticles as drug delivery systems. Nanomedicine. 2010;6:662–71.
23. Bharti N, Harikumar SL, Buddiraja A. Development and characterization of albumin nanoparticles for pulmonary drug delivery. World J Pharm Sci. 2014;3(1):86–92.
24. Abraham J. International conference on harmonisation of technical requirements for registration of pharmaceuticals for human use. In: Tietje C, Brouder A, editors. Handbook of Transnational Economic Governance Regimes. Brill | Nijhoff; 2010 [cited 2020 Sep 5]. p. 1041–53. Available from: https://brill.com/view/book/edcoll/9789004181564/Bej.9789004163300.i-1081_085.xml.
25. Bagari R, Bansal D, Gulbake A, Jain A, Soni V, Jain SK. Chondroitin sulfate functionalized liposomes for solid tumor targeting. J Drug Target. Taylor & Francis. 2011;19:251–7.
26. Lo Y-L, Sung K-H, Chiu C-C, Wang L-F. Chemically conjugating polyethylenimine with chondroitin sulfate to promote CD44-mediated endocytosis for gene delivery. Mol Pharm. 2013;10:664–76.
27. Chen Z, Chen J, Wu L, Li W, Jun C, Cheng H, et al. Hyaluronic acid-coated bovine serum albumin nanoparticles loaded with brucine as selective nanovectors for intra-articular injection. Int J Nanomedicine. 2013;8:3843.
28. Rakotoarisoa M, Angelov B, Garamus VM, Angelova A. Curcumin- and fish oil-loaded spongosome and cubosome nanoparticles with neuroprotective potential against H2O2-induced oxidative stress in differentiated human SH-SY5Y cells. ACS Omega. 2019;4:3061–73.
29. Shen Y, Li W. HA/HSA co-modified erlotinib-albumin nanoparticles for lung cancer treatment. Drug Des Devel Ther. 2018;12:2285–92.
30. Zhang H, Huang N, Yang G, Lin Q, Su Y. Bufalin-loaded bovine serum albumin nanoparticles demonstrated improved anti-tumor activity against hepatocellular carcinoma: preparation, characterization, pharmacokinetics and tissue distribution. Oncotarget. 2017;8:63311–23.
31. Mishra V, Mahor S, Rawat A, Gupta PN, Dubey P, Khatri K, et al. Targeted brain delivery of AZT via transferrin anchored pegylated albumin nanoparticles. J Drug Target. 2006;14:45–53.
32. Gao J, Wang Z, Liu H, Wang L, Huang G. Liposome encapsulated of temozolomide for the treatment of glioma tumor: preparation, characterization and evaluation. Drug Discov Ther. 2015;9:205–12.
33. Kumari S, Ahsan SM, Kumar JM, Kondapi AK, Rao NM. Overcoming blood brain barrier with a dual purpose temozolomide loaded lactoferrin nanoparticles for combating glioma (SERP-17-12433). Sci Rep. 2017;7:6602.

Materials Science & Engineering C 81 (2017) 607–626

Contents lists available at ScienceDirect

Materials Science & Engineering C

journal homepage: www.elsevier.com/locate/msec

Review

Albumin based versatile multifunctional nanocarriers for cancer therapy: Fabrication, surface modification, multimodal therapeutics and imaging approaches

Ritu R. Kudarha, Krutika K. Sawant*

Pharmacy Department, The Maharaja Sayajirao University of Baroda, India

ARTICLE INFO

Keywords:
Human serum albumin
Nanoconjugates
Nanoparticles
Prodrugs
Gene delivery
Photothermal and photodynamic therapy

ABSTRACT

Albumin is a versatile protein used as a carrier system for cancer therapeutics. As a carrier it can provide tumor specificity, reduce drug related toxicity, maintain therapeutic concentration of the active moiety like drug, gene, peptide, protein etc. for long period of time and also reduce drug related toxicities. Apart from cancer therapy, it is also utilized in the imaging and multimodal therapy of cancer. This review highlights the important properties, structure and types of albumin based nanocarriers with regards to their use for cancer targeting. It also provides brief discussion on methods of preparation of these nanocarriers and their surface modification. Applications of albumin nanocarriers for cancer therapy, gene delivery, imaging, phototherapy and multimodal therapy have also been discussed. This review also provides brief discussion about albumin based marketed nano formulations and those under clinical trials.

1. Introduction

Cancer is a deadly and life threatening disease with high mortality rate worldwide. According to GLOBOCAN, it caused 8.2 million deaths in 2012 [1]. The most common cancer deaths were due to lung cancer (1.6 million deaths), liver cancer (745,000 deaths), and stomach cancer (723,000 deaths) [2]. This high mortality rate may be due to several reasons like late diagnosis and detection of cancer, inability of therapeutic moiety to reach the tumor site, adverse and toxic effects towards the normal cells etc. [3]. The current strategy for the treatment of cancer lies in chemotherapy, radiotherapy, hormonal therapy and surgery. The existing conventional chemotherapy has several draw backs like less concentration of therapeutic moiety to the tumor site, less target specificity, toxicity towards normal cells and tissues, inability to cross different biological barriers like blood brain barrier, and drug and dosage form related factors which includes less solubility, less permeability, poor dissolution, less stability (photo, thermal and pH stability), degradation of drug, variable drug release from dosage form, multi drug resistance etc. [4,5].

So there is a need to develop novel delivery system which has ability to overcome all these drawbacks of conventional chemotherapy. In past several decades, nanoparticles have gained lots of attention for treatment of cancer. Nanoparticles have potential to overcome the drawbacks of conventional cancer chemotherapy because of unique properties like small size, surface charge, variable shape, several binding sites for the attachment of target specific ligands, antibodies, peptides etc. They can also enhance the tumor targeting by both passive and active targeting mechanism. Passive targeting is possible due to enhanced permeability and retention (EPR) effect [6,7]. Nanoparticles based delivery systems are also approved by the FDA for clinical use (Abraxane, Doxil, Genexol-PM, DepoCyt, Myocet etc.) and many more are in the clinical trials (NK105, CYt-6091, Genexol-PM, Rexin-G etc.) [6,8]. As compared to conventional chemotherapy, nanoparticles based delivery systems have several advantages and features, including: 1) improved delivery of poorly water soluble drugs, peptides, and genes; 2) better protection of drugs, peptides or genes from harsh environments (e.g., enzymatic degradation and the highly acidic environment in the lysosomes or stomach); 3) enhanced treatment efficiency and reduced systemic side effects by cell or tissue specific targeted delivery of drugs, peptides or genes; 4) overcome multidrug resistance by co delivery of drugs, peptides, genes and/or diagnostic agents; 5) stimuli-responsive systems (pH sensitive, temperature sensitive, redox sensitive) can control release of drugs, peptides or genes over a manageable period of time at precise doses [6,9].

Nanoparticles used as a carrier for cancer therapeutics may be of several types viz. protein based nanoparticles (albumin nanoparticles, gelatin nanoparticles etc.) [10,11], polymer based nanoparticles (poly lactide co glycolide nanoparticles, polycaprolactone nanoparticles,

* Corresponding author.
E-mail address: dr_krutikasawant@rediffmail.com (K.K. Sawant).

http://dx.doi.org/10.1016/j.msec.2017.08.004
Received 20 June 2017; Received in revised form 13 July 2017; Accepted 2 August 2017
Available online 03 August 2017

polylactide nanoparticles, chitosan nanoparticles etc.) [12–15], lipid based nanoparticles (solid lipid nanoparticles, nanostructured lipid carriers, liposomes etc.) [16–18], lipid polymer hybrid nanoparticles [19], metal nanoparticles [20–22], polymeric micelles (cationic micelles, unimolecular micelles, dual responsive and triple responsive micelles etc.) [23–31], dendrimers [32] etc. Among all these nanoparticles, protein based nanoparticles have gained much more attention in cancer therapy due to unique properties viz. relatively safe and easy to prepare, capability to deliver proteins, peptides, genes, nucleic acid, and hydrophilic as well as hydrophobic anticancer molecules, site specific targeting by surface modification, greater stability profile during storage, etc. [33]. In this review, albumin based nanocarriers and their role in cancer therapy have been discussed in detail.

2. Albumin

Albumin is a protein based macromolecule and the most abundant plasma protein (35–50 g/L human serum) of human blood which is synthesized in the liver at the rate of approximately 0.7 mg/h for every gram of liver (10–15 g daily) [34,35]. It is nontoxic, biodegradable, biocompatible, highly water soluble, non-immunogenic, easy to purify and stable plasma protein [36].

2.1. Types of albumin

Albumins are of various type viz. Ovalbumin (OVA), bovine serum albumin (BSA), human serum albumin (HSA), rat albumin etc. Commercially, albumins are obtained from egg white, bovine serum and human serum. Apart from these, it can also obtained from soybeans, milk and grains [36].

Ovalbumin (OVA) is monomeric phosphoglycoprotein obtained from egg white and is utilized in designing food matrix as it is a food protein. It has molecular weight of 4.7 kDa, isoelectric point (pI) of 4.8 and consists of 385 amino acid residues, with each molecule having one internal disulfide bond and four free sulphydryl groups and has 3D structure with helical reactive loop arrangement. It is used as a drug delivery carrier due to its properties like low cost, easy availability, emulsion and foam stabilization ability, pH and temperature sensitive properties [36,37].

Bovine serum albumin (BSA) is obtained from bovine serum and has a molecular weight of 6.93 kDa with pI of 4.7 in water at 25 °C. It is a water soluble monomeric protein that consists of 583 amino acid residues and contains 17 disulfide bonds resulting in nine loops formed by the bridges, one cysteine and 8 pairs of disulfide bonds. It also contains high content of aspartate (Asp), glutamic acid (Glu), alanine (Ala), luciene (Luc) and lysine (Lys). It is also used as a drug carrier because of its low cost, ease of purification, unusual ligand binding properties, biocompatibility, biodegradability, non-toxicity, lesser immunogenicity (as compared to OVA and rat albumin) and wide acceptance in pharmaceutical industry [36,38].

Human serum albumin (HSA) is heart shaped monomeric globular protein obtained from human serum. It consists of 585 amino acid residues and contains 17 disulfide bridges and 1 sulfhydryl group which is formed by cysteinyl (Cys35) residues. It contains single tryptophan residue (Trp 214) and one free cysteine (Cys34) and high amount of glutamic acid, arginine, and lysine. HSA contains negative charge due to presence of more acidic amino residue as compared to basic amino acid. Disulfide bridges provide stability and longer biological half life (~19 days). It has similar properties as BSA and is also used as a versatile carrier for drugs, genes, hormones, peptides and several other molecules [36,39].

HSA and BSA are homologous proteins and share 76% sequential identity. The major difference between the two is with respect to the number and positioning of tryptophan residues in them. HSA has only one tryptophan, located at position 214 which is equivalent to Trp-212 for BSA present buried in a hydrophobic pocket at sub domain IIA. BSA has one more additional tryptophan Trp-134, which is more exposed to solvent and found at sub domain IB. As compared to other albumins, HSA is more non immunogenic plasma protein due to which it is widely used as a safe and effective carrier protein in different delivery systems [40,41].

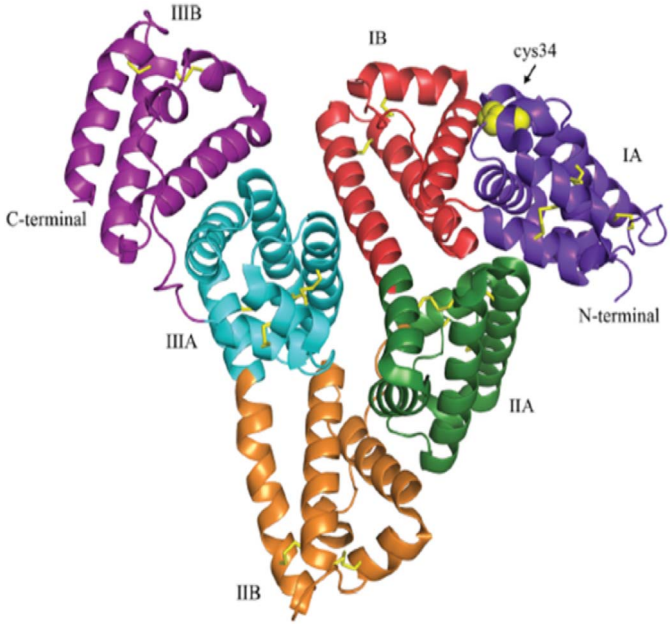

Fig. 1. Structure of human serum albumin.

2.2. Structure of albumin

The three dimensional (3D) structure of HSA (Fig.1), shown by X-ray crystallography, proposed that HSA molecule is formed from three homologous domains I, II and III which themselves contain two separate helical sub-domains A (4 α-helices) and B (6 α-helices) [35]. A heart shaped albumin with 67% α-helix and no β sheet is very stable to changes in pH, denaturating solvents and exposure to heat because it contains 17 disulfide bonds and one free thiol from an unpaired cysteine (Cyc34) in domain I [42].

2.3. Binding sites in albumin

HSA has two main binding sites namely, Sudlow site I (present in sub-domain IIA) and Sudlow site II (present in sub-domain IIIA). Bulky heterocyclic anions such as anticoagulant drug warfarin bind to site I and aromatic carboxylates such as diazepam bind to site II. Apart from these two binding sites, albumin also contains other binding sites like Cys34 (binding site for Au(I), Hg(II) and complexed Pt(II) in the form of cisplatin, nitric oxide) and fatty acid binding sites. Cys34 site is also used to conjugate small molecules as well as protein and peptide based drugs [42]. Different ligand binding sites are summarized in Table 1.

3. Albumin based nanocarriers

Albumin is a versatile protein used as a carrier system for cancer therapeutics. As a carrier it can provide tumor specificity, reduce drug related toxicity, maintain therapeutic concentration of therapeutic moiety like drug, gene, peptide, protein etc. for long period of time and also reduce drug related toxicities. It also has the potential in the half life extension of drug. As albumin has various binding sites, ligand functionalized delivery of therapeutic moiety is also possible which can provide site specific delivery of the therapeutic moiety [11]. Two basic approaches are utilized in the development of albumin based cancer

Table 1
Different ligand binding sites present in albumin tertiary structure (modified from Sleep et al. [42]).

Sr. no.	Binding site	Location	Ligands	Notes
1.	N-terminal site	IA	Co (II), Ni(II) and Cu(II)	Consists of the 3 N-terminal amino acids, Asp-Ala-His
2.	Cys34	IA	Au(I), Hg(II), Pt(II) and NO	Cisplatin-binding site
3.	FA1	IB	Fatty acids, haem-Fe(III), bilirubin, hemin, synthetic Fe(II) porphoryrins and Al(III) phthalocyanines (tumor localizing photosensitisers) and prostaglandins	Low-affinity FA-binding site
4.	FA2	Between IA and IIA	Fatty acids	High-affinity FA-binding site
5.	MBS (also known as site A or cadmium site A)	I/II inter-domain contact region	Cu(II), Ni(II), Cd(II) and Zn(II)	Surrounded by FA1, FA2 and FA7
6.	FA7	IIA	Fatty acids, thyroxine, bulky heterocyclic anions such as warfarin, CMPF, phenylbutazone, tolbutamide, iodipamide and indomethacin	Major drug-binding site I, or Sudlow's site I, Low-affinity FA site
7.	FA6	Between IIA and IIB	Fatty acids	Low-affinity FA-binding site
8.	Met298	Between IIA and IIB	Cisplatin (Pt(II))-binding site	–
9.	FA3-FA4	DIIIA	Fatty acids, aromatic carboxylates, ibuprofen, diazepam, diflunisal, diclofenac, iopanoic acid and thyroxine	Major drug-binding site II, or Sudlow's site II. FA3 low affinity FA binding, while FA4 high-affinity FA binding
10.	FA5	IIIB	Fatty acids and thyroxine	High-affinity FA binding
11.	FA8-FA9	Between IA-IB-IIA and IIB-IIIA-IIIB	Fatty acids	Supplementary sites only. FA8 short-chain FA and FA9 induced during FA saturation
12.	Secondary MBS (site B or cadmium site B)	Currently not defined	Cd(II), Co(II), Mn(II) and Zn(II)	–

therapy system i.e. conjugation of therapeutic moiety directly to the albumin or formulation of nanoparticles incorporated with therapeutic moiety like drug, peptide, gene etc. Some of biological applications of albumin conjugates are: use as a reagent for immunoassay and immunohistochemistry, used for elucidating hormone receptor interactions and used in the treatment of various diseases like cancer, viral infection and diabetes [11,34]. Albumin based nanoparticles are utilized for cancer treatment as they are biodegradable, non-antigenic and can be also surface modified which may help in avoiding the undesirable toxicity of drugs by modifying their body distribution and improve their cellular uptake. They also have targeting potential because proteins themselves act as passive as well as active targeting moiety. Other targeting ligands can also attach in these carriers to provide site specificity [11]. Different albumin based carrier systems are depicted in Fig. 2 and their roles in the treatment of cancer will be discussed in subsequent sections of this review.

3.1. Albumin nanoparticles

Albumin nanoparticles can be prepared by several methods like desolvation, emulsification, thermal gelation, nano spray drying, nab technology and self-assembly etc. All preparation methods are summarized in Table 2. The selection of the method is based on several factors such as type of system, area of application, required size, type of drug (hydrophilic or hydrophobic), etc.

3.2. Albumin micelles

Protein derived copolymers are used in preparation of micelles (core/shell structure) in which core acts as a reservoir for drug or gene and hydrophilic side chains form shell that reduces nonspecific interactions, immunogenicity and antigenicity of proteins and peptides. These micelles are used for gene delivery, targeted anticancer drug delivery, surface engineered multimodal therapy etc. [48]. Wu et al. developed albumin copolymer micelles for delivery of doxorubicin in which polycationic albumin precursor protein cBSA-147 was used to formulate nanosized micelles and doxorubicin (DOX) was loaded by hydrophobic interaction with polypeptide scaffold. The obtained results showed higher drug cytotoxicity and cellular uptake as compared to free DOX and also higher pH dependent stability in various physiological buffers [48]. In another study, amphiphilic adriamycin-human serum albumin (HSA-ADR) conjugates were developed by Chen et al. This amphiphilic HSA-ADR conjugate self assembled into redox sensitive micelles like nanoparticles. These redox sensitive micelles showed higher in vitro cytotoxicity in gastric cancer cell line and also higher intra tumor accumulation as compared to HAS/ADR NPs. An in-vivo tumor suppression was also observed after i.v. administration which showed the promising potential of glutathione sensitive (redox) micelles in gastric cancer therapy [49]. Apart from drugs, proteins can be also delivered by the albumin based micelles to their target site. Jiang et al. prepared albumin (BSA) based polyionic complex micelles for protein delivery. Although BSA itself directly formed complex with the positively charged proteins and self assembled into nanoparticles, but these nanoparticles were not stable and aggregated into large particles after some days. To overcome this drawback, maleimide functionalized poly(oligo (ethylene glycol) methyl ether methacrylate) was conjugated with BSA and this was used to deliver Spry 1 by forming polyionic complexed micelles. These micelles showed improved cytotoxicity of Spry1 on the breast cancer cell lines (MCF7 and MDA-MB-23) and exhibited high anticancer efficacy by inhibiting the growth of three dimensional MCF-7 multicellular tumor spheroids [50]. The formed pegylated albumin based polyionic complex micelles also revealed their potential in gene delivery [51]. Jiang et al. also developed albumin micelles for drug delivery. They formulated albumin - poly(methyl methacrylate) (PMMA) conjugate which self assembled into micelles for delivery of curcumin [52].

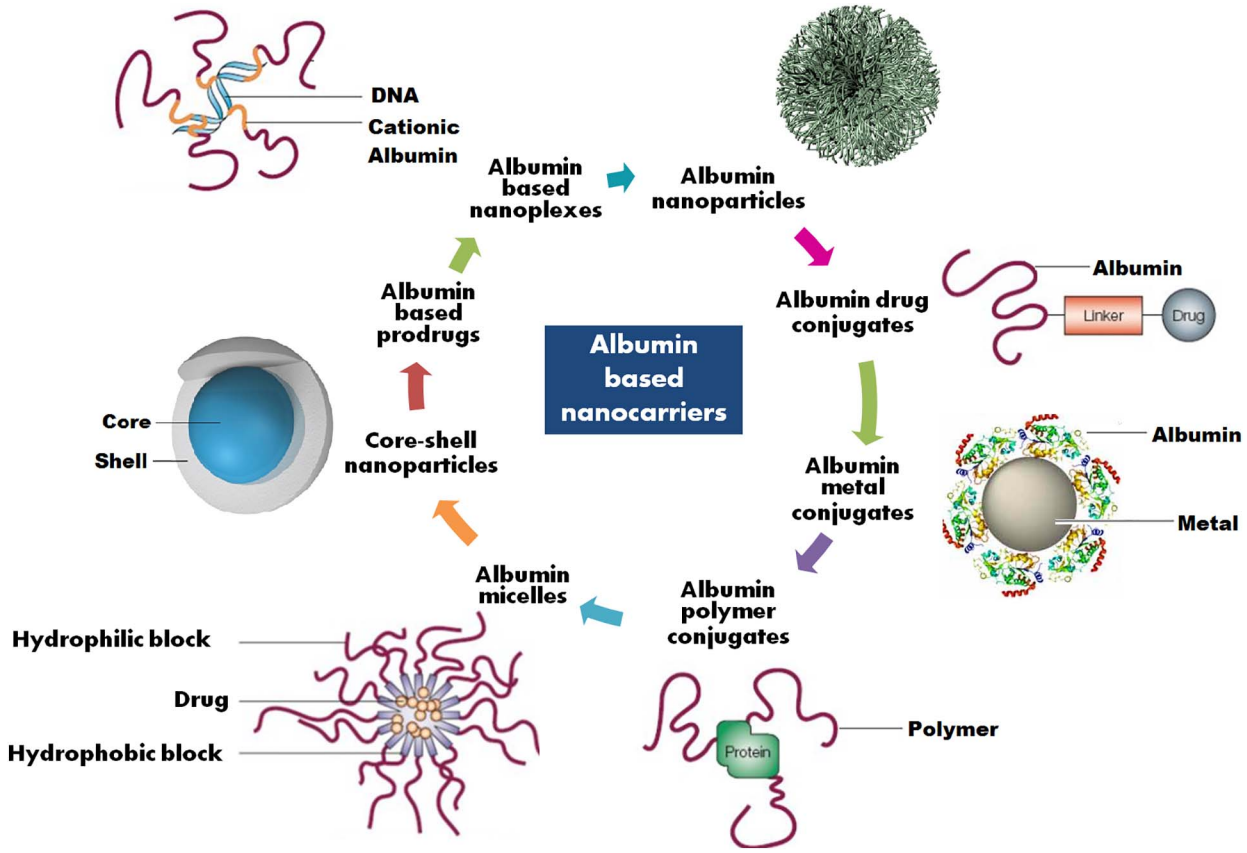

Fig. 2. Albumin based nanocarriers.

3.3. Albumin based nanoconjugates

Apart from nanoparticles, various albumin based nanoconjugates have also been investigated for drug and gene delivery in past few years. These nanoconjugates are formed by the interaction of albumin with different conjugation moieties like polymers, drugs, metals, DNA or RNA and known as albumin-polymer conjugate, albumin-drug conjugate, albumin-metal conjugate and albumin based nanoplexes respectively. These interactions may be of two types: either non covalent interaction or covalent interactions and are possible because of the unique structure of albumin as it has various binding sites (Fig. 3). The non-covalent interaction between albumin and conjugation moiety is because of hydrophobic and electrostatic interaction which act as driving force in the formation of albumin conjugates. Albumin contains different functional groups due to presence of different amino acid residues and these functional groups are utilized to prepare albumin based nanoconjugates by different chemical coupling reactions like thiol-maleimide coupling, Michael addition reaction and carbodiimide coupling reactions which form covalent bonds between the albumin and conjugation moiety. Such nanoconjugates are more stable as compared to nanoconjugates formed by non-covalent interactions. Among the various amino acid residues present in the albumin structure, cysteine (Cys) and lysine (Lys) residues are most widely explored targeting residues for the preparation of covalently conjugated albumin nanoconjugates [53].

3.3.1. Albumin based prodrugs and albumin-drug conjugates

Albumin based prodrugs and drug conjugates are widely used in cancer therapy. The unique properties of albumin like biodegradability, solid tumor accumulation ability, non-toxicity etc. makes it suitable drug carrier. Albumin also has different binding sites which can bind drugs by covalent or non-covalent bonding. Binding of drugs with albumin alters the properties of the drug molecule like toxicity profile, circulation half life and other pharmacokinetic properties [54]. Albumin-drug conjugate enhances the circulation half of drug due to long plasma half life (~19 days) of albumin in human body. Apart from this, it also overcomes the multi drug resistance of anticancer drugs [55]. On the basis of above mentioned properties of albumin-drug conjugates, lots of research work is carried out in last few years for the treatment of cancer and is also in clinical trials.

Many anticancer drugs like methotrexate (MTX), doxorubicin (DOX), cisplatin, oxaliplatin, carboplatin, docetaxel etc. were used to prepare albumin-drug conjugates. Stehle et al. prepared MTX-HSA conjugate for the treatment of cancer and this was the first albumin-drug conjugate that was under gone clinical trials. MTX-HSA conjugate was prepared by the direct coupling of MTX with the lysine residue of HSA and found to be more effective in targeting tumor [56,57]. 7-Ethyl-10-hydroxycamptothecin (SN38) - HSA conjugate was prepared by Sepeheri et al. to improve the solubility as well as tumor tissue targeting as compared to active form of SN38 by chemical coupling using carbodiimide chemistry (EDC/NHS) [55]. The results revealed better solubility and stability of SN38-HSA conjugate along with prolonged circulation time in blood as compared to free SN38. Esmaeili et al. developed docetaxel-albumin conjugate for enhancing the solubility and tumor targeting [58]. Apart from drugs, different dyes and photosensitizing agents have also been conjugated to albumin for cancer diagnosis and therapy. Jeong et al. prepared chlorin e6 (Ce6) conjugated HSA nanoparticles for photodynamic therapy. Ce6-HSA conjugate was prepared by the carbodiimide chemistry using EDC/NHS. This conjugate was able to form self-assembled nanoparticles which upon illumination with specific wavelength light produced singlet oxygen which damaged the target tumor cells in cell culture. The in vivo results also revealed superior biodistribution of Ce6-HSA conjugate at the tumor site as compared to free Ce6 [59].

Table 2
Methods of preparation of albumin based nanoparticles [36,37,41–47].

Sr. no.	Method	Key factors/variables	Advantages	Disadvantages
1.	Desolvation 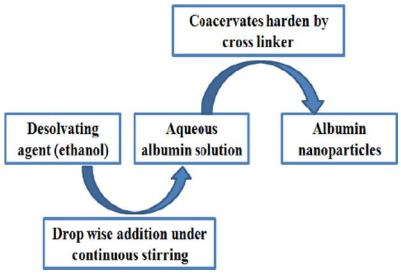	• Albumin concentration • pH of albumin solution • Aqueous phase: Desolvating agent volume ratio • Rate of addition of desolvating agent • Amount of cross linker • Stirring speed • Stirring time • Solvent polarity	• Most accepted method • Robust • Reproducible • No surfactant required • Used for encapsulation of hydrophilic molecule.	• Chemical cross linking agent may cause toxicity • Require removal of organic solvent
2.	Emulsification 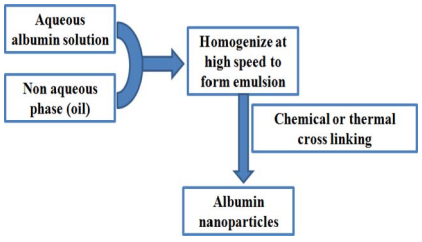	• Albumin concentration • Aqueous phase: oil phase volume ratio • Rate of addition of emulsion • Emulsification time • Speed of homogenizer • Heating temperature for thermal stabilization • Amount of surfactant • Type of surfactant • Amount of cross linker	• Hydrophobic drugs can be entrapped • Both chemical as well as thermal stabilization methods can be used for stabilization of nanoparticles	• Require organic solvent • Require removal of oily residue and surfactant • Chemical cross linking agent may cause toxicity • Require high temperature for crosslinking • Larger particle size than desolvation method
3.	Thermal gelation 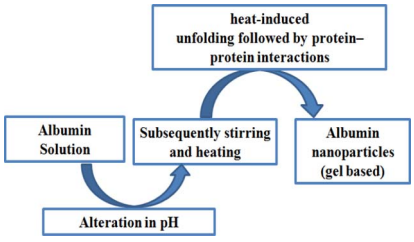	• pH • Temperature • Protein concentration • Ionic strength • Nature and concentration of other solids	• Used for fabrication of nano hydrogels	• Thermolabile drugs cannot be used • Require high temperature
4.	Nano spray drying 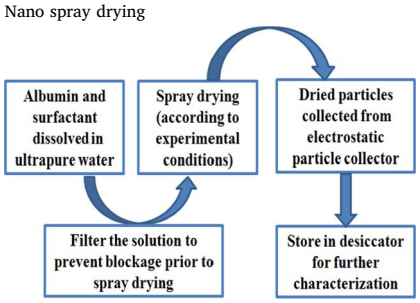	• Albumin solution concentration • Surfactant concentration • Drying air flow rate • Inlet temperature • Spray mesh size • Organic solvent content of spray solution	• Single step • Continuous and scalable method • Final drying not required • High reproducibility • High encapsulation efficiency • Cost effective • Also overcome biopharmaceutical disadvantage of drug	• Large particle size • Higher processing time • Highly viscous polymer solution can't be use because of small diameter of orifice of spray nozzle • Crust may contaminate fine particles • Mechanical shear can alter the properties of shear sensitive substance • Require high temperature
5.	Nab-technology 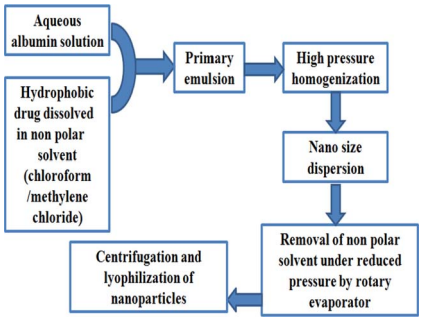	• Albumin solution concentration • Aqueous phase: organic phase volume ratio • Homogenization time • Homogenization cycle • Homogenization pressure	• No surfactant required • No denaturation of albumin • High loading of poorly water soluble drugs • Nanoparticles formed are safe and suitable for intravenous use of hydrophobic drug	

Different prodrugs have been designed to target the cancer cells that utilized endogenous albumin as drug carrier. These prodrugs are designed in such a way that binds rapidly and selectively to the cysteine-34 position (Cys-34) of circulating serum albumin after administration because approximately 70% of blood circulating albumin is mercaptalbumin containing an accessible Cys-34 [34]. Many platinum based prodrugs have been designed to selectively bind with the serum albumin for cancer treatment. Zheng et al. designed Pt (IV) prodrugs to bind non-covalently to HSA for drug delivery. In this study, axial ligand of cisplatin was asymmetrically functionalized by two different groups i.e. succinate and an unbranched aliphatic carbamate. Optimized compound of this study (compound 4e) bound with serum albumin non-covalently and after conversion of active form demonstrated 9 to 70 time better anticancer activity than parent compound cisplatin in lung

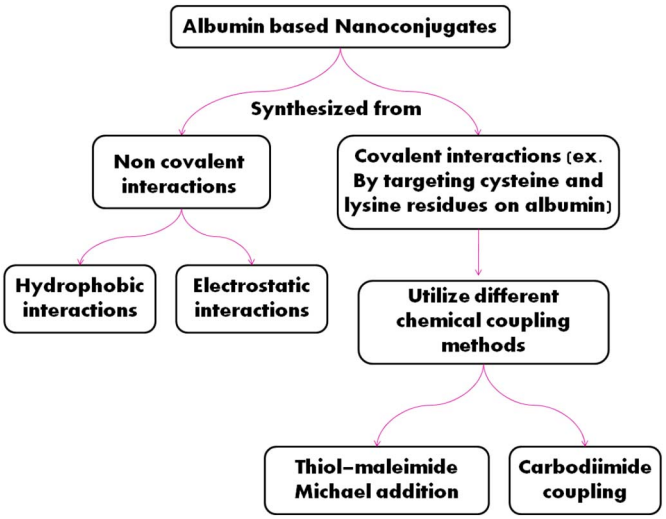

Fig. 3. Interactions involved in the synthesis of albumin based nanoconjugates.

and ovarian cancer cell lines along with prolonged half life (6.8 h) in blood as compared to cisplatin (t1/2 ~ 20 min) or satraplatin (t1/2 ~ 6 min). This prodrug compound (compound 4e) was interacted with the biological reductants, present in the cancer cells, which convert it into Pt(II) form. This Pt(II) form further interacted with DNA and causes DNA damage, cell cycle arrest and apoptosis [60]. In another study, Mayr et al. prepared oxaliplatin prodrugs to bind with HSA and improve the anticancer activity. Prodrugs were designed by the functionalization of the maleimide group in the parent compound which converted the Pt (II) form of oxaliplatin to Pt (IV) prodrug. Apart from oxaliplatin, cisplatin prodrug was also prepared with the same functional moiety and results were compared. The results indicated the faster reduction of cisplatin analogue as compared to oxaliplatin analogues. Apart from the reducibility, tumor-targeting potential of the albumin-bound drugs 24 h after i.v. administration also varied which may be due to different reducibility of the drugs. All these results revealed the potential of prodrug of oxaliplatin in enhancing plasma half life of drug by avoiding fast renal clearance and better tumor accumulation of the drug due to EPR effect [61]. Apart from the platinum based prodrugs, ferric prodrugs have also been designed to interact with serum albumin and targeting cancer. Qi et al. designed the ferric prodrug based on N-donor residues (Lys199 or/and His242) of human serum albumin (HSA) carrier IIA subdomain for cancer treatment. They synthesized six Fe (III) compounds derived from 2-hydroxy-1-naphthaldehyde thiosemicarbazone and compared their potential alone as well as after binding with the HSA. Among these compounds, compound 12 and compound 12-HSA complex demonstrated better in vivo performance. As compared to compound 12, compound 12-HAS complex exhibited better targeting ability and activity in liver cancer [62]. All these results suggest that HSA carrier prodrug strategy for intravenous administration of novel anticancer compounds may be a promising approach for targeted cancer therapy.

In the development of albumin based prodrugs and albumin-drug conjugates, several factors may affect the activity of the compound. The major factors are: molar ratio of drug and albumin, structure and stereochemistry of the drug, nature of the drug and substitution moiety etc. For example, presence of hydrophobic moiety in the drug may enhance the affinity of drug to bind with the serum albumin which leads to stabilization of the drug-albumin conjugate [47,59].

3.3.2. Albumin-polymer conjugates

Apart from tremendous advantageous properties, some draw backs are also associated with albumin that restrict its use in drug delivery such as lack of intrinsic targeting group, limited proteolytic stability and lesser suitability for hydrophilic and charged drugs [63,64]. These drawbacks can be overcome by conjugating albumin with another polymer. Similar to albumin-drug conjugates and other protein polymer hybrids, albumin-polymer conjugates can be prepared either by chemical conjugation using covalent or non-covalent conjugation strategies or simply by the physical attachment of different polymers with albumin. Interactions between albumin and polymers are possible because of the presence of various active groups present on the surface of albumin like amino (Lys residues), carboxyl (Asp and Glu residues) and thiol (Cys residue). As compared to non-covalent conjugation strategy, covalent conjugates of albumin-polymer are more stable under physiological conditions. But on the basis of preparation method, non-covalent conjugation methods are relatively simple and flexible [47,64]. There are two basic techniques for preparing the albumin-polymer conjugates: 1) conjugation of polymer to albumin by various coupling reactions like maleimide coupling, carbodiimide chemistry etc. [65] and 2) in-situ polymerization method (atom transfer radical polymerization (ATRP), reversible addition fragmentation chain transfer polymerization (RAFT), ring opening polymerization (ROP) etc.) [65–68]. Albumin-polymer conjugates have been prepared by conjugating several polymers like polyethylene glycol (PEG) and its derivatives [69], poly(methyl methacrylate) (PMMA) [66,70], poly (lactide co glycolide) (PLGA) [71], poly(N-isopropylacrylamide) (PNIPAAm) [68], poly(ε-caprolactone) (PCL) [65], hydroxyethylacrylate (HEA) [67] etc. Albumin-polymer conjugates based nanoparticles can be prepared by different methods like self assembly, coating/conjugation of polymer over the albumin nanoparticles and vice-versa [65,70,71] and have been extensively explored in the treatment of cancer. Dag et al. developed polymer-albumin conjugate for the delivery of macromolecular platinum drugs and its effectiveness was tested against the ovarian cancer. In their study, two monomers N-(2-hydroxypropyl)methacrylamide (HPMA) and Boc protected 1,3-diaminopropan-2-yl acrylate (Ac-DAP-Boc) were copolymerized using RAFT polymerization to form macromolecular ligand and this was further conjugated with the platinum drug. This polymer-platinum conjugate was further conjugated with albumin to form self assembled core (polymer-platinum)-shell (albumin) nanoparticles having the size of 80 nm. Albumin coated polymer-platinum conjugate was readily taken up by the ovarian cancer cells and demonstrated superior toxicity as compared to albumin coating free polymer-platinum conjugate [72]. In another study, Liu et al. prepared DOX-encapsulated cetuximab-functionalized BSA–PCL nano vesicle as a tumor-targeted nanocarrier. BSA-PCL conjugates were synthesized by maleimide–sulfhydryl coupling reaction. DOX-encapsulated cetuximab-functionalized BSA–PCL nano vesicle showed enhanced antitumor activity as compared to free DOX [65]. Camptothecin (CPT) encapsulated BSA-PMMA nanoparticles were prepared by the simple nanoprecipitation method and showed enhanced anti-tumor activity both in vitro and in animals [70].

3.3.3. Albumin-metal conjugates (albumin coated inorganic nanoparticles)

Inorganic nanoparticles are widely used in the drug delivery system not only for delivering the active moiety but also for diagnostic and imaging application because of their unique optical, magnetic and other properties. For target specificity, effective bioavailability and colloidal stability of these inorganic nanoparticles, surface modification with suitable targeting moiety or biocompatible moiety is necessary [47,73]. Albumin coated inorganic nanoparticles have been explored extensively because of the unique properties of albumin. It provides the stability, enhanced circulation and better accumulation of inorganic nanoparticles to the desired target site and can also provide target specificity due to the presence of reactive surface functional groups for the attachment of targeting ligands [74]. Chen et al. developed pH-/H_2O_2-Responsive albumin-MnO_2 Nanoparticles for combinational cancer therapy to modulate tumor hypoxia. To prevent the decomposition of MnO_2 nanoparticles in acidic environment, premodified HSA either with Ce6 or with c,t,c-[$Pt(NH_3)2$-$(O_2CCH_2CH_2COOH)(OH)Cl_2$] (cis-Pt

(IV)SA), as pro-drug of cis-platinum, were used which acted as a template and coating molecules to induce the formation of MnO_2 nanoclusters through biomineralization in alkaline conditions, obtaining multicomponent HSA-MnO_2-Ce6 & Pt (HMCP) nanoparticles. These HMCP nanoparticles acted as a multimodal therapeutic system in which pH-/H_2O_2-responsive behaviors of MnO_2 simultaneously generated O_2 in situ by reaction with endogenous H_2O_2 inside the tumor and overcame the tumor hypoxia-associated resistance of photodynamic therapy. On the other side, HMCP nanoparticles within the acidic tumor microenvironment were gradually degraded into individual therapeutic albumin-drug complexes with small sizes (< 10 nm) and exhibited greatly enhanced intratumoral permeability for improved effectiveness in combined photodynamic and chemotherapy [75]. Attachment of albumin with the inorganic nanoparticles can alter the biological behavior like cellular uptake of nanoparticles, blood circulation time, higher penetration and retention of nanoparticles in the tumor cells etc. and these were also verified by different studies [47,74,76–79].

4. Surface modification of albumin nanocarriers

Surface modification of protein based nanocarriers is necessary to alter the surface properties and enhance the targeting potential of the delivery system. Presence of different binding sites and functional groups like carboxyl and amino groups on albumin offers several possibilities for surface modification of albumin based nanocarriers. Surface modification of albumin nanocarriers with the specific ligand can be done by conjugating functional group of albumin with the ligand by covalent bond. For surface modification of albumin nanocarriers, electrostatic adsorption or surface coating techniques may be utilized as non-covalent attachment of ligands. In surface modified albumin nanocarrier, albumin plays a role of carrier for delivering therapeutic moiety whereas the ligand is used to modify the pharmacokinetic parameters, improve stability, prolonging circulation half life, modifying the release pattern of therapeutic moiety or as a targeting agent [11,36]. For the surface modification of protein based systems, different ligation strategies are utilized viz. thiol–maleimide Michael addition ligation, biotin/avidin ligation, carbodiimide coupling strategy and disulfide bridging [80].

4.1. Ligands as a targeting agent

Various ligands like small molecules, carbohydrates, peptides, proteins or antibodies have been utilized for targeting of different nanocarriers. These act as receptor mediated targeting ligand for cancer treatment because several receptors like folate (FR), transferrin (TfR), epidermal growth factor receptor (EGFR), and lipoprotein receptors etc. are over expressed in the cancer cells and these ligands bind with the receptor and shows their action [80]. Some examples of ligand conjugated albumin nanoparticles for targeted delivery in cancer are summarized in Table 3.

4.1.1. Small molecules

Small molecules like folate and biotin are widely used as targeting ligand for cancer cell targeting because of their easy availability, inexpensiveness, ease in handling and flexibility in chemical modification and characterization [80]. Folic acid, FR binding ligand, is an inexpensive and non-immunogenic small molecule having molecular weight of 44 Da. Folate conjugated drugs or biomarkers retain their ability to bind specifically with FR because of the high stability of folate over a wide range of temperatures and pH values [92]. It significantly binds with the glycosylphosphatidylinositol-linked FR which is over expressed (100–300 times higher than those observed in normal tissues) in different cancerous cells [80]. Folate conjugated proteins like albumin are selectively internalized into cytoplasm by receptor mediated endocytosis and promotes cellular uptake of therapeutic moiety like drug into cancerous cells [93]. Biotin is another vitamin used to target the cancer cells. It is basically cell growth promoter and present in significantly higher concentration in the cancer cells as compared to normal cells. Biotin receptors are also over expressed on the cancer cell surface because rapid proliferation occurs in cancer cells which need a higher quantity of biotin so it can also be utilized as a cancer targeting ligand [94].

4.1.2. Carbohydrates

Carbohydrate molecules (galactose, lactose and mannose) specifically bind to asialoglycoprotein receptors (membrane lectin receptors) commonly found in liver cells and are used for targeting hepatic and cervical cancer cells [95]. Hyaluronic acid which is a polysaccharide is also used as ligand for CD44 receptor mediated cancer targeting [96,97].

4.1.3. Peptides

Integrin receptors ($\alpha_v\beta_3$) (membrane receptor for extracellular matrix ligands) are over expressed on the cancer cells surface and in tumor proliferating neovascular endothelial cells while lesser expressed in normal quiescent endothelial cells. These integrin receptors are very well targeted by the use of peptides. Among the various peptides, cyclic arginine-glycine-aspartic acid (RGD) is mostly used to target cancer cells because of high affinity to $\alpha_v\beta_3$ integrin which can enhance cellular uptake and prolong retention of drug in the cancer cells [80,83]. Some examples are mentioned in Table 3. Apart from RGD, other peptides like cell penetrating peptide (i.e. TAT), tumor homing peptide like CREKA and LyP-1 are also used in the targeted delivery of albumin based carrier for cancer [98].

Table 3
Ligand conjugated albumin nanoparticles for targeted delivery in cancer.

Albumin based architecture	Ligand	Ligand category	Formulation method	Morphology	Size (nm)	Target cancer	Ref.
HSA-biotin	Biotin	Small molecule	Cross linked HSA with EDC	Nanoparticles	125–145	Breast and cervical	[81]
BSA-lysine-galactose	Galactose	Carbohydrate	Desolvation/crosslinking	Nanoparticles	180–200	Liver	[82]
HSA-PEG-cyclic RGD	Cyclic RDG	Peptide	Self assembly	Micelles	30	Skin	[83]
BSA-cyclic RGD	Cyclic RDG	Peptide	Desolvation/crosslinking	Nanoparticles	130	Pancreas	[84]
HSA-PEG-anti-HER-2 Mab	Anti-HER-2 MAb	MAb	Desolvation/crosslinking	Nanoparticles	390–410	Breast	[85]
HSA-PEG-anti-HER-2 Mab	Anti-HER-2 MAb	MAb	Desolvation/crosslinking	Nanoparticles	220	Breast	[86]
HSA-PEGDI17E6/IgG	DI17E6 MAb	Mab	Desolvation/crosslinking	Nanoparticles	165–180	Skin	[87]
FA-BSA-SPIO NPs	Folate	Small molecule	Chemical coprecipitation then coating of BSA	Albumin-magnetic nanoparticles	–	Brain tumor (MRI imaging)	[88]
Cationic and Mannose modified HSA	Mannose	Carbohydrate	High-pressure homogenization	Nanoparticles	90.3	Brain tumor	[89]
cRGD conjugated HSA	Cyclic RGD	Peptide	Nab technology	Nanoparticles	160	Pancreatic	[90]
Glycyrrhetinic acid-BSA	Glycyrrhetinic acid	Carbohydrate	Desolvation	Nanoparticles	258.8	Hepato-cellular carcinoma	[91]

4.1.4. Proteins

Proteins like transferrin, lactoferrin and Apolipoprotein E (Apo E) bind with the transferrin receptor, lactoferrin receptor and low density lipoprotein receptor respectively. These ligands are used for brain targeting because of over expression in blood brain barrier also. Apo E and transferrin conjugated HSA nanoparticles loaded with loperamide were also prepared for brain targeting. The results indicated higher concentration of drug after the conjugation of these ligands with HSA nanoparticles in the brain [99–102]. Zhigui et al. prepared lactoferrin-modified polyethylene glycol grafted BSA nanoparticles as a dual targeting system for gliomas. Results showed higher permeability and cellular uptake in both primary brain capillary endothelial cells (BCECs) and glioma cells (C6) [103].

4.1.5. Monoclonal antibody (MAb)

MAbs (Y-shaped proteins) have been also utilized as a ligand for tumor targeting because of their unique properties like higher affinity ($K_d \sim 0.1$ nM) even with a low density and ability to recognize a specific part of their target [104]. Different MAbs used as ligands for tumor targeting are: anti-CD3 MAb, Herceptin, EGFRMAb, DI17E6 MAb, anti FAS MAb, anti-antigen rich breast cancer cells MAb, AMB8LK MAb, anti-CD20 MAb, anti-CEA MAb etc. [80]. MAb functionalized albumin nanocarriers are also summarized in Table 3.

4.2. Ligands as pharmacokinetic parameter modifier

Surfactants like polysorbate 80 (Tween 80), poloxamer etc. are used to alter the pharmacokinetics of the formulation. These surfactants are coated over the surface of the nanoparticles which significantly reduces various toxicities of the drug [11]. This can be explained by tween 80 coated DOX loaded HSA nanoparticles. Coating of tween 80 significantly reduced the toxicities (hematological, cardiac and testicular) of DOX which may be due to alteration of pharmacokinetic properties of drug [36,105–107].

4.3. Ligands as circulation half life enhancer

Polyethylene glycol (PEG) coating or chemical coupling, known as pegylation, to protein or particles (the delivery system) is used to improve the circulation half life and reduce the immunogenicity. It also enhances the accumulation of carrier system in the tumor because of EPR effect [108]. Methoxy PEG2000 was used for the pegylation of BSA nanoparticles. In vivo pharmacokinetic studies demonstrated long circulation time and higher uptake and cytotoxicity of doxorubicin in both primary brain capillary endothelial cells (BCECs) and glioma cells (C6) [103]. Moreover, pegylation also modified the release of drug from the nanoparticles. The release of 5-Flurouracil from methoxy PEG-succinimididyl propionate modified BSA nanoparticles was much slower than non-pegylated nanoparticles due to presence of mPEG which acted as a barrier to drug diffusion [108]. Pegylation of HSA nanoparticles were done by conjugation of two different PEG: poly (thioetheramido acid) poly (ethylene glycol) and methoxy poly (ethylene glycol) [109]. The loading of Rose Bengal in HSA-mPEG nanoparticles was much lesser as compared to unmodified HSA due to lesser drug-protein binding sites in modified HSA. The drug release from the modified HSA was also slow due to steric stabilization of nanoparticles provided by PEG which prevented the enzymatic degradation of nanoparticles [109].

4.4. Ligands used to modify the drug release and stability of nanocarrier

Different polymers are used to modify the drug release from the albumin based carrier and to stabilize them. The polymers can be chemically or physically attached with the albumin which potentially alters the properties of albumin like solubility, biocompatibility etc. and enhances its stability. These polymers can be either coated on the surface of the nanocarrier or conjugated with the albumin prior to the preparation of nanocarrier [64]. A large number of polymers viz. PEG, PLGA, PCL, PLA cationic polymers like polyethylenimine (PEI), poly-L-lysine (PLL), thermoreversible and thermosensitive polymers like poly (N-isopropylacrylamide) (PNIPAAm), poly(methylmethacrylate) (PMMA) etc. have been exploited to alter the drug release and stability of nanocarriers [64,110–117]. Cationic polymers are mainly used to alter the release behavior of drug from the nanocarriers. These are used to retard and control the drug release which depends on the concentration of coated polymer [11]. Zhang et al. prepared bone morphogenetic protein − 2 (BMP-2) encapsulated PEI coated BSA nanoparticles and study results showed release alteration due to PEI [118,119]. As PEI is a cationic polymer, surface charge of BSA nanoparticles shifted towards the neutral or slightly negative side and facilitated in vivo application of nanoparticles due to reduced opsonization and improved stability of system [119]. In another study, PEI coating over the HSA nanoparticles improved the therapeutic index of DOX against MCF-7 breast cancer cells because PEI coating enhanced cellular uptake of the particles [120]. PLL is another cationic polymer used to coat the albumin based nanocarriers. PLL coating enhances the nanoparticles stability by providing proteolytic resistance. This was reported for SiRNA encapsulated BSA nanoparticles in which stability of nanoparticles in aqueous solution was improved with increasing PLL molecular weight and concentration [11,121]. Apart from cationic polymers, thermoresponsive polymers are also used for controlling the release of encapsulated therapeutic active from the albumin nanocarrier. Poly (N-isopropylacrylamide)-*block*-polyallylamine (PNIPAM-AAm-b-PAA) conjugated albumin nanospheres were developed by Shen et al. to control the release of adriamycin. The results indicated that as compared to unconjugated nanoparticles, release of adriamycin from conjugated nanoparticles in trypsin solution was slower and decreased with increasing the conjugation amount or molecular weight of PNIPAM-AAm-b-PAA. This may be due to steric stabilization of nanoparticles which makes the degradation of unconjugated nanoparticles more difficult [122,123].

5. Role of albumin and albumin nanocarriers in cancer therapy

Albumin has been widely explored for cancer diagnosis and therapy due to its unique properties like biocompatibility, biodegradability, non-toxicity and low immunogenicity [36]. Albumin accumulates in the malignant tumor tissue/cells because of leaky vasculature and impaired (absent or defective) lymphatic drainage system of tumor cells. These properties of tumor cells enhance the accumulation of albumin in tumor by EPR effect [124–126]. Albumin or albumin nanocarrier binds with gp60 (60 kDa glycoprotein also known as albondin) receptors over-expressed on epithelium wall of tumor blood vessels. This ligand-receptor binding initiates transcytosis and leads to formation of invagination at the surface of membrane and ultimately form caveolae (transcytotic vesicles). Then fusion of these caveolae with the plasma membrane takes place by the extra vascular deposition and passing through other side of cell followed by release of albumin into the extracellular space (tumor interstitium). In the tumor interstitium, SPARC (secreted protein, acidic and rich in cysteine) are over expressed which enhance the accumulation of albumin inside the tumor by providing a mediated albumin transport pathway to the subendothelial space [127]. The process of accumulation of albumin-drug complex in the solid tumor is demonstrated in the Fig. 4.

5.1. Albumin nanocarriers for cancer therapy

Albumin based nanoparticles are widely explored protein based nanocarriers for cancer therapy. Several categories of drugs can be encapsulated in albumin via covalent conjugation, electrostatic interaction or hydrophobic interaction. This makes albumin a versatile drug delivery carrier. Apart from this, its accumulation in the tumor also makes it suitable candidate for cancer therapy. Different albumin based

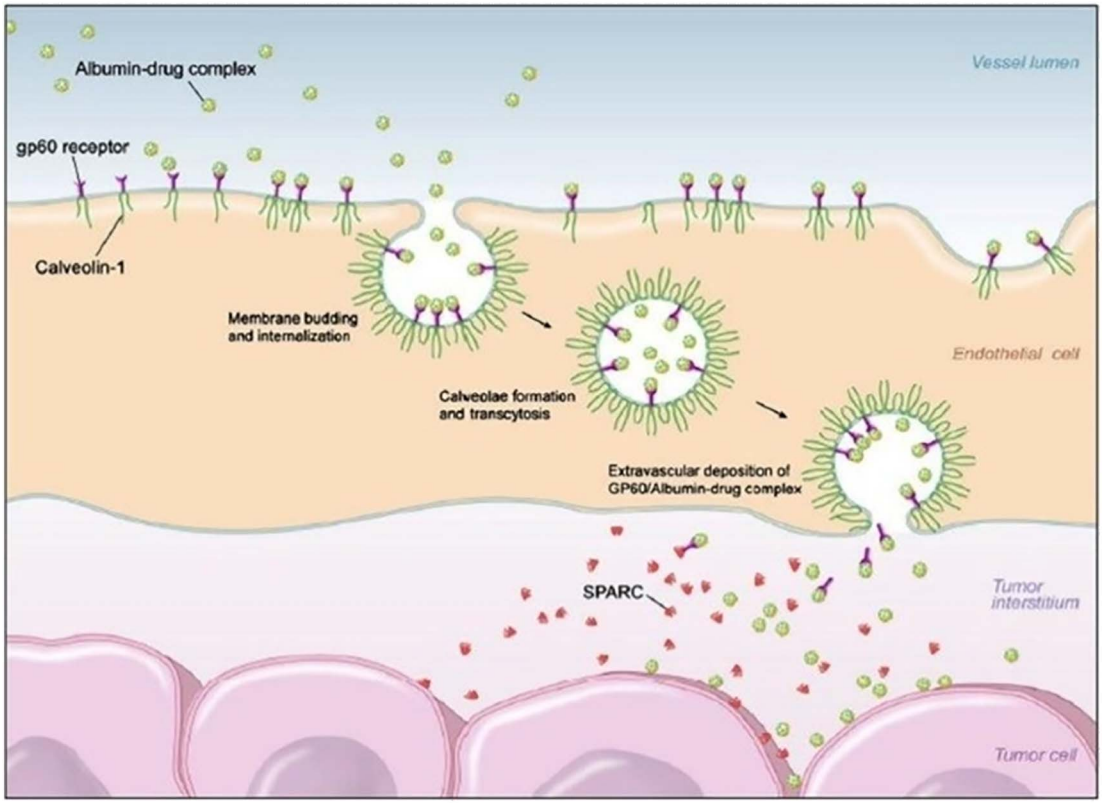

Fig. 4. Accumulation and uptake of albumin-drug conjugate in tumor cell [reproduced from B. Elsadek and F. Kratz [220]].

nanocarriers and their applications in cancer therapy are summarized in Table 4.

5.2. Albumin nanocarriers for gene therapy

Gene therapy is a highly potential therapeutic strategy for the treatment of genetic disorders such as cancer, hemophilia, hypercholesterolemia, neurodegenerative diseases and autoimmune diseases by intentionally altering the gene expression in pathological cells. Gene therapy has been widely studied for the treatment of cancer and currently explored in the clinical trials [159–161]. However, internalization of the naked genetic molecules by the target cells are not very effective because of their high susceptibility to nuclease, rapid renal clearance, phagocyte uptake, reduced uptake by target cells and toxic effect arising by immune response stimulation, which severely restricts their clinical application [159,162]. To overcome all these problems, several viral and non-viral vectors are used to deliver the genetic materials. Viral vector based gene delivery is significantly potent and ensures long-term expression of genes but their utility in gene therapy is limited and restricted because of several pitfalls like carcinogenicity, immunogenicity, inflammation, or high-cost production [163–166]. These pitfalls were overcome by the use of non-viral vectors such as lipid-based nanoparticles, polymer based nanoparticles, polymer based micelles and inorganic nanoparticles [159,167–175].

Serum albumin as a polymer can be also utilized for the gene therapy because of its ability to efficiently deliver genetic material like small interfering RNA (siRNA), DNA etc. to the desired cell type, tissue or organ [176]. However, unmodified albumin or albumin nanocarrier has negative surface charge which prevents or decreases the binding of negatively charged plasmid DNA, making it inefficient in gene delivery [177]. To overcome this drawback, several researchers have developed modified albumin nanocarriers for effective gene therapy. Bcl-2 specific siRNA and gold nanorod encapsulated BSA nanocomplex (SREB) were developed by Choi et al. with the aim of synergistic anticancer activity in treatment of breast cancer by utilizing both siRNA-mediated gene silencing and photothermal therapy. This SREB nanocomplex was further modified with PEG and anti-ErbB-2 antibodies to achieve active targeting. Results indicated that SREB nanocomplex decomposed intracellularly by proteolytic enzymes and led to simultaneous RNA interference and thermal ablation, thus leading to apoptosis in the targeted cancer cells [178]. In another study, Wei Lu et al. developed plasmid pORF-hTRAIL (pDNA) incorporated cationic albumin nanoparticles (CBSA-NP-hTRAIL) for brain tumors by intravenous (i.v.) route. After i.v. administration, CBSA-NP-hTRAIL crossed the BBB and accumulated in glioma xenograft by absorptive-mediated transcytosis. The results suggested that the encapsulated pDNA containing the hTRAIL gene was released and rapidly translocated to the nucleus, where hTRAIL expressed and induced apoptosis of tumor cells but not normal cells. The study showed the feasibility of systemic administration of CBSA-NP-hTRAIL as a nonviral vector for gene therapy of glioma [179]. Albumin-chitosan based core-shell nanoparticles were developed for DNA (psiRNA-hH1GFPzeo) delivery. Cellular uptake studies on HeLa cells showed higher cellular uptake [180]. In another study, albumin nanospheres were simultaneously loaded with super-paramagnetic iron oxide nanoparticles (as gene vector and anticancer gene), and plasmid pDONR223-IFNG and modified with anti-EGFR monoclonal antibody cetuximab (cetuximab [C225]-IFNG-IMANS) for treatment of lung carcinoma and its activity was estimated on GLC-82 cell lines [181]. Results showed targeting ability of nanospheres by combination of thermal treatment, molecular targeted treatment, and gene treatment. It also suggested that C225-IFNG-IMANS may be useful in gene delivery [182]. Han et al. prepared Bcl2-specific siRNA encapsulated cationic bovine serum albumin (CBSA) nanoparticles for lung metastatic cancer. The study concluded that CBSA had excellent ability to intracellularly deliver siRNA and mediate significant accumulation in the lung. It also produced an efficient gene silencing effect that induced notable cancer cell apoptosis and subsequently inhibited the tumor growth in a B16 lung metastasis model [177,182]. In another

Table 4
Application of albumin nanocarriers in cancer therapy.

Albumin nanocarrier	Targeting ligand	Preparation method	Size	Morphology	Drug	Cell line	Study outcome	Ref
Brain tumor								
Peptide functionalized albumin nanoparticles	Cell penetrating peptide (cRGD and KALA)	Self assembly	241 nm	Spherical nanoparticles	Doxorubicin (DOX)	U87-MG glioblastoma cells	Better tumor targeting, cell penetrating, and endolysosomal pH-responsive properties.	[127]
PEG grafted BSA nanoparticles	Lactoferrin	Desolvation	150–155 nm	Nanoparticles	DOX	BCECs and C6	Better permeation enhancement property, increased dual targeting effect of nanoparticles for brain delivery and facilitated the uptake of DOX in the brain tissue	[103]
HSA nanoparticles	–	Desolvation	80–90 nm	Nanoparticles	Imatinib base (IMTb)	U87-MG glioblastoma cells	Cytotoxic effect of the IMTb loaded HSA nanoparticles was higher than that of free IMTb for glioblastoma	[128]
HSA nanoparticles	Cationic albumin and mannose	High pressure homogenization	90.5 nm	Spherical nanoparticles	DOX	bEnd.3 cell, and U87 MG glioblastoma cells	Better tumor targeting	[89]
Albumin lipid nanoparticles	–	Emulsification solvent evaporation	110.1 nm	Core shell nanoparticles	Docetaxel (DXT)	U87 MG, A549, bEnd.3, HUVEC, BMEC cells	Lower toxicity and a superior anti-glioma effect as compared to standard DTX preparations.	[129]
Cationic albumin conjugated pegylated nanoparticles	–	(o/w) emulsion technique	57.7 nm	Nanoparticles	Aclarubicin (ACL)	C6 glioma cells	Higher accumulation of cationic albumin conjugated nanoparticles in tumor mass as compared to non-conjugated nanoparticles with better retention, Survival time also increased.	[130]
Breast cancer								
HSA nanoparticles	–	High pressure homogenization	156.9 ± 3.2 nm	Nanoparticles	Pirarubicin (THP) and Paclitaxel (PTX)	4T1 cells	Increased apoptosis and G2/M cell cycle arrest against 4T1 cells and significantly lower side effects regarding bone marrow suppression and organ and gastrointestinal toxicities.	[131]
HSA nanoparticles	–	Nab technology	137.3 nm	Nanoparticles	Lapatinib	SKBr3 cells	Better inhibit HER2 phosphorylation of tumor cells and exhibited superior anti-tumor efficacy in tumor-bearing mice with no subchronic toxicity	[132]
HSA nanoparticles	–	Nab technology	147 nm	Nanoparticles	DXT	MCF7 cells	DTX nanoparticles showed dose and time dependent cytotoxicity in MCF-7 cells. Real-time PCR analysis showed higher alteration of pro-apoptotic gene expression in MCF-7 cells after treatment with DTX nanoparticles compared with free DTX.	[133]
Methotrexate–human serum albumin nanoparticles	Luteinizing-hormone releasing hormone (LHRH)	MTX firstly conjugated with HSA by using EDC and NHS and this conjugate is further cross-linked by EDC to form nanoparticles	120.5 nm–138.56 nm	Nanoparticles	Methotrexate (MTX)	4T1 breast cancer cells	Significant tumor growth delay was observed in 4T1 tumor bearing mice treated with LHRH targeted MTX–HSA NPs compared to non-targeted MTX–HSA NPs treated group. The body weight loss of LHRH targeted nanoparticles treated groups was very low.	[134]
HSA nanoparticles	Biotin/Folate	Emulsification method	185 nm and 205 nm	Drug-HSA conjugated nanoparticles	DXT	MDA-MB-231, A549 and 4T1 cells	Conjugated nanoparticles more significantly reduce tumor size and increases survival rate of animal compared to free drug.	[135]
PEI-enhanced HSA nanoparticles	–	Desolvation	137 nm	Nanoparticles	DOX	MCF7 cells	Coating of cationic polymer over the HSA nanoparticles improved the cell penetration and showed more potent	[120]

(continued on next page)

Table 4 *(continued)*

Albumin nanocarrier	Targeting ligand	Preparation method	Size	Morphology	Drug	Cell line	Study outcome	Ref
							cytotoxic effects on MCF 7 cells.	
Cervical cancer								
Aptamer Functionalized Cisplatin-Albumin Nanoparticles (Apt-Pt NPs)	EGFR RNA Aptamer	Desolvation	40 nm	Nanoparticles	Cisplatin	Human Hela cell line	Enhanced intracellular cisplatin release rather than extracellular and avoid unnecessary accumulation of drug in body.	[136]
Colon cancer								
HSA nanoparticles	Folate	Emulsification	165.6 ± 15 nm	Nanoparticles	Curcumin	–	Nanoparticles showed sustained release of Curcumin and in vivo study showed prolonged retention time of drug and better antitumor activity.	[137]
Prototype of HSA nanoparticles	–	Self assembly	267.3 nm	Nanoparticles	DOX	HCT 116 and A549 cells	excellent tumor target ability probably due to gp60-mediated transcytosis mechanism	[138]
HSA nanoparticles	–	Nab technology	60–120 nm	Nanoparticles	DOX and TRAIL protein	HCT116 cells	Co delivery of DOX and TRAIL offered potential synergistic apoptosis-based anticancer therapy	[139]
Gastric cancer								
HSA nanoparticles	–	BSA cross linked by Schiff base-containing vanillin to form nanoparticles	100.5 nm	Nanoparticles	DOX	BGC-823 cells	Formulation showed superior extension of survival time than free DOX and DOX-BSA-NPs, and greater tumor suppression than free DOX.	[140]
Liver cancer								
BSA nanoparticles	Glycyrrhizic acid	Emulsification (High pressure homogenization)	157.5 nm	Nanoparticles	10-hydroxy camptothecin	SMMC7721 cells	Promising new vehicle for hepatocellular carcinoma-targeting therapy	[141]
Recombinant HSA nanoparticles	Glycyrrhetinic Acid (GA)	Desolvation	170 nm	Nanoparticles	DOX	HepG2 cells	The targeted NPs exhibited higher cellular uptake in a GA receptor-positive liver cancer cell line than non-targeted NPs and biodistribution experiments showed that targeted NPs exhibited a much higher level of tumor accumulation than non-targeted NPs	[142]
Albumin nanoparticles	Glycyrrhetinic acid	Desolvation	258.8 ± 6.4 nm	Nanoparticles	Curcumin	HepG2 cells	NPs were significantly more cytotoxic to HepG2 cells and in a concentration-dependent manner.	[91]
BSA nanoparticles	Hematoporphyrin (HP)	Desolvation	372.6 ± 10.9 nm	Nanoparticles	DOX	HepG2 cells	Cellular uptake from HP-NPs was proportional to the expression level of LDL receptors on the cells, indicating possible involvement of LDL receptor-mediated endocytosis (RME) in uptake.	[143]
Lung cancer								
Self-assembled albumin nanoparticles	–	Self assembly	~340 nm	Nanoparticles	DOX and TRAIL protein	H226 cells	Improved anti-tumor efficacy was found to be due to the synergistic apoptotic effects of DOX and TRAIL	[144]
Albumin nanoparticles	–	Emulsion-evaporation cross-link method	163–169 nm	Nanoparticles	DXT	A549 cells	Pegylated nanoparticles showed higher cellular uptake and superior antitumor activity as compared to non-pegylated nanoparticles.	[145]
Multi Drug Resistance (MDR) cancer								
TPGS modified reduced BSA nanoparticles	–	Ultrasonication	173–338 nm	Albumin-polymer conjugated nanoparticles	PTX	MCF-7 and MCF-7/ADR cells	Polymer-protein conjugate based nanoparticles showed higher drug loading and entrapment of lipophilic	[146]

(continued on next page)

Table 4 *(continued)*

Albumin nanocarrier	Targeting ligand	Preparation method	Size	Morphology	Drug	Cell line	Study outcome	Ref
							drug and in vitro revealed its ability to overcome MDR by inhibiting P-gp efflux.	
BSA nanoparticles	–	Self assembly	50 nm	Nanoparticles	DOX and Verapamil (VER)	HCT-15 cells and 293T cells	As compared with free DOX and DOX/BSA nanoparticles, DOX/VER/BSA nanoparticles exhibited a stronger tumor cell inhibitory effect because of the enhanced intracellular DOX concentration caused by the efflux pump inhibition of VER.	[147]
Ovarian cancer								
BSA nanoparticles	–	Modified desolvation	10–200 nm	Nanoparticles	Albendazole (ABZ)	SKOV3, OVCAR3, and HOSE cells	BSA-ABZ may hold promise for the treatment and control of progression of ovarian cancer with ascites. However further studies are also required.	[148]
Pancreatic cancer								
HSA nanoparticles	–	Nab technology	150 ± 27 nm	Nanoparticles	Gemcitabine (GEM)	BxPC-3 cell	The enhanced in vivo efficacy of GEM-HSA-NPs towards the pancreatic cancer cell line suggests their potential role for use in the clinical field.	[149]
HSA nanoparticles	cRGD peptide	Nab technology	160 ± 23 nm	Nanoparticles	GEM	BxPC-3 cell	The in vitro results confirmed that cRGD-anchored nanoparticles can deliver gemcitabine to a pancreatic cancer cell line more efficiently.	[92]
Paclitaxel (PTX)-bound albumin nanoparticles	TRAIL	Nab technology	170–230 nm	Nanoparticles	PTX and TRAIL protein	Mia Paca-2 cells	TRAIL/PTX HSA-NP would have potential as a novel apoptosis-based anticancer agent because of enhanced in vitro and in vivo performance.	[150]
Miscellaneous								
HSA nanoparticles	–	High pressure homogenization	170.5 ± 4.0	Nanoparticles	Cabazitaxel (CBX) and indocyanine green (ICG)	4T1, PC3, C6 cells	CBX and ICG could be co-delivered to the tumor tissue specifically via receptor mediated pathway and possessed high accumulation in the tumor area	[151]
MTX–HSA conjugated nanoparticles	Biotin	MTX firstly conjugated with HSA by using EDC and NHS and this conjugate is further cross-linked by EDC to form nanoparticles	111.46 nm–144.36 nm	Albumin-drug conjugated nanoparticles	Methotrexate (MTX)	4T1 breast cancer cells	The in vivo anticancer experiment showed that biotin targeted MTX-HSA NPs had stronger antitumor activity and lower toxic effect than non-targeted MTX-HSA NPs and free MTX in a mouse breast tumor model.	[152]
BSA nanoparticles	Folate	Desolvation	195.3 ± 5.6 nm,	Nanoparticles	Bexarotene (BEX)	A549 and MCF-7 cells	Both the BEX-BSANPs and FA-BEX-BSANPs induced an enhanced cancer cell apoptotic effect in contrast to BEX solution.	[153]
Albumin nanoparticles	TRAIL	Modified desolvation and Electrostatic layer by layer assembly	< 200 nm	Core shell nanoparticles	DOX and TRAIL	H460 and DOX resistance L929 cells.	The assembled core/shell structure of the nanoparticles was internalized more easily with the cancer cells, which was attributed to TRAIL binding with death receptors.	[154]
BSA nanoparticles	Hyaluronic acid (HA)	Modified desolvation and Layer by layer assembly	119–238 nm	Core shell nanoparticles	DOX	MDA-MB-231 cells	Nanoparticles with HA as the final layer showed maximum cellular uptake in MDA-MB-231 cells owing to the CD44 receptor-mediated endocytosis and hence, exhibited more cytotoxicity as compared to free Dox.	[155]
Lipid hybrid albumin	–	High pressure homogenization	128.4 ± 12.9 nm	Lipid hybrid	Pirarubicin (THP)	–	Significantly reduced bone marrow	[156]

(continued on next page)

Table 4 *(continued)*

Albumin nanocarrier	Targeting ligand	Preparation method	Size	Morphology	Drug	Cell line	Study outcome	Ref
nanoparticle				albumin nanoparticles			suppression, cardiotoxicity, renal toxicity, and gastrointestinal toxicity	
Targeted albumin based nanoparticles	Cyclic RGD peptide	Self assembly	30 nm	Nano micelles	DOX	Human melanoma cells (M21 +)	Higher uptake and longer retention of DOX with RGD modified micelles as compared to non-modified micelles and free DOX	[157]
Multi-stimuli-responsive biohybrid nanoparticles		Self-assembly	30–60 nm	Nano micelles	–	HepG2 cells	pH, temperature and enzyme responsive delivery. Highly biocompatible and higher internalization of nanoparticles by cells make it suitable candidate for cancer therapy	[158]

study, Son et al. used thiolated HSA (tHSA) for delivery of VEGF siRNA to the tumor sites by forming nanosized complexes. This nanosized complex accumulated significantly in the tumor site after being administered by i.v. route. It produced gene silencing in tumor and inhibited tumor related angiogenesis in PC-3 tumor xenografts which resulted in growth retardation of PC-3 tumors [183]. Kummitha et al. showed that albumin coating reduced the interaction of other serum proteins with lipid nanoparticles and enhanced siRNA delivery [184].

5.3. Albumin nanocarriers for phototherapy

Phototherapy is a light-triggered, noninvasive and effective approach for cancer therapy which has improved selectivity and fewer side effects as compared to conventional chemotherapy and radiotherapy. Phototherapy may be either photodynamic therapy (PDT) or photothermal therapy (PTT) or combination of both [185–187]. In phototherapy, photosensitizer (PS) or photothermal agent is used to selectively and efficiently destroy the targeted cells by the application of light [188–191]. In cancer phototherapy, different types of imaging technologies such as computed tomography (CT), positron emission tomography (PET), magnetic resonance imaging (MRI), ultrasonic imaging and photoacoustic imaging are used as a tool for guiding assistance [192].

5.3.1. Albumin nanocarrier for photodynamic therapy

Photodynamic therapy (PDT) refers to cancer treatment through the selective uptake of a light-sensitive agent, a photosensitizer (PS), which can produce highly reactive oxygen species (ROS) followed by exposure to a specific wavelength that irreversibly induces cell apoptosis or necrosis in the targeted tissue. PDT is a noninvasive and effective cancer therapy with minimum side effects and more selectivity as compared to chemotherapies and radiotherapies [192–194]. Albumin is used as nanocarrier in PDT because of its biocompatibility, abundance, better accumulation in tumors, strong EPR effect, non-antigenic nature and binding with several organic and inorganic molecules. Chen et al. prepared pheophorbide-HSA (Pheo-HSA) nanoparticles (PHSA40 and PHSA100) and investigated their photophysical and photosensitizing properties for photodynamic therapy [195]. Results indicated that, Pheo-HSA nanoparticles caused a much lower phototoxicity than free Pheo molecules in Jurkat cells and this may because of different cellular uptake mechanisms which influenced photoactivity of Pheo. After 24 h incubation, PHSA40 and PHSA100 showed a higher phototoxicity than Pheo [195]. In another study, Chen et al. developed mTHPC-loaded HSA nanoparticles and reported that their photophysical properties such as absorption, fluorescence, and fluorescence lifetime mainly depended on loading ratio [196]. To improve the generation of singlet oxygen upon irradiation, Monila et al. developed redox sensitive Ce6-HSA nanoparticles. Results showed enhanced generation of singlet oxygen production upon reduction of crosslinking and led to increased cell death upon radiation. It also prevented the dark toxicity in non-targeted and healthy tissues [197]. In another study, Yang et al. developed Hematoporphyrin (HP) linked albumin nanoparticles (HP-ANP) by solvent diffusion method for photodynamic therapy and modified them with gamma-emitting nuclides (^{99m}Tc) for scintigraphic imaging. HP-ANP showed higher accumulation in A549 and CT-26 cells. Upon UV exposure, HP-ANP showed photodynamic action against A549 cell line. As compared to ^{99m}Tc-HP, ^{99m}Tc-HP-ANP demonstrated good imaging properties in rabbits with a much more extended biological half life. These results suggested the suitability of the system as radio-diagnostic as well as photodynamic tool for cancer therapy [198]. Butzbach et al. prepared albumin folate conjugate for PDT using polar β-carboline derivatives as photosensitizers (PS). The results showed phototoxic effects of folate-albumin-β-carbolinium conjugate with or without irradiation as compared to albumin–*b*-carbolinium conjugates without FA. For phototoxicity cellular uptake and lysosomal degradation of the conjugates was required [199]. Use of PS induced skin

photosensitivity after exposure in sunlight is the main limitation of using it for the PDT. To overcome this limitation, Zhang et al. developed a hydrophobic Near-infrared (NIR) dye IR-780 iodide (IR780) to induce the self-assembly of albumin-PS conjugates, as a switchable PDT (Switch-PDT) agent. Their results showed inhibited PDT effect of PS by IR780 and recovered by NIR light irradiation in vitro. This quench/recovery strategy does not sacrifice the anti-tumor ability in vivo, and the combined PDT and PTT (photothermal) effect contributes a very effective tumor inhibition rate of 100%. NP (IR780 + Ce6) causes negligible skin photosensitization in mice and rabbit model. The activatable PDT still has tumor ablation ability equivalent to traditional PDT agent. These data suggested suitability of switchable PDT for reducing photo sensitization [200]. In another study, Ce6 conjugated HSA self assembled nanoparticles (Ce6-HSA-NPs) were prepared and injected through the tail vein into tumor-bearing HT-29 mice. As compared to free Ce6, Ce6-HSA-NPs revealed enhanced tumor-specific biodistribution and successful therapeutic results following laser irradiation [58]. All these studies indicate the suitability of albumin and albumin based nanocarriers for PDT.

5.3.2. Albumin nanocarriers for photothermal therapy

Photothermal therapy (PTT) is a new type of light-induced cancer treatment strategy in which near-infrared (NIR)-absorbing photothermal agents can effectively convert NIR light (λ = 700–1100 nm) into heat, resulting in the thermal ablation of cancer without affecting the surrounding healthy tissues [201,202]. Albumin and its nanocarriers are being used in PTT because of its aforementioned properties like biocompatibility, better tumor accumulation etc. Chen et al. prepared NIR dye (IR825) bounded HSA noncomplex imaging guided PTT. The results revealed enhanced fluorescence quantum yield (QY) under 600 nm excitation wavelengths compared to that of free IR825, together with a rather high absorbance but low fluorescence QY at 808 nm. This HSA-IR825 complex when intravenously injected in mice revealed high tumor uptake and lesser biodistribution in other organs and 100% tumor ablation [203]. Chen et al. developed albumin based nanotheranostic agents for multimodal image guided PTT to inhibit lymphatic metastasis of cancer post-surgery [204]. In this work, they firstly conjugated HSA with diethylenetriamine penta-acetic acid (DTPA) to chelate gadolinium (Gd) ions and then bound IR825 to it. The formed HSA-Gd-IR825 nanocomplex exhibited strong fluorescence for fluorescence imaging as well as in MRI (using as T1 contrast agent). After intratumor injection, HSA-Gd-IR825 quickly migrated into tumor-associated sentinel lymph nodes through lymphatic circulation and after NIR laser exposure caused photothermal ablation of tumor cells. This photothermal ablation of tumor when combined with surgical removal of primary tumors would be able to prevent further lymphatic metastatic spread of cancer cells and remarkably prolong animal survival [200,205]. In another study, Chen et al. developed Albumin-NIR dye self-assembled nanoparticles for photoacoustic pH imaging and pH-responsive PTT for large tumors. In this, croconine (Croc) was used as a pH responsive NIR dye which induced the self assembly of HSA to form stable HSA-Croc nanoparticles upon simple mixing without the need of chemical cross-linkers. Upon i.v. injection of these nanoparticles into tumor bearing mice, the pH values in the tumor microenvironment were accurately detected by dual-wavelength ratiometric photoacoustic imaging and upon NIR absorption, photothermal ablation of large tumors took place [206]. HSA coated Prussian blue nanoparticles (PB NPs) loaded with DOX were synthesized by Li et al. for cancer thermochemotherapy. DOX loaded NPs exhibited a dual-modal pH-/thermal-sensitive drug release, resulting in a high chemotherapy effect on cancer cells. Furthermore, the NPs showed strong NIR absorbance, excellent capability, stability of photothermal conversion for PTT applications. These nanoparticles showed synergistic anticancer activity [207].

5.3.3. Albumin nanocarriers for combinational photothermal and photodynamic therapy

Combinational therapies include both photothermal and photodynamic activity with or without imaging guided therapy. Sheng et al. developed programmed assembly strategy for the preparation of human serum albumin (HSA)-indocyanine green (ICG) nanoparticles (HSA-ICG NPs) by intermolecular disulfide conjugations for imaging guided cancer phototherapy [190]. Upon NIR laser irradiation, HSA-ICG NPs efficiently induced ROS and local hyperthermia simultaneously for synergetic PDT/PTT treatments. Results showed that after an i.v. injection of HSA-ICG NPs followed by imaging-guided precision phototherapy (808 nm, 0.8 W/cm^2 for 5 min), the tumor was completely suppressed, no tumor recurrence and treatments-induced toxicity were observed [190]. Multifunctional theranostic PB-BSA-ICG nanoparticles were prepared by Sahu et al. for bimodal imaging guided laser mediated combinatorial phototherapy. Results revealed lesser photo instability of ICG and higher solution stability of nanoparticles. Upon NIR irradiation, significant cell death was observed which may be due to combined PTT-PDT effect. In vivo studies results suggested higher tumor accumulation and lesser biodistribution of nanoparticles in other major organ were observed when analyzed by T1-weighted MRI and NIR fluorescence bimodal imaging. The nanoparticles efficiently suppressed the tumor growth through combinatorial phototherapy with no tumor recurrence upon a single NIR laser irradiation [207]. In another study, Song et al. developed Ce6 conjugated albumin-polypyrrole (PPy@BSA-Ce6) nanoparticles for imaging guided PTT/PDT therapy. Results revealed stability of these nanoparticles in physiological solutions as well as photodynamic and photothermal activity along with MRI contrasting activity (with Gd^{3+} − labeling). In vivo fluorescence imaging and MRI also revealed higher tumor uptake of nanoparticles. In vivo data also suggested synergistic therapeutic effect by combinational PTT/PDT therapy [208]. All these results indicate the suitability of albumin nanocarriers for combinational photothermal and photodynamic therapy.

5.4. Albumin nanocarriers for imaging and diagnosis

Various dye conjugated albumin nanocomplexes are utilized in the fluorescence imaging and MRI of tumor cells. Apart from the NIR dyes, albumin can also be conjugated with other contrast agents like gadolinium (Gd) and DTPA or can be labeled with the radioactive material for MRI or PET imaging [204]. Watcharin et al. developed Gd-DTPA and rhodamine 123 (Rho) conjugated HSA nanoparticles (Gd-Rho-HSA-NPs) for the detection of hepatocellular carcinomas (HCC) by T1-weighted MRI. These nanoparticles were injected in HCC tumor bearing transgenic mice by intravenous route and MRI scan revealed strong negative contrast of tumor. Gadolinium-ethoxybenzyl-diethylenetriaminepentaacetic acid-enhanced MRI is used for the detection of HCC in patients. Gd-Rho-HSA-NPs enhanced MRI required lesser Gd for the contrasting of HCC as compared to previous one. These results indicate the suitability of nanoparticles for detection of HCC by T1-weighted MRI in mice [209]. Wang et al. prepared folic acid functionalized BSA coated superparamagnetic iron nanoparticles (FA-BSA-SPIO NPs) as a contrast agent for MRI. These nanoparticles were labeled with fluorescein isothiocyanate (FITC) for interacellular imaging after cellular uptake and internalization by glioma U251 cells. The results showed that the fabricated FA-BSA-SPIO NPs did not affect cell proliferation, viability and cell cycle, possessed unobservable cytotoxicity, and were more suitable as contrast agents for MR imaging. These results make it suitable for tumor cell labeling and intracellular imaging in human brain tumor diagnosis and treatment [88]. In another study, Liu et al. prepared BSA-poly(ε-caprolactone) (PCL) conjugate coated $CuInS_2$/ZnS quantum dots (CIS/ZnS QDs) and used it as a NIR fluorescent probe for targeted cell imaging. The prepared nanoprobe showed excellent fluorescent properties over the pH range of 3–10 and also had stability in physiological condition. This nanoprobe was further functionalized by cRGD peptide for integrin αvβ3-overexpressed tumor cell imaging

Table 5
Clinically approved albumin nanocarriers for therapy and diagnosis of cancer and other diseases and ongoing clinical trials for cancer therapy (modified from: reference [35, 219, 220]).

Name and company	Particle type/drug	Approved application/indication	Approval (year)	Investigated application/indication	ClinicalTrials.gov identifier
Abraxane (Celgene)	Albumin-particle bound paclitaxel	Advanced non-small cell lung cancer (surgery or radiation is not an option) Metastatic breast cancer (secondary), Metastatic pancreatic cancer (primary)	FDA (2005) EMA (2008)	Various cancers including: solid malignancies, breast, lymphomas, bladder, lung, pancreatic, head and neck, prostate, melanoma, or liver	295 studies mention Abraxane
Optison (GE Healthcare)	Human serum albumin stabilized perflutren microspheres	Ultrasound contrast agent	FDA (1997) EMA (1998)	Ultrasound enhancement for: lymph node, renal cell carcinoma, myocardial infarction, pulmonary transit times, or heart transplant rejections	11 currently active or recruiting studies
^{9m}Tc-Albures® (GIPHARMA)	^{99m}Tc aggregated albumin	Diagnostic agent used in screening of primary cancers		Various cancers including breast cancer, lymphomas, esophageal squamous cell carcinoma and other solid tumors	–
^{99m}Tc-Nanocoll® (GIPHARMA)	^{99m}Tc aggregated albumin	Diagnostic agent used in detection of metastasis		Various cancers including breast cancer, lymphomas, esophageal squamous cell carcinoma and other solid tumors	–
Levemir® (Novo Nordisk)	(Insulin detemer) Albumin binding derivative of human insulin	Diabetes type 1 and type 2	Europe (2004) FDA (2005)	Diabetes type 1 and type 2	–
Victoza® (Novo Nordisk)	(Liraglutide) Albumin binding derivative of GLP-1	Diabetes type 2	Europe (2009) FDA (2010)	Diabetes type 2	–
Eperzan®/Tanzeum® (Albiglutide) (Glaxo Smith Kline)	GLP-1 receptor agonist genetically fused with albumin	Diabetes type 2	FDA (2014)	Diabetes type 2	
ABI-008 (Celgene)	Albumin bound Docetaxel	–	–	Prostate and colon cancer	Phase I/II completed
ABI-009 (Aadi with Celgene)	Albumin bound rapamycin	–	–	Bladder cancer, PEComa, or pulmonary arterial hypertension	NCT02009332 (Phase I/II) NCT02587325 (Phase I) NCT02494570 (Phase II)
ABI-010 (Celgene)	HSP90 inhibitor	–	–	Cancer (hematological malignancies)	Withdraw before enrollment
ABI-011 (NantBioScience)	Albumin bound thiocolchicine analog (IDN 5405)	–	–	Solid tumors or lymphomas	NCT02582827 (Phase I)
Aldoxorubicin (INNO-206 or DOXO-EMCH) (CytRx, Inc.)	Albumin-Doxorubicin conjugate	–	–	Cancer (soft tissue sarcoma, small cell lung cancer etc.)	Phase I completed and Phase II ongoing for small cell lung cancer
MTX-HAS (Access Pharmaceuticals Inc.)	Albumin-drug conjugate	–	–	Cancer and autoimmune disease	Phase II
Ozoralizumab (Ablynx)	Albumin binding antibody derivative	–	–	Rheumatoid arthritis	Phase II completed
Albuferon®/Zalbin/Jouleferon (Human genome Sciences in collaboration with Novartis)	Genetically Fused protein of albumin and INFalpha-2b	–	–	Hepatitis C	Phase III completed, Development ceased

and showed high selectivity towards the targeted tumor cells [210]. Albumin based fluorescent carbon dots (CDs) were prepared by Hu et al. for biological imaging. These CDs showed fluorescent effect by photoluminescent mechanism and its biological imaging application was tested on human breast cancer Bcap-37 cell. They also suggested the suitability of these CDs for substituting organic dyes or semiconductor quantum dots (SQDs) in biological imaging [211]. Moon et al. developed ultrasound microbubbles conjugated PTX loaded HSA nanoparticles (PTX-HSA-NPs-MBs) as ultra sound contrast agent for tumor diagnosis and therapy. They injected these nanoparticles in tumor bearing mice by intravenous route and reported enhanced echogenisity in tumor as well as enhanced survival rate of mice. This indicates the suitability of PTX-HSA-NPs-MBs in early cancer diagnosis and possibility of theragnosis [212].

5.5. Albumin nanocarriers for cancer theranostics and multimodal therapy

Theranostics is a combination of diagnosis and therapy which provides a platform for simultaneous imaging and therapy of the disease affected cell, tissue or organ. Cancer theranostics is a multimodal therapy which gives us opportunity for simultaneous imaging and therapy of the tumor [213,17]. Simkina et al. developed albumin based core-shell superparamagnetic iron oxide nanoparticles (SPIONs) loaded with DOX for cancer theranostics. The nanoparticles were prepared by adsorption of the BSA shell onto the Fe_3O_4 core followed by cross-linking of the protein layer and PEG was grafted over it by carbodiimide chemistry. These nanoparticles showed stimuli sensitive drug release of DOX, reduced toxicity towards the normal cells and due to superparamagnetic properties these were also used as a MRI diagnostic agent [214]. DOX and NIR dye (ICG) encapsulated albumin nanoparticles were developed by Kolluru et al. using coacervation/nanoprecipitation method for tumor targeting. Preliminary in vivo real time imaging studies revealed significant breast tumor passive targeting. The in vivo studies also showed enhanced accumulation of the dye loaded NPs at the tumor site as compared to dye solution, and also allowed non-invasive tumor imaging and monitoring [215]. Chen et al. developed albumin based nanotheranostic particles by drug induced protein assembly for tumor targeted combination (phototherapy and chemotherapy) therapy. PTX loaded HSA nanoparticles were either modified by Ce6 as photosensitizing agent to chelate $Mn2^+$ ions or cRGDyK peptide to target Rvβ3-integrin overexpressed on tumor angiogenic endothelium. These nanoparticles showed promising results for multimodel imaging-guided combination therapy of cancer [216]. In other study, Khandelia et al. developed gold (Au) nanocluster embedded nanotheranostic BSA nanoparticles in which Au nanoclusters act as a luminescent probe for imaging of cancer cells. It also contained DOX that kills the cancer cells by apoptotis. These nanoparticles were stable and retained their luminescence in human blood serum which makes it suitable system used clinical for in vivo imaging and combination therapy where the nanoclusters in conjunction with the conventional drug would be used for therapy using radiation [217]. Wei et al. prepared BCNU loaded BSA nanoparticles for MRI as well as fluorescence imaging for tracking of therapeutic agent in chemotherapy. In this Gd and FITC were used as MR contrast agent and fluorescent imaging agent respectively and these nanoparticles were water dispersible, stable, and biocompatible as confirmed by XTT cell viability assay. Results indicated potential bioimaging tracking of chemotherapeutic agent ability in vitro and in vivo for cancer therapy and can be potentially utilized in clinical applications [218].

6. Clinically approved albumin nanocarriers and ongoing clinical trials

Owing to huge advancement in albumin based drug delivery systems, especially nanocarriers, the albumin based nano formulations have been projected as potential carrier systems feasible for market translations, leading to their approval for clinical trials. The first product to get green flag for clinical trials dates back to late nineties with the first FDA approval for human use in 2005 Abraxane developed by Celgene Ltd. Thereafter, various other albumin based formulations for cancer therapy and other diseases such as diabetes got approval for clinical trials, some of which made it to the market. Some of the major albumin based formulations specifically for cancer treatment and diagnosis have been summarized in Table 5. Vast amount of research is still going on in the same area and sooner or later we will see albumin based novel therapeutic and diagnostic platforms getting approval for cancer treatment which will serve as a major stepping stone for better healthcare system for cancer patient.

7. Conclusion and perspectives

Albumin based nanocarriers have gained more attention in cancer therapy due to the its unique properties viz. relatively safe and easy to prepare, capability to deliver proteins, peptides, genes, nucleic acid, and hydrophilic as well as hydrophobic anticancer molecules, site specific targeting by surface modification, greater stability profile during storage, etc. All these properties make albumin a very versatile and popular polymer for designing cancer targeted delivery systems like nanoparticles.

Albumin also forms micelles (after conjugation with drugs and polymers) by self assembly. These micelles are used for gene delivery, targeted anticancer drug delivery, surface engineered multimodel therapy etc. Albumin micelles increase stability as well as decrease immunogenicity and non-specificity of proteins. It also enhances cellular uptake of drugs and genes and also increases the cytotoxic effects of drugs towards cancer cells. So act as a suitable carrier for cancer therapy.

Apart from nanoparticles, various albumin based nanoconjugates have also been investigated for drug and gene delivery. Albumin based prodrug strategies for i.v. administration of novel anticancer compounds may be a promising approach for targeted cancer therapy. Apart from this, albumin metal conjugates and albumin coated inorganic nanoparticles have been explored extensively as they can provide stability, enhanced circulation and better accumulation to the desired target site and can also provide target specificity due to the presence of reactive surface functional groups for the attachment of targeting ligands. Although albumin based nanoconjugates have demonstrated a lot of promising advantages and benefits, there are still a lot of issues especially related to their synthesis. For the preparation of these nanoconjugates, several hazardeous chemicals and harsh chemical or environmental conditions are utilized which may also affect the structure and stability of the albumin and may also alter its performance. So the challenge is to develop such methods which may utilize mild reaction conditions and avoid the usage of hazardeous chemical reagents for preparing albumin based nanoconjugates.

Besides better tumor accumulation of albumin due to EPR effect, surface modification of albumin based nanocarriers is necessary to alter the surface properties and enhance the targeting potential of the delivery system. The utilization and development of new targeting strategies may open new doors in the field of targeted cancer therapy. The various binding sites and functional groups present on albumin can be utilized to develop new targeting ligands and other targeting strategies.

After the successful and wide application of albumin and albumin based nanocarriers in delivery of anticancer drugs, they are also utilized for gene delivery. Unmodified albumin or albumin nanocarrier has negative surface charge which prevents or decreases the binding of negatively charged plasmid DNA, making it inefficient in gene delivery; so cationic albumin is used for better gene delivery. Besides cationic albumin, there is still scope for the development of other modified forms of albumin or albumin based nanocarriers for improved gene delivery.

Apart from cancer targeting, albumin based nanocarriers have also

been explored for biomedical and imaging applications. Various dye conjugated albumin nanocomplexes are utilized in the fluorescence imaging and MRI of tumor cells. Apart from the NIR dyes, albumin can also be conjugated with other contrast agents like gadolinium (Gd) and DTPA or can be labeled with the radioactive material for MRI or PET imaging. Albumin nanocarriers have also been explored in the photothermal and photodynamic therapy of cancer alone or with combination of anticancer drug, providing multimodal platform in the cancer therapeutics. The combination of anticancer drug delivery with the image guided therapy provides better anticancer activity by synergistic action. All the studies included in the review indicate the suitability of albumin and albumin based nanocarriers in the field of imaging and phototherapy (PTT, PDT and combination of both) of cancer. The fabricated albumin based nanocarriers are also utilized as a contrast agent for MR imaging which makes it suitable for tumor cell labeling and intracellular imaging in tumor diagnosis and treatment. Vast amount of research is still going on in the same area and sooner or later we will see albumin based novel therapeutic and diagnostic platforms getting approval for cancer treatment which will serve as a major stepping stone for improved cancer therapeutics.

Acknowledgment

The authors would like to thank DST-INSPIRE, New Delhi, India, for providing financial assistances in the form of INSPIRE fellowship to Ritu Kudarha (No. DST/INSPIRE Fellowship/2015/IF150242).

Declaration of interest

The authors state no conflict of interest.

References

[1] Globocan, IARC 2013, (2012).
[2] J. Ferlay, I. Soerjomataram, R. Dikshit, S. Eser, C. Mathers, M. Rebelo, D.M. Parkin, D. Forman, F. Bray, Cancer incidence and mortality worldwide: sources, methods and major patterns in GLOBOCAN 2012, Int. J. Cancer 136 (2015) E359–E386.
[3] U. Aruna, R. Rajalakshmi, Y.I. Muzib, V. Vinesha, M. Sushma, K.R. Vandana, N.V. Kumar, Inter. J. Inn. Pharm. Res. 4 (2013) 318–324.
[4] K.B. Sutradhar, L. Amin, Nanotechnology in cancer drug delivery and selective targeting, ISRN Nanotechnol. 2014 (2014) 1–12.
[5] J. Mondal, A.K. Panigrahi, A.R. Khuda-Bukhsh, Conventional chemotherapy: problems and scope for combined therapies with certain herbal products and dietary supplements, Austin J. Mol. Cell Biol. 1 (1) (2014) 10.
[6] T. Sun, Y.S. Zhang, B. Pang, D.C. Hyun, M. Yang, Y. Xia, Engineered nanoparticles for drug delivery in cancer therapy, Angew. Chem. Int. Ed. 53 (2014) 2–47.
[7] A.Z. Wang, R. Langer, O.C. Farokhzad, Annu. Rev. Med. 63 (2012) 185–198.
[8] G. Pillai, Nanomedicines for cancer therapy: an update of FDA approved and those under various stages of development, SOJ Pharm. Pharm. Sci. 1 (2) (2014) 13.
[9] M.E. Davis, Z. Chen, D.M. Shin, Nanoparticle therapeutics: an emerging treatment modality for cancer, Nat. Rev. Drug Discov. 7 (2008) 771–782.
[10] X. Yu, C. Jin, Application of albumin-based nanoparticles in the management of cancer, J. Mater. Sci. Mater. Med. 27 (2016) 4.
[11] C. Yewale, D. Baradia, I. Vhora, A. Misra, Proteins: emerging carrier for delivery of cancer therapeutics, Expert Opin. Drug Del. 10 (10) (2013).
[12] N.L. Dhas, P.P. Ige, R.R. Kudarha, Design, optimization and in vitro study of folic acid conjugated-chitosan functionalized PLGA nanoparticle for delivery of bicalutamide in prostate cancer, Powder Technol. 283 (2015) 234–245.
[13] P. Kumar, R. Srivastava, IR 820 stabilized multifunctional polycaprolactone glycol chitosan composite nanoparticles for cancer therapy, RSC Adv. 5 (2015) 56162–56170.
[14] N. Yang, Y. Jiang, H. Zhang, B. Sun, C. Hou, J. Zheng, Y. Liu, P. Zuo, Active targeting docetaxel-PLA nanoparticles eradicate circulating lung cancer stem-like cells and inhibit liver metastasis, Mol. Pharm. 12 (1) (2015) 232–239.
[15] M. Prabaharan, Chitosan-based nanoparticles for tumor-targeted drug delivery, Int. J. Bio. Macromol. 72 (2015) 1313–1322.
[16] R.K. Kudarha, N.L. Dhas, A.P. Pandey, V.S. Belgamwar, P.P. Ige, Box–Behnken study design for optimization of bicalutamide-loaded nanostructured lipid carrier: stability assessment, Pharm. Del. Tech. 20 (2015) 608–618.
[17] A. Tupal, M. Sabzichi, F. Ramezani, M. Kouhsoltani, H. Hamishehkar, Dermal delivery of doxorubicin-loaded solid lipid nanoparticles for the treatment of skin cancer, J. Microencapsul. 33 (4) (2016) 372–380.
[18] V.P. Torchilin, Multifunctional, stimuli-sensitive nanoparticulate systems for drug delivery, Nat. Rev. Drug Discov. 13 (2014) 813–827.
[19] S. Krishnamurthy, R. Vaiyapuri, L. Zhang, J.M. Chan, Lipid-coated polymeric nanoparticles for cancer drug delivery, Biomater. Sci. 3 (2015) 923.
[20] S. Bhattacharyya, R.A. Kudgus, R. Bhattacharya, P. Mukherjee, Inorganic nanoparticles in cancer therapy, Pharm. Res. 28 (2) (2011) 237–259.
[21] M.P. Vinardell, M. Mitjans, Antitumor activities of metal oxide nanoparticles, Nano 5 (2015) 1004–1021.
[22] N.S. Chaudhari, A.P. Pandey, P.O. Patil, A.R. Tekade, S.B. Bari, P.K. Deshmukh, Graphene oxide based magnetic nanocomposites for efficient treatment of breast cancer, Mat. Sci. Eng. C. 37 (2014) 278–285.
[23] Y. Zhang, Y. Huang, S. Li, Polymeric micelles: nanocarriers for cancer-targeted drug delivery, AAPS. Pharm. Sci. Tech. 15 (4) (2014) 862–871.
[24] C.K. Liu, Q. Dou, S.S. Liow, J.N. Kumar, X.J. Loh, Cationic micelles based on polyhedral oligomeric Silsesquioxanes for enhanced gene transfection, Aust. J. Chem. 69 (2016) 363.
[25] X. Fan, Z. Li, X.J. Loh, Recent development of unimolecular micelles as functional materials and applications, Polym. Chem. 7 (2016) 5898.
[26] X.J. Loh, S.J. Ong, Y.T. Tung, H.T. Choo, Co-delivery of drug and DNA from cationic dual-responsive micelles derived from poly (DMAEMA-co-PPGMA), Mat. Sci. Eng. C 33 (2013) 4545–4550.
[27] X.J. Loh, S.J. Ong, Y.T. Tung, H.T. Choo, Dual responsive micelles based on poly [(R)-3-hydroxybutyrate] and poly(2-(di-methylamino)ethyl methacrylate) for effective doxorubicin delivery, Polym. Chem. 4 (2013) 2564.
[28] X.J. Loh, Poly (DMAEMA-co-PPGMA): dual-responsive “reversible” micelles, J. Appl. Polym. Sci. 127 (2013) 992.
[29] X.J. Loh, M.-H. Tsai, J. Barrio, E.A. Appel, T.-C. Lee, O.A. Scherman, Triggered insulin release studies of triply responsive supramolecular micelles, Polym. Chem. 3 (2012) 3180.
[30] X.J. Loh, J. Barrio, P.P.C. Toh, T.-C. Lee, D. Jiao, U. Rauwald, E.A. Appel, O.A. Scherman, Triply triggered doxorubicin release from supramolecular nanocontainers, Biomacromolecules 13 (2012) 84.
[31] X.J. Loh, Z.-X. Zhang, Y.-L. Wu, T.S. Lee, J. Li, Synthesis of novel biodegradable thermoresponsive triblock copolymers based on poly [(*R*)-3-hydroxybutyrate] and poly(*N*-isopropylacrylamide) and their formation of thermoresponsive micelle, Macromolecules 42 (2008) 194.
[32] S. Somani, C. Dufès, Applications of dendrimers for brain delivery and cancer therapy, Nanomedicine 9 (15) (2014) 2403–2414.
[33] W. Lohcharoenkal, L. Wang, Y.C. Chen, Y. Rojanasakul, Protein nanoparticles as drug delivery carriers for cancer therapy, Bio. Med. Res. Int. 2014 (2014) 12, http://dx.doi.org/10.1155/2014/180549.
[34] F. Kratz, Albumin as a drug carrier: design of prodrugs, drug conjugates and nanoparticles, J. Control. Release 132 (2008) 171–183.
[35] M.T. Larsen, M. Kuhlmann, M.L. Hvam, K.A. Howard, Albumin-based drug delivery: harnessing nature to cure disease, Mol. Cell. Ther. 4 (2016) 1–12.
[36] A.O. Elzoghby, W.M. Samy, N.A. Elgindy, Albumin-based nanoparticles as potential controlled release drug delivery systems, J. Control. Release 157 (2012) 168–182.
[37] M. Karimi, S. Bahrami, S.B. Ravari, P.S. Zangabad, H. Mirshekari, M. Bozorgomid, S. Shahreza, M. Sori, M.R. Hamblin, Albumin nanostructures as advanced drug delivery systems, Expert Opin. Drug. Del. (2016), http://dx.doi.org/10.1080/17425247.2016.1193149.
[38] R. Tantra, J. Tompkins, P. Quincey, Characterisation of the de-agglomeration effects of bovine serum albumin on nanoparticles in aqueous suspension, Colloids Surf. B: Biointerfaces 75 (2010) 275–281.
[39] U. Bairagi, P. Mittal, B. Mishra, Albumin: a versatile drug carrier, Austin Ther. 2 (2) (2015) 1021.
[40] T. Peters Jr., All About Albumin, Academic Press, USA, 1996.
[41] D.C. Carter, J.X. Ho, Serum albumin, Ad. V. Protein Chem. 45 (1994) 153–203.
[42] D. Sleep, Albumin and its application in drug delivery, Expert Opin. Drug Deliv. 12 (6) (2014) 1–20.
[43] S.K. Podaralla, O.P. Perumal, R.S. Kaushik, Design and formulation of Protein based NPDDS, in: Y. Pathak, D. Thassu (Eds.), Drug Delivery Nanoparticles Formulation and Characterization, CRC Press, Informa Health Care, New York, 2016, pp. 69–91.
[44] S.H. Lee, D. Heng, W.K. Ng, H.K. Chan, R.B. Tan, Nano spray drying: a novel method for preparing protein nanoparticles for protein therapy, Int. J. Pharm. 403 (2011) 192–200.
[45] A. Sosnik, K.P. Seremet, Advantages and challenges of the spray-drying technology for the production of pure drug particles and drug-loaded polymeric carriers, Adv. Colloid Interf. Sci. (2015), http://dx.doi.org/10.1016/j.cis.2015.05.003.
[46] E.S. Lee, Y.S. Youn, Albumin-based potential drugs: focus on half-life extension and nanoparticle preparation, J. Pharm. Inves. 6 (2016) 305–315.
[47] Ana Loureiroa, Nuno G. Azoiaa, Andreia C. Gomesb, Artur Cavaco-Paulo, Albumin-based nanodevices as drug carriers, Curr. Pharm. Des. 22 (2016) 1371–1390.
[48] Y. Wu, E.K. Shih, A. Ramanathan, S. Vasudevan, T. Weil, Nano-sized albumin-copolymer micelles for efficient doxorubicin delivery, Biointerphases 7 (2012) 5, http://dx.doi.org/10.1007/s13758-011-0005-7.
[49] L. Chen, F. Chen, M. Zhao, X. Zhu, C. Ke, J. Yu, Z. Yan, F. Zhang, Y. Sun, D. Chen, C. Jiang, X. Zhao, Y. Gao, S. Guo, W. Li, A redox-sensitive micelle-like nanoparticle self-assembled from amphiphilic adriamycin-human serum albumin conjugates for tumor targeted therapy, Biomed. Res. Int. 2015 (2015) 1–10.
[50] Y. Jiang, H. Lu, F. Chen, M. Callari, M. Pourgholami, D.L. Morris, M.H. Stenzel, Pegylated albumin-based polyion complex micelles for protein delivery, Biomacromolecules 17 (2016) 808–817.
[51] Y. Jiang, H. Lu, Y.Y. Khine, A. Dag, M.H. Stenzel, Polyion complex micelle based on albumin-polymer conjugates: multifunctional oligonucleotide transfection vectors for anticancer chemotherapeutics, Biomacromolecules (2014), http://dx.doi.org/10.1021/bm501205x.
[52] Y. Jiang, M. Liang, D. Svejkar, G. Hart-Smith, H. Lu, W. Scarano, M.H. Stenze, Albumin-micelles via a one-pot technology platform for the delivery of drugs, Chem. Commun. 50 (2014) 6394.
[53] F. Liu, J. Mu, B. Xing, Recent advances on the development of pharmacotherapeutic agents on the basis of human serum albumin, Cur. Pharm. Des. 21 (00) (2015) 1–23.

[54] F. Krats, Drug conjugates with albumin and transferrin, Expert Opin. Ther. Patents 12 (3) (2002) 433–439.
[55] N. Sepehri, H. Rouhani, A.R. Ghanbarpour, M. Gharghabi, F. Tavassolian, M. Amini, S.N. Ostad, M.H. Ghahremani, R. Dinarvand, Human serum albumin conjugates of 7-ethyl-10-hydroxycamptothecin (SN38) for cancer treatment, Bio. Med. Res. Int. 2014 (2014) 1–11.
[56] G. Stehle, H. Sinn, A. Wunder, H.H. Schrenk, S. Schutt, W. Maier-Borst, D.L. Heene, The loading rate determines tumor targeting properties of methotrexate-albumin conjugates in rats, Anti-Cancer Drugs 8 (1997) 677–685.
[57] G. Stehle, A. Wunder, H. Sinn, H.H. Schrenk, S. Schutt, E. Frei, G. Hartung, W. Maier-Borst, D.L. Heene, Pharmacokinetics of methotrexate-albumin conjugates in tumor-bearing rats, Anti-Cancer Drugs 8 (1997) 835–844.
[58] F. Esmaeili, R. Dinarvand, M.H. Ghahremani, M. Amini, H. Rouhani, N. Sepehri, S.N. Ostad, F. Atyabi, Docetaxel–albumin conjugates: preparation, in vitro evaluation and biodistribution studies, J. Pharm. Sci. 98 (8) (2009) 2718–2730.
[59] H. Jeong, M.S. Huh, S.J. Lee, H. Koo, I.C. Kwon, S.Y. Jeong, K. Kim, Photosensitizer-conjugated human serum albumin nanoparticles for effective photodynamic therapy, Theranostics 1 (2011) 230–239.
[60] Y.R. Zheng, K. Suntharalingam, T.C. Johnstone, H. Yoo, W. Lin, J.G. Brooks, S.J. Lippard, Pt(IV) prodrugs designed to bind non-covalently to human serum albumin for drug delivery, J. Am. Chem. Soc. 136 (2014) 8790–8798.
[61] J. Mayr, P. Heffeter, D. Groza, L. Galvez, G. Koellensperger, A. Roller, B. Alte, M. Haider, W. Berger, C.R. Kowoland, B.K. Keppler, An albumin-based tumor-targeted oxaliplatin prodrug with distinctly improved anticancer activity in vivo, Chem. Sci. (2016), http://dx.doi.org/10.1039/c6sc03862j.
[62] J. Qi, Y. Gou, Y. Zhang, K. Yang, S. Chen, L. Liu, X. Wu, T. Wang, W. Zhang, F. Yang, Developing anticancer ferric prodrugs based on the N-donor residues of human serum albumin carrier IIa subdomain, J. Med. Chem. 59 (2016) 7497–7511.
[63] Y. Wu, D.Y.W. Ng, S.L. Kuan, T. Weil, Protein–polymer therapeutics: a macromolecular perspective, Biomater. Sci. (2014), http://dx.doi.org/10.1039/c4bm00270a.
[64] Y. Jiang, M. Stenzel, Drug delivery vehicles based on albumin–polymer conjugates, Macromol. Biosci. 16 (2016) 791–802.
[65] Z. Liu, C. Dong, X. Wang, H. Wang, W. Li, J. Tan, J. Chang, Self-assembled biodegradable protein − polymer vesicle as a tumor-targeted nanocarrier, ACS Appl. Mater. Interfaces 26 (2014) 2393.
[66] J. Liu, V. Bulmus, D.L. Herlambang, C. Barner-Kowollik, M.H. Stenzel, T.P. Davis, In situ formation of protein–polymer conjugates through reversible addition fragmentation chain transfer polymerization, Angew. Chem. Int. Ed. 46 (2007) 3099.
[67] N. Vanparijs, S. Maji, B. Louage, L. Voorhaar, D. Laplace, Q. Zhang, Y. Shi, W.E. Hennink, R. Hoogenboom, B.G. De Geest, Polymer-protein conjugation via a 'grafting to' approach – a comparative study of the performance of protein-reactive RAFT chain transfer agents, Polym. Chem. 6 (2015) 5602.
[68] I. Cobo, M. Li, B.S. Sumerlin, S. Perrier, Smart hybrid materials by conjugation of responsive polymers to biomacromolecules, Nat. Mater. 14 (2015) 143.
[69] K.L. Heredia, H.D. Maynard, Synthesis of protein-polymer conjugates, Org. Biomol. Chem. 5 (2007) 45–53.
[70] J. Ge, E. Neofytou, J. Lei, R.E. Beygui, R.N. Zare, Protein–polymer hybrid nanoparticles for drug delivery, Small 8 (2012) 3573.
[71] S. Manoochehri, B. Darvishi, G. Kamalinia, M. Amini, M. Fallah, S.N. Ostad, F. Atyabi, R. Dinarvand, Surface modification of PLGA nanoparticles via human serum albumin conjugation for controlled delivery of docetaxel, Daru J. Pharm. Sci. 21 (2013) 58.
[72] A. Dag, Y. Jiang, K.J.A. Karim, G. Hart-Smith, W. Scarano, M.H. Stenzel, Polymer–Albumin Conjugate for the Facilitated Delivery of Macromolecular Platinum Drugs, Macromol. Rapid Commun. (2015), http://dx.doi.org/10.1002/marc.201400576.
[73] P.H. Chan, Y.C. Chen, Human serum albumin stabilized gold nanoclusters as selective luminescent probes for staphylococcus aureus and methicillin-resistant staphylococcus aureus, Anal. Chem. 84 (2012) 8952–8956.
[74] F. Cañaveras, R. Madueño, J.M. Sevilla, M. Blázquez, T. Pineda, Role of the functionalization of the gold nanoparticle surface on the formation of bioconjugates with human serum albumin, J. Phys. Chem. C 116 (2012) 10430–10437.
[75] Q. Chen, L. Feng, J. Liu, W. Zhu, Z. Dong, Y. Wu, Z. Liu, Intelligent albumin–MnO_2 nanoparticles as pH/H_2O_2-responsive dissociable nanocarriers to modulate tumor hypoxia for effective combination therapy, Adv. Mater. (2016), http://dx.doi.org/10.1002/adma.201601902.
[76] L. Treuel, S. Brandholt, P. Maffre, S. Wiegele, L. Shang, G.U. Nienhaus, Impact of protein modification on the protein corona on nanoparticles and nanoparticle-cell interactions, ACS Nano 8 (2014) 503–513.
[77] J. Mariam, S. Sivakami, D. Kothari, P. Dongre, Bioactivity of albumins bound to silver nanoparticles, Protein J. 33 (2014) 258–266.
[78] M. Schäffler, F. Sousa, A. Wenk, et al., Blood protein coating of gold nanoparticles as potential tool for organ targeting, Biomaterials 35 (2014) 3455–3466.
[79] Q. Quan, J. Xie, H. Gao, et al., HSA coated iron oxide nanoparticles as drug delivery vehicles for cancer therapy, Mol. Pharm. 8 (2011) 1669–1676.
[80] J. Nicolas, S. Mura, D. Brambilla, N. Mackiewicz, P. Couvreur, Design, functionalization strategies and biomedical applications of targeted biodegradable/biocompatible polymer-based nanocarriers for drug delivery, Chem. Soc. Rev. (2013), http://dx.doi.org/10.1039/c2cs35265f.
[81] A. Taheri, R. Dinarvand, F. Atyabi, F. Nouri, F. Ahadi, M.H. Ghahremani, S.N. Ostad, A.T. Borougeni, P. Mansoori, J. Biomed. Nanotechnol. 7 (2011) 743.
[82] Z. Shen, W. Wei, H. Tanaka, K. Kohama, G. Ma, T. Dobashi, Y. Maki, H. Wang, J. Bi, S. Dai, Pharmacol. Res. 64 (2011) 410.
[83] R. Xu, M. Fisher, R.L. Juliano, Targeted albumin-based nanoparticles for delivery of amphipathic drugs, Bioconjug. Chem. 22 (2011) 870.
[84] S. Ji, J. Xu, B. Zhang, W. Yao, W. Xu, W. Wu, Y. Xu, H. Wang, Q. Ni, H. Hou, X. Yu, Cancer Biol. Ther. 13 (2012) 206.
[85] M.G. Anhorn, S. Wagner, J. Kreuter, K. Langer, H. von Briesen, Bioconjug. Chem. 19 (2008) 2321.
[86] I. Steinhauser, B. Spänkuch, K. Strebhardt, K. Langer, Biomaterials 27 (2006) 4975.
[87] S. Wagner, F. Rothweiler, M.G. Anhorn, D. Sauer, I. Riemann, E.C. Weiss, A. Katsen-Globa, M. Michaelis, J. Cinatl Jr., D. Schwartz, J. Kreuter, H. von Briesen, K. Langer, Biomaterials 31 (2010) 2388.
[88] X. Wang, M. Tu, B. Tian, Y. Yi, Z. Wei, F. Wei, Synthesis of tumor-targeted folate conjugated fluorescent magnetic albumin nanoparticles for enhanced intracellular dual-modal imaging into human brain tumor cells, Anal. Biochem. (2016), http://dx.doi.org/10.1016/j.ab.2016.08.010.
[89] H.J. Byeon, L.Q. Thao, S. Lee, S.Y. Min, E.S. Lee, B.S. Shin, H.G. Choi, Y.S. Youn, Doxorubicin-loaded nanoparticles consisted of cationic- and mannose-modifiedalbumins for dual-targeting in brain tumors, J. Control. Release (2016), http://dx.doi.org/10.1016/j.jconrel.2016.01.046.
[90] X. Yu, Y. Song, Y. Di, H. He, D. Fu, C. Jin, Enhanced tumor targeting of cRGD peptide-conjugated albumin nanoparticles in the BxPC-3 cell line, Sci Rep 6 (2016) 31539, http://dx.doi.org/10.1038/srep31539.
[91] J. Li, T. Chen, F. Deng, J. Wan, Y. Tang, P. Yuan, L. Zhang, Synthesis, characterization, and in vitro evaluation of curcumin-loaded albumin nanoparticles surface-functionalized with glycyrrhetinic acid, Int. J. Nanomedicine 10 (2015) 5475–5487.
[92] C. Muller, R. Schibli, Folic acid conjugates for nuclear imaging of folate receptorpositive cancer, J. Nucl. Med. 52 (2011) 1–4.
[93] Y. Lu, P.S. Low, Folate-mediated delivery of macromolecular anticancer therapeutic agents, Adv. Drug Deliv. Rev. 64 (2012) 342–352.
[94] W. Yang, Y. Cheng, T. Xu, X. Wang, L.P. Wen, Eur. J. Med. Chem. 44 (2009) 862.
[95] M. Goto, H. Yura, C.-W. Chang, A. Kobayashi, T. Shinoda, A. Maeda, S. Kojima, K. Kobayashi, T. Akaike, J. Control. Release 28 (1994) 223.
[96] E.A. Turley, P.W. Noble, L.Y. Bourguignon, J. Biol. Chem. 277 (2002) 4589.
[97] R.E. Eliaz, F.C. Szoka, Cancer Res. 61 (2001) 2592.
[98] P.P. Karmali, V.R. Kotamraju, M. Kastantin, M. Black, D. Missirlis, M. Tirrell, E. Ruoslahti, Targeting of albumin-embedded paclitaxel nanoparticles to tumors, Nanomedicine 5 (2009) 73–82.
[99] K. Ulbrich, T. Hekmatara, E. Herbert, J. Kreuter, Transferrin- and transferrinreceptor-antibody-modified nanoparticles enable drug delivery across the blood–-brain barrier (BBB), Eur. J. Pharm. Biopharm. 71 (2009) 251–256.
[100] A. Zensi, D. Begley, C. Pontikis, C. Legros, L. Mihoreanu, S. Wagner, C. Büchel, H. von Briesen, J. Kreuter, Albumin nanoparticles targeted with Apo E enter the CNS by transcytosis and are delivered to neurons, J. Control. Release 137 (2009) 78–86.
[101] J. Kreuter, T. Hekmatara, S. Dreis, T. Vogel, S. Gelperina, K. Langer, Covalent attachment of apolipoprotein A-I and apolipoprotein B-100 to albumin nanoparticles enables drug transport into the brain, J. Control. Release 118 (2007) 54–58.
[102] V. Mishra, S. Mahor, A. Rawat, P.N. Gupta, P. Dubey, K. Khatri, S.P. Vyas, Targeted brain delivery of AZT via transferrin anchored pegylated albumin nanoparticles, J. Drug Target. 14 (2006) 45–53.
[103] Z. Su, L. Xing, Y. Chen, Y. Xu, F. Yang, C. Zhang, Q. Ping, Y. Xiao, Lactoferrin-modified poly(ethylene glycol)-grafted BSA nanoparticles as a dual-targeting carrier for treating brain gliomas, Mol. Pharm. 11 (2014) 1823–1834.
[104] D. Sutton, N. Nasongkla, E. Blanco, J. Gao, Pharm. Res. 24 (2007) 1029.
[105] E. Pereverzeva, I. Treschalin, D. Bodyagin, O. Maksimenko, K. Langer, S. Dreis, B. Asmussen, J. Kreuter, S. Gelperina, Influence of the formulation on the tolerance profile of nanoparticle-bound doxorubicin in healthy rats: focus on cardio- and testicular toxicity, Int. J. Pharm. 337 (2007) 346–356.
[106] R. Zucchi, R. Danesi, Cardiac toxicity of antineoplastic anthracyclines, Curr. Med. Chem. Anticancer Agent. 3 (2003) 151–171.
[107] L.D. Russell, J.A. Russell, Short-term morphological response of the rat testis to administration of five chemotherapeutic agents, Am. J. Anat. 192 (1991) 142–168.
[108] H. Kouchakzadeh, S.A. Shojaosadati, A. Maghsoudi, E.V. Farahani, Optimization of PEGylation conditions for BSA nanoparticles using response surface methodology, AAPS Pharm. Sci. Tech. 11 (2010) 1206–1211.
[109] W. Lin, M.C. Garnett, S.S. Davis, E. Schacht, P. Ferruti, L. Illum, Preparation and characterization of Rose Bengal-loaded surface-modified albumin nanoparticles, J. Control. Release 71 (2001) 117–126.
[110] C. Zheng, H. Gao, D.-P. Yang, M. Liu, H. Cheng, Y.-L. Wu, X.J. Loh, PCL-based thermo-gelling polymers for in vivo delivery of chemotherapeutics to tumors, Mat. Sci. Engi. C. 74 (2017) 110–116.
[111] S.S. Liow, Q. Dou, D. Kai, Z. Li, S. Sugiarto, C. Yu, R. Kwok, X. Chen, Y.-L. Wu, S.T. Ong, A. Kizhakeyil, N.K. Verma, B.Z. Tang, X.J. Loh, Long-term real-time in vivo drug release monitoring with AIE thermogelling polymer, Small 13 (2017) 1603404.
[112] H. Ye, C. Owh, S. Jiang, C. Zhen, Q. Ng, D. Wirawa, X.J. Loh, A thixotropic polyglycerol Sebacate-based supramolecular hydrogel as an injectable drug delivery matrix, Polymer 8 (2016) 130.
[113] Y.-L. Wu, H. Wang, Y.-K. Qiud, X.J. Loh, PLA-based thermogel for the sustained delivery of chemotherapeutics in a mouse model of hepatocellular carcinoma, RSC Adv. 6 (2016) 44506.
[114] X.J. Loh, T.-C. Lee, Q. Doua, G.R. Deene, Utilising inorganic nanocarriers for gene delivery, Biomater. Sci. 4 (2016) 70.
[115] X.J. Loh, B.J.H. Yee, F.S. Chia, Sustained delivery of paclitaxel using thermogelling poly(PEG/PPG/PCL urethane)s for enhanced toxicity against cancer cells, J. Biomed. Mater. Res. A. 100 (2012) 2686.
[116] X.J. Loh, W. Guerinb, S.M. Guillaume, Sustained delivery of doxorubicin from thermogelling poly(PEG/PPG/PTMC urethane)s for effective eradication of cancer cells, J. Mater. Chem. 22 (2012) 21249.
[117] X.J. Loh, J. Li, Biodegradable thermosensitive copolymer hydrogels for drug delivery, Expert Opin. Ther. Patents 17 (2007) 965.
[118] S. Zhang, G. Wang, X. Lin, M. Chatzinikolaidou, H. Jennissen, M. Laub, Polyethylenimine-coated albumin nanoparticles for BMP-2 delivery, Biotechnol. Prog. 24 (2008) 945–956.

[119] S. Zhang, M.R. Doschak, H. Uludağ, Pharmacokinetics and bone formation by BMP-2 entrapped in polyethylenimine-coated albumin nanoparticles, Biomaterials 30 (2009) 5143–5155.
[120] S. Abbasi, A. Paul, W. Shao, et al., Cationic albumin nanoparticles for enhanced drug delivery to treat breast cancer: preparation and in vitro assessment, J. Drug Deliv. 2012 (2012) 686108.
[121] H.D. Singh, G. Wang, H. Uludağ, L.D. Unsworth, Poly-L-lysine-coated albumin nanoparticles: stability, mechanism for increasing. In vitro enzymatic resilience and siRNA release characteristics, Acta Biomater. 6 (2010) 4277–4284.
[122] Z.Y. Shen, G.H. Ma, T. Dobashi, Y. Maki, Z.G. Su, Preparation and characterization of thermo-responsive albumin nanospheres, Int. J. Pharm. 346 (2008) 133–142.
[123] Z. Shen, W. Wei, Y. Zhao, G. Ma, T. Dobashi, Y. Maki, Z. Su, J. Wan, Thermosensitive polymer-conjugated albumin nanospheres as thermal targeting anti-cancer drug carrier, Eur. J. Pharm. Sci. 35 (2008) 271–282.
[124] T.A. John, S.M. Vogel, C. Tiruppathi, A.B. Malik, R.D. Minshall, Quantitative analysis of albumin uptake and transport in the rat microvessel endothelial monolayer, Am. J. Phys. Lung Cell. Mol. Phys. 284 (2003) L187–L196.
[125] R.D. Minshall, C. Tiruppathi, S.M. Vogel, A.B. Malik, Vesicle formation and trafficking in endothelial cells and regulation of endothelial barrier function, Histochem. Cell Biol. 117 (2002) 105–112.
[126] S.M. Vogel, R.D. Minshall, M. Pilipovic, C. Tiruppathi, A.B. Malik, Albumin uptake and transcytosis in endothelial cells in vivo induced by albumin-binding protein, Am. J. Phys. Lung Cell. Mol. Phys. 281 (2001) L1512–L1522.
[127] B. Chen, X.Y. He, X.Q. Yi, R.X. Zhuo, S.X. Cheng, Dual-peptide functionalized albumin-based nanoparticles with ph dependent self-assembly behavior for drug delivery, ACS Appl. Mater. Interfaces (2015), http://dx.doi.org/10.1021/acsami.5b03866.
[128] M. Kamali, R. Dinarvand, H. Maleki, H. Arzani, P. Mahdaviani, H. Nekounam, M. Adabi, M. Khosravani, Preparation of imatinib base loaded human serum albumin for application in the treatment of glioblastoma, RSC Adv. 5 (2015) 62214–62219.
[129] H. Gao, S. Cao, Z. Yang, S. Zhang, Q. Zhang, X. Jiang, Preparation, characterization and anti-glioma effects of docetaxel-incorporated albumin-lipid nanoparticles, J. Biomed. Nanotechnol. 11 (2015) 2137–2147.
[130] W. Lu, J. Wan, Q. Zhang, Z. She, X. Jiang, Aclarubicin-loaded cationic albumin-conjugated pegylated nanoparticles for glioma chemotherapy in rats, Int. J. Cancer 120 (2006) 420–431.
[131] X. Yi, X. Lian, J. Dong, Z. Wan, C. Xia, X. Song, Y. Fu, T. Gong, Z. Zhang, Co-delivery of pirarubicin and paclitaxel by human serum albumin nanoparticles to enhance antitumor effect and reduce systemic toxicity in breast cancers, Mol. Pharm. (2015), http://dx.doi.org/10.1021/acs.molpharmaceut.5b00536.
[132] X. Wan, X. Zheng, X. Pang, Z. Zhang, Q. Zhang, Incorporation of lapatinib into human serum albumin nanoparticles with enhanced anti-tumor effects in HER2-positive breast cancer, Colloids Surf. B: Biointerfaces (2015), http://dx.doi.org/10.1016/j.colsurfb.2015.10.018.
[133] M. Kordezangeneh, S. Irani, R. Mirfakhraie, M. Esfandyari-Manesh, F. Atyabi, R. Dinarvand, Regulation of BAX/BCL2 gene expression in breast cancer cells by docetaxel-loaded human serum albumin nanoparticles, Med. Oncol. 32 (2015) 208.
[134] A. Taheri, R. Dinarvand, F. Ahadi, M.R. Khorramizadeh, F. Atyabi, The in vivo antitumor activity of LHRH targeted methotrexate–human serum albumin nanoparticles in 4T1 tumor-bearing Balb/c mice, Int. J. Pharm. 431 (2012) 183–189.
[135] N. Nateghian, N. Goodarzi, M. Amini, F. Atyabi, M. Reza, K.R. Dinarvand, Biotin/folate-decorated human serum albumin nanoparticles of docetaxel: comparison of chemically conjugated nanostructures and physically loaded nanoparticles for targeting of breast cancer, Chem. Biol. Drug Des. 87 (2016) 69–82.
[136] Y. Chen, J. Wang, J. Wang, L. Wang, X. Tan, K. Tu, X. Tong, L. Qi, Aptamer functionalized cisplatin-albumin nanoparticles for targeted delivery to epidermal growth factor receptor positive cervical cancer, J. Biomed. Nanotechnol. 12 (2016) 656–666.
[137] Z. Song, Y. Lu, X. Zhang, H. Wang, J. Han, C. Dong, Novel curcumin-loaded human serum albumin nanoparticles surface functionalized with folate: characterization and in vitro/vivo evaluation, Drug Des. Dev. Ther. 10 (2016) 2643–2649.
[138] S. Lee, C. Lee, B. Kim, L.Q. Thao, E.S. Lee, J.O. Kim, K.T. Oh, H.G. Choi, Y.S. Youn, A novel prototype of albumin nanoparticles fabricated bysupramolecular cyclodextrin-adamantane association, Colloids Surf. B: Biointerfaces 147 (2016) 281–290.
[139] L.Q. Thao, H.J. Byeon, C. Lee, S. Lee, E.S. Lee, Y.W. Choi, H.G. Choi, E.S. Park, K.C. Lee, Y.S. Youn, Doxorubicin bound albumin nanoparticles containing a trail protein for targeted treatment of colon cancer, Pharm. Res. (2015), http://dx.doi.org/10.1007/s11095-015-1814-z.
[140] F. Li, C. Zheng, J. Xin, F. Chen, H. Ling, L. Sun, T.J. Webster, X. Ming, J. Liu, Enhanced tumor delivery and antitumor response of doxorubicin-loaded albumin nanoparticles formulated based on a Schiff base, Int. J. Nanomedicine 11 (2016) 3875–3890.
[141] Y. Zu, L. Meng, X. Zhao, Y. Ge, X. Yu, Y. Zhang, Y. Deng, Preparation of 10-hydroxycamptothecin-loaded glycyrrhizic acid-conjugated bovine serum albumin nanoparticles for hepatocellular carcinoma-targeted drug delivery, Int. J. Nanomedicine 8 (2013) 1207–1222.
[142] W.W. Qi, H. Yu, H. Guo, J. Lou, Z. Wang, P. Liu, A. Sapin-Minet, P. Maincent, X.C. Hong, X. Hu, Y. Xiao, Doxorubicin-loaded glycyrrhetinic acid-modified recombinant human serum albumin nanoparticles for targeting liver tumor chemotherapy, Mol. Pharm. (2015), http://dx.doi.org/10.1021/mp500394v.
[143] J.E. Chang, W.S. Shim, S.G. Yang, E.Y. Kwak, S. Chong, D.D. Kim, S.J. Chung, C.K. Shim, Liver cancer targeting of doxorubicin with reduced distribution to the heart using hematoporphyrin-modified albumin nanoparticles in rats, Pharm. Res. 29 (2012) 795–805.
[144] S.H. Choi, H.J. Byeon, J.S. Choi, L. Thao, I. Kim, E.S. Lee, B.S. Shin, K.C. Lee, Y.S. Youn, Inhalable self-assembled albumin nanoparticles for treating drug-resistant lung cancer, J. Control. Release (2014), http://dx.doi.org/10.1016/j.jconrel.2014.11.008.
[145] G. Jin, M. Jin, X. Yin, Z. Jin, L. Chen, Z. Gao, A comparative study on the effect of docetaxel-albumin nanoparticles and docetaxel-loaded PEG-albumin nanoparticles against non-small cell lung cancer, Int. J. Oncol. 47 (2015) 1945–1953.
[146] F. Chen, J. Wu, C. Zheng, J. Zhu, Y. Zhang, X. You, F. Cai, V. Shah, J. Liu, L. Ge, TPGS modified reduced bovine serum albumin nanoparticles as a lipophilic anticancer drug carrier for overcoming multidrug resistance, J. Mater. Chem. 4 (2016) 3959–3968.
[147] B. Chen, C. Wu, R.X. Zhuo, S.X. Cheng, A self-assembled albumin based multiple drug delivery nanosystem to overcome multidrug resistance, RSC Adv. 5 (2015) 6807–6814.
[148] L. Noorani, M. Stenzel, R. Liang, M.H. Pourgholami, D.L. Morris, Albumin nanoparticles increase the anticancer efficacy of albendazole in ovarian cancer xenograft model, J. Nanobiotechnol. 13 (25) (2015) 1–12.
[149] X. Yu, Y. Di, C. Xie, Y. Song, H. He, H. Li, X. Pu, W. Lu, D. Fu, C. Jin, An in vitro and in vivo study of gemcitabine-loaded albumin nanoparticles in a pancreatic cancer cell line, Int. J. Nanomedicine 10 (2015) 6825–6834.
[150] S.Y. Min, H.J. Byeon, C.K. Lee, J. Seo, E.S. Lee, B.S. Shin, H.G. Choi, K.C. Lee, Y.S. Youn, Facile one-pot formulation of TRAIL-embedded paclitaxel-bound albumin nanoparticles for the treatment of pancreatic cancer, Int. J. Pharm. (2015), http://dx.doi.org/10.1016/j.ijpharm.2015.08.055.
[151] X. Tai, Y. Wang, L. Zhang, Y. Yang, K. Shi, S. Ruan, Y. Liu, H. Gao, Z. Zhang, Q. He, Cabazitaxel and indocyanine green codelivery tumor-targeting nanoparticle for improved antitumor efficacy and minimized drug toxicity, J. Drug Target. (2016), http://dx.doi.org/10.1080/1061186X.2016.1233975.
[152] A. Taheri, R. Dinarvand, F.S. Nouri, M.R. Khorramizadeh, A.T. Borougeni, P. Mansoori, F. Atyabi, Use of biotin targeted methotrexate–human serum albumin conjugated nanoparticles to enhance methotrexate antitumor efficacy, Int. J. Nanomedicine 6 (2011) 1863–1874.
[153] L. Qi, Y. Guo, J. Luan, D. Zhang, Z. Zhao, Y. Luan, Folate-modified bexarotene-loaded bovine serum albumin nanoparticles as a promising tumor targeting delivery system, J. Mater. Chem. B 2 (2014) 8361.
[154] W. Cui, A. Wang, J. Zhao, X. Yang, P. Cai, J. Li, Layer by layer assembly of albumin nanoparticles with selective recognition of tumor necrosis factor-related apoptosis-inducing ligand (TRAIL), J. Colloid Interface Sci. 465 (2016) 11–17.
[155] S. Pulakkat, S.A. Balaji, A. Rangarajan, A.M. Raichur, Surface engineered protein nanoparticles with hyaluronic acid based multilayers for targeted delivery of anticancer agents, ACS Appl. Mater. Interfaces (2016), http://dx.doi.org/10.1021/acsami.6b04179.
[156] J. Zhou, X. Zhang, M. Li, W. Wu, X. Sun, L. Zhang, T. Gong, Novel lipid hybrid albumin nanoparticle greatly lowered toxicity of pirarubicin, Mol. Pharm. 10 (2013) 3832–3841.
[157] R. Xu, M. Fisher, R.L. Juliano, Targeted albumin-based nanoparticles for delivery of amphipathic drugs, Bioconjug. Chem. 22 (2011) 870–878.
[158] Wang Lin, Li Liu, Bingyang Dong, Hanying Zhao, Mingming Zhang, Wenjuan Chen, Yanhang Hong, Multi-stimuli-responsive biohybrid nanoparticles with cross-linked albumin coronae self-assembled by a polymer-protein biodynamer, Acta Biomater. 54 (2017) 259–270.
[159] J. Chen, Z. Guo, H. Tian, X. Chen, Production and clinical development of nanoparticles for gene delivery, Mol. Ther. Meth. Clin. Dev. 3 (2016) 16023, http://dx.doi.org/10.1038/mtm.2016.23.
[160] Y.S. Choi, M.Y. Lee, A.E. David, Y.S. Park, Nanoparticles for gene delivery: therapeutic and toxic effects, Mol. Cell Toxicol. 10 (2014) 1–8.
[161] C.Y. Chen, Y.N. Chang, P. Ryan, M. Linscott, G.J. McGarrity, Y.L. Chiang, Effect of herpes simplex virus thymidine kinase expression levels on ganciclovir-mediated cytotoxicity and the “bystander effect”, Hum. Gene Ther. 6 (11) (1995) 1467–1476.
[162] J. Chen, X. Dong, T. Feng, L. Lin, Z. Guo, J. Xia, et al., Charge-conversional zwitterionic copolymer as pH-sensitive shielding system for effective tumor treatment, Acta Biomater. 26 (2015) 45–53.
[163] J.C. Marx, J.A. Allay, D.A. Persons, S.A. Nooner, P.W. Hargrove, P.F. Kelly, E.F. Vanin, E.M. Horwitz, High-efficiency transduction and long-term gene expression with a murine stem cell retroviral vector encoding the green fluorescent protein in human marrow stromal cells, Hum. Gene Ther. 10 (7) (1999) 1163–1173.
[164] H. Boulaiz, J.A. Marchal, J. Prados, C. Melguizo, A. Aranega, Non-viral and viral vectors for gene therapy, Cell Mol. Biol. (Noisy-legrand). 51 (1) (2005) 3–22.
[165] J.Y. Sun, V. Anand-Jawa, S. Chatterjee, K.K. Wong, Immune responses to adeno-associated virus and its recombinant vectors, Gene Ther. 10 (11) (2003) 964–976.
[166] A.K. Zaiss, D.A. Muruve, Immune responses to adenoassociated virus vectors, Curr. Gene Ther. 5 (3) (2005) 323–331.
[167] A. Pensado, B. Seijo, A. Sanchez, Current strategies for DNA therapy based on lipid nanocarriers, Expert Opin. Drug Deliv. 11 (2014) 1721–1731.
[168] A.P. Pandey, K.K. Sawant, Polyethylenimine: A versatile, multifunctional non-viral vector for nucleic acid delivery, Mat. Sci. Engi. C 68 (2016) 904–918.
[169] D. Ibraheem, A. Elaissari, H. Fessi, Gene therapy and DNA delivery systems, Int. J. Pharm. 459 (2014) 70–83.
[170] Y.S. Lee, S.W. Kim, Bioreducible polymers for therapeutic gene delivery, J. Control. Release 190 (2014) 424–439.
[171] X. Fan, S. Jiang, Z. Li, X.J. Loh, Conjugation of poly(ethylene glycol) to poly(lactide)-based polyelectrolytes: an effective method to modulate cytotoxicity in gene delivery, Mater. Sci. Eng. C 73 (2017) 275–284.
[172] Advanced Healthcare Materials, 5 (2016), p. 2679.
[173] X.J. Loh, Y.-L. Wu, Cationic star copolymers based on b-cyclodextrins for efficient gene delivery to mouse embryonic stem cell colonies, Chem. Commun. (Camb.) 51 (2015) 10815.
[174] Q.Q. Dou, X. Fang, S. Jiang, P.L. Chee, T. Lee, X.J. Loh, Multi-functional fluorescent carbon dots with antibacterial and gene delivery properties, RSC Adv. 5 (2015) 46817.
[175] J. Li, X.J. Loh, Cyclodextrin-based supramolecular architectures: syntheses, structures, and applications for drug and gene delivery, Adv. Drug Deliv. Rev. 60 (2008) 1000–1017.

[176] A. Malhotra, B.R. Mittal, SiRNA gene therapy using albumin as a carrier, Pharmacogenet. Genomics 24 (12) (2014) 582–587.
[177] J. Look, N. Wilhelm, H. von Briesen, N. Noske, C. Günther, K. Langer, E. Gorjup, Ligand-modified human serum albumin nanoparticles for enhanced gene delivery, Mol. Pharm. 12 (2015) 3202–3213.
[178] J.-H. Choi, H.-J. Hwang, S.W. Shin, J.-W. Choi, S.H. Umand, B.-K. Oh, A novel albumin nanocomplex containing both small interfering RNA and gold nanorods for synergetic anticancer therapy, Nanoscale (2015), http://dx.doi.org/10.1039/c5nr00211g.
[179] W. Lu, Q. Sun, J. Wan, Z. She, X.-G. Jiang, Cationic albumin–conjugated pegylated nanoparticles allow gene delivery into brain tumors via intravenous administration, Cancer Res. 66 (24) (2006) 11878–11887.
[180] M. Karimi, P. Avci, R. Mobasseri, M.R. Hamblin, H. Naderi-Manesh, The novel albumin–chitosan core–shell nanoparticles for gene delivery: preparation, optimization and cell uptake investigation, J. Nanopart. Res. 15 (4) (2013) 1651, http://dx.doi.org/10.1007/s11051-013-1651-0.
[181] H. Zhang, X. Hou, M. Lin, L. Wang, H. Li, C. Yuan, C. Liang, J. Zhang, D. Zhang, The study on the preparation and characterization of gene-loaded immunomagnetic albumin nanospheres and their anti-cell proliferative effect combined with magnetic fluid hyperthermia on GLC-82 cells, Drug Des. Dev. Ther. 9 (2015) 6445–6460.
[182] J. Han, Q. Wang, Z. Zhang, T. Gong, X. Sun, Cationic bovine serum albumin based self-assembled nanoparticles as siRNA delivery vector for treating lung metastatic cancer, Small 10 (2014) 524–535.
[183] S. Son, S. Song, S.J. Lee, S. Min, S.A. Kim, J.Y. Yhee, et al., Self-crosslinked human serum albumin nanocarriers for systemic delivery of polymerized siRNA to tumors, Biomaterials 34 (2013) 9475–9485.
[184] C.M. Kummitha, A.S. Malamas, Z.R. Lu, Albumin pre-coating enhances intracellular siRNA delivery of multifunctional amphiphile/siRNA nanoparticles, Int. J. Nanomedicine 7 (2012) 5205–5214.
[185] J.P. Celli, B.Q. Spring, I. Rizvi, C.L. Evans, K.S. Samkoe, S. Verma, B.W. Pogue, T. Hasan, Imaging and photodynamic therapy: mechanisms, monitoring, and optimization, Chem. Rev. 110 (2010) 2795–2838.
[186] S. Lal, S.E. Clare, N.J. Halas, Nanoshell-enabled photothermal cancer therapy: impending clinical impact, Acc. Chem. Res. 41 (2008) 1842–1851.
[187] P. Huang, J. Lin, X. Wang, Z. Wang, C. Zhang, M. He, K. Wang, F. Chen, Z. Li, G. Shen, et al., Light-triggered theranostics based on photosensitizer-conjugated carbon dots for simultaneous enhanced-fluorescence imaging and photodynamic therapy, Adv. Mater. 24 (2012) 5104–5110.
[188] M. Guo, H. Mao, Y. Li, A. Zhu, H. He, H. Yang, Y. Wang, X. Tian, C. Ge, Q. Peng, et al., Dual imaging-guided photothermal/photodynamic therapy using micelles, Biomaterials 35 (2014) 4656–4666.
[189] R. Chen, X. Wang, X. Yao, X. Zheng, J. Wang, X. Jiang, Near-IR-triggered photothermal/photodynamic dual-modality therapy system via chitosan hybrid nanospheres, Biomaterials 34 (2013) 8314–8322.
[190] Z. Sheng, D. Hu, M. Zheng, P. Zhao, H. Liu, D. Gao, P. Gong, G. Gao, P. Zhang, Y. Ma, L. Cai, Smart human serum albumin-indocyanine green nanoparticles generated by programmed assembly for dual-modal imaging-guided cancer synergistic phototherapy, ACS Nano 8 (12) (2014) 12310–12322.
[191] Z. Li, E. Ye, David, R. Lakshminarayanan, X.J. Loh, Recent advances of using hybrid nanocarriers in remotely controlled therapeutic delivery, Small 12 (2016) 4782.
[192] C.A. Robertson, D. Hawkins Evans, H. Abrahamse, Photodynamic therapy (PDT): a short review on cellular mechanisms and cancer research applications for PDT, J. Photochem. Photobiol. B Biol. 96 (2009) 1–8.
[193] Y. Ge, Y. Ma, L. Li, The application of prodrug-based nano-drug delivery strategy in cancer combination therapy, Colloids Surf. B: Biointerfaces 146 (2016) 482–489.
[194] P. Agostinis, et al., Photodynamic therapy of cancer: an update, CA Cancer J. Clin. 61 (4) (2011) 250–281.
[195] K. Chen, A. Preuß, S. Hackbarth, M. Wacker, K. Langer, B. Röder, Novel photosensitizer-protein nanoparticles for photodynamic therapy: photophysical characterization and in vitro investigations, J. Photochem. Photobiol. B Biol. 96 (2009) 66–74.
[196] K. Chen, M. Wacker, S. Hackbarth, C. Ludwig, K. Langer, B. Röder, Photophysical evaluation of mTHPC-loaded HSA nanoparticles as novel PDT delivery systems, J. Photochem. Photobiol. B Biol. 101 (2010) 340–347.
[197] A.M. Molina, M. Morales-Cruz, M. Benítez, K. Berríos, C.M. Figueroa, et al., Redox-sensitive cross-linking enhances albumin nanoparticle function as delivery system for photodynamic cancer therapy, J. Nanomed. Nanotechnol. 6 (2015) 294, http://dx.doi.org/10.4172/2157-7439.1000294.
[198] S.-G. Yang, J.-E. Chang, B. Shin, S. Park, K. Na, C.-K. Shim, 99mTc-hematoporphyrin linked albumin nanoparticles for lung cancer targeted photodynamic therapy and imaging, J. Mater. Chem. 20 (2010) 9042–9046.
[199] K. Butzbach, F.A.O. Rasse-Suriani, M.M. Gonzalez, F.M. Cabrerizo, B. Epe, Albumin–folate conjugates for drug-targeting in photodynamic therapy, Photochem. Photobiol. 92 (2016) 611–619.
[200] Y. Zhang, L. He, J. Wu, K. Wang, J. Wang, W. Dai, A. Yuan, J. Wu, Y. Hu, Switchable PDT for Reducing Skin Photosensitization by a NIR dye Inducing Self-Assembled and Photo Disassembled Nanoparticles, Biomaterials, (2016), http://dx.doi.org/10.1016/j.biomaterials.2016.08.03 7.
[201] Q. Chen, Z. Liu, Albumin carriers for cancer theranostics: a conventional platform with new promise, Adv. Mater. (2016), http://dx.doi.org/10.1002/adma.201600038.
[202] Y. Jin, Y. Li, X. Ma, Z. Zha, L. Shi, J. Tian, Z. Dai, Encapsulating tantalum oxide into polypyrrole nanoparticles for X-ray CT/photoacoustic bimodal imaging-guided photothermal ablation of cancer, Biomaterials 35 (22) (2014) 5795–5804.
[203] Q. Chen, C. Wang, Z. Zhan, W. He, Z. Cheng, Y. Li, Z. Liu, Near-infrared dye bound albumin with separated imaging and therapy wavelength channels for imaging-guided photothermal therapy, Biomaterials 35 (2014) 8206–8214.
[204] Q. Chen, C. Liang, X. Wang, J. He, Y. Li, Z. Liu, An albumin based theranostic nano-agent for dual-modal imaging guided photothermal therapy to inhibit lymphatic metastasis of cancer post surgery, Biomaterials 35 (2014) 9355–9362.
[205] Q. Chen, X. Liu, J. Zeng, Z. Cheng, Z. Liu, Albumin-NIR dye self-assembled nanoparticles for photoacoustic pH imaging and pH-responsive photothermal therapy effective for large tumors, Biomaterials 98 (2016) 23–30.
[206] Z. Li, Y. Hu, T. Jiang, K.A. Howard, Y. Li, X. Fan, Y. Sun, F. Besenbacher, Y. Miao, Human-serum-albumin-coated Prussian blue nanoparticles as ph-/thermo-triggered drug-delivery vehicles for cancer thermochemotherapy, Part. Part. Syst. Charact. 33 (2016) 53–62.
[207] A. Sahu, J.H. Lee, H.G. Lee, Y.Y. Jeong, G. Tae, Prussian blue/serum albumin/indocyanine green as a multifunctional nanotheranostic agent for bimodal imaging guided laser mediated combinatorial phototherapy, J. Control. Release 236 (2016) 90–99.
[208] X. Song, C. Liang, H. Gong, Q. Chen, C. Wang, Z. Liu, Photosensitizer-conjugated albumin – polypyrrole nanoparticles for imaging-guided in vivo photodynamic/photothermal therapy, Small 11 (32) (2015) 3932–3941.
[209] W. Watcharin, C. Schmithals, T. Pleli, V. Köberle, H. Korkusuz, F. Hübner, O. Waidmann, S. Zeuzem, H.-W. Korf, A. Terfort, S. Gelperina, T.J. Vogl, J. Kreuter, A. Piiper, Detection of hepatocellular carcinoma in transgenic mice by Gd-DTPA- and rhodamine 123-conjugated human serum albumin nanoparticles in T1 magnetic resonance imaging, J. Control. Release 199 (2015) 63–71.
[210] Z. Liu, N. Chen, C. Dong, W. Li, W. Guo, H. Wang, S. Wang, J. Tan, Y. Tu, J. Chang, Facile construction of near infrared fluorescence nanoprobe with amphiphilic protein-polymer bioconjugate for targeted cell imaging, ACS Appl. Mater. Interfaces (2015), http://dx.doi.org/10.1021/acsami.5b05406.
[211] X. Hu, X. An, L. Li, Easy synthesis of highly fluorescent carbon dots from albumin and their photoluminescent mechanism and biological imaging applications, Mat. Sci. Eng. C (2015), http://dx.doi.org/10.1016/j.msec.2015.09.066.
[212] H. Moon, C. Yoon, T.W. Lee, K.-S. Ha, J.H. Chang, T.-K. Song, K. Kim, H. Kim, Therapeutic ultrasound contrast agents for the enhancement of tumor diagnosis and tumor therapy, J. Biomed. Nanotechnol. 11 (2015) 1183–1192.
[213] D. Yoo, J.H. Lee, T.H. Shin, J. Cheon, Theranostic magnetic nanoparticles, Acc. Chem. Res. 44 (2011) 863–874.
[214] A. Semkina, M. Abakumov, N. Grinenko, A. Abakumov, A. Skorikov, E. Mironova, G. Davydova, A.G. Majouga, N. Nukolova, A. Kabanov, V. Chekhonin, Core-shell-corona doxorubicin-loaded superparamagnetic Fe_3O_4 nanoparticles for cancer theranostics, Colloids Surf. B: Biointerfaces (2015), http://dx.doi.org/10.1016/j.colsurfb.2015.11.009.
[215] L.P. Kolluru, S.A.A. Rizvi, M. D'Souza, M.J. D'Souza, Formulation development of albumin based theragnostic nanoparticles as a potential delivery system for tumor targeting, J. Drug Target. 21 (1) (2013) 77–86.
[216] Q. Chen, X. Wang, C. Wang, L. Feng, Y. Li, Z. Liu, Drug-induced self-assembly of modified albumins as nanotheranostics for tumor-targeted combination therapy, ACS Nano (2015), http://dx.doi.org/10.1021/acsnano.5b00640.
[217] R. Khandelia, S. Bhandari, U.N. Pan, S.S. Ghosh, A. Chattopadhyay, Gold nanocluster embedded albumin nanoparticles for two-photon imaging of cancer cells accompanying drug delivery, Small (2015), http://dx.doi.org/10.1002/smll.201500216.
[218] K.-C. Wei, F.-W. Lin, C.-Y. Huang, C.-C.M. Ma, J.-Y. Chen, L.-Y. Feng, H.-W. Yang, 1,3-Bis(2-chloroethyl)-1-nitrosourea-loaded bovine serum albumin nanoparticles with dual magnetic resonance–fluorescence imaging for tracking of chemotherapeutic agents, Int. J. Nanomedicine 11 (2016) 4065–4075.
[219] A.C. Anselmo, S. Mitragotri, Nanoparticles in the clinic, Bioeng. Transl. Med. 1 (2016) 10–29.
[220] B. Elsadek, F. Kratz, Impact of albumin on drug delivery - new applications on the horizon, J. Control. Release 157 (2012) 4–28.

Journal of Drug Delivery Science and Technology
Available online 10 October 2020, 102129
In Press, Corrected Proof

Research paper

Hyaluronic acid conjugated albumin nanoparticles for efficient receptor mediated brain targeted delivery of temozolomide

Ritu R. Kudarha, Krutika K. Sawant
NDDS Research Laboratory, Faculty of Pharmacy, The Maharaja Sayajirao University of Baroda, Donor's Plaza, Fathegunj, Vadodara, 390002, India

Received 25 June 2020, Revised 17 September 2020, Accepted 29 September 2020, Available online 10 October 2020.

Highlights

- Hyaluronic acid conjugated albumin nanoparticles for brain tumor targeting via CD44 receptor mediated targeting.
- Development and optimization of albumin nanoparticles using Box Bhenken response surface design.
- CD44 receptor blocking assay and elucidation of cellular uptake mechanism.
- Enhancement of temozolomide concentration in brain via target specific drug delivery.
- Pharmacokinetic, biodistribution and toxicity studies of developed nanoparticles.

Abstract

In the present investigation, temozolomide (TMZ) loaded albumin nanoparticles (TNPs) were prepared by desolvation method and optimized by Box-Behnken design. Hyaluronic acid (HA) was used to modify the surface of TNPs to achieve CD44 receptor mediated targeting (HA-TNPs). The developed nanoparticles were characterized and evaluated using various in vitro and in vivo techniques. HA-TNPs were able to cross the blood brain barrier (BBB) as demonstrated in BBB passage study performed on monolayer and co-culture models. Cell viability assay demonstrated superior suppression of growth of U87 MG cells by HA-TNPs as compared to pure drug. HA-TNPs were able to generate reactive oxygen species (ROS) in U87 MG cells and their uptake was both endocytosis mediated (caveolae pathway) and CD44 receptor mediated as confirmed by CD44 receptor blocking study. In vivo results showed improvement in pharmacokinetics of TMZ as significant enhancement in plasma AUC, $t_{1/2}$ and MRT from HA-TNPs was observed as compared to TMZ alone. Biodistribution results demonstrated higher accumulation of TMZ in brain and significant decrease of drug in other vital organs like liver and lungs by HA-TNPs as compared to pure drug. From all these results, it was concluded that HA-TNPs have potential to target brain tumor more specifically as compared to pure TMZ and may act as a promising targeted delivery platform.

Graphical abstract

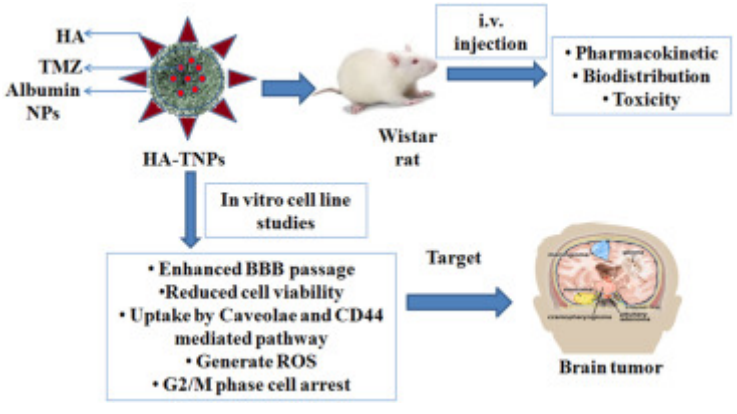

Download : Download high-res image (313KB) Download : Download full-size image

Keywords

Temozolomide; Albumin nanoparticles; Brain targeting; CD44 blocking assay; Pharmacokinetics and biodistribution

Recommended articles Citing articles (0)

View full text